Use of an Inducible Promoter to Characterize Type IV Pili Homologues in *Clostridium perfringens*

Andrea H. Hartman

Thesis submitted to the Faculty of the
Virginia Polytechnic Institute and State University
in partial fulfillment of the requirements for the degree of

Master of Science
in
Biological Sciences

Stephen B. Melville, Committee Chair
David L. Popham
Jiann-Shin Chen
Florian D. Schubot

13 September 2012
Blacksburg, Virginia

Keywords: *Clostridium perfringens*, inducible promoter, Type IV pili, Type II secretion

Use of an Inducible Promoter to Characterize Type IV Pili Homologues in *Clostridium perfringens*

Andrea H. Hartman

ABSTRACT

Researchers of *Clostridium perfringens*, a Gram-positive anaerobic pathogen, were lacking a tightly-regulated, inducible promoter system in their genetic toolbox. We constructed a lactose-inducible plasmid-based system utilizing the transcriptional regulator, BgaR. Using the *E. coli* reporter GusA, we characterized its induction in three different strains of *C. perfringens*.

We then used a newly-developed mutation system to create in-frame deletion mutants in three genes with homology to Type IV pilins, and we used the promoter system described above to complement the mutants. We analyzed each pilin for localization and expression, as well as tested each of the mutants for various phenotypes frequently associated with type IV pili (TFP) and type II secretion systems. PilA2, PilA3, and PilA4 localized to the poles of the cells. PilA2 was expressed in the wildtype when *C. perfringens* was grown on agar plates, and the PilA3 mutant lacked a von Willebrand factor A domain-containing protein in its secretome.

We used our promoter system to express GFP-tagged versions of the TFP ATPase homologues and view them in cells growing on surfaces. We saw that PilB1 and PilB2 co-localized nearly all of the time, while a portion of PilT was independent of the PilB proteins. PilT appeared necessary for the localization of PilB, and it localized independently of TFP proteins in *Bacillus subtilis*. PilT's typical localization in *Bacillus subtilis* was disrupted when the GTPase and polymerization activity of cell division protein FtsZ was blocked, suggesting that PilT associates with cell division proteins.

Dedication

This work is dedicated to Tim and Piper, for their flexibility and patience this past year. I am looking forward to taking care of them next year and in future years.

Acknowledgments

I would like to acknowledge my advisor, Stephen Melville, for his guidance in investigating this project. Whenever I was unable to think of any further beneficial experiments, he redirected me. I must also thank him for his patience with my mistakes, constant questions, and frequent frustration. He always remained calm and helpful regardless of the situation.

My committee members David Popham, Jiann-Shin Chen, and Florian Schubot also contributed many useful ideas toward this project. Aside from the actual project, they were continually exhorting me toward better professionalism, and helping me have realistic expectations. I really appreciate their care.

My Melville lab colleagues, Hualan Liu and Will Hendrick, are one reason I am very sad to be concluding my time here. Hualan and I have been in graduate school four years together, and I am cheering her on to the finish. Her co-workers can always count on her for kindness, encouragement, hard work and humor. Will is always quick to help with anything protein-related, and he knows more random things than any other young person I know. I wish him the best in his doctoral pursuits.

I have also been blessed to have several competent undergraduates working in the lab. Brittany Gianetti worked for three and a half years, preparing plasmids, counting fluorescent spots, videoing cells under the microscope, and running attachment assays. Elizabeth Pickering analyzed hundreds of computer images to produce quantitative data. I thank them and wish them each the best in their future endeavors.

Contents

List of Figures

List of Tables

List of Videos

Attribution

Hualan Liu performed half of the GusA assays in Chapter 2. Brittany Gianetti did half of the image analysis and video microscopy in Chapters 3 and 4 as well as the attachment and clumping assays. Stephen Melville was the principle investigator. Each co-author has given written permission to reproduce the material in this thesis.

Chapter 1

Introduction and Literature Review

***Clostridium perfringens*.**

Clostridium perfringens belongs to a genus of Gram-positive, endospore-producing, anaerobic rods with a low G and C content in their chromosome [1]. Their A and T content comprises on average 75% of the genome [2]. *C. perfringens* lives in soil and sewage, and is part of the intestinal flora of animals and humans. It acts as an opportunistic pathogen, causing gas gangrene and many intestinal diseases in both animals and humans [1, 3]. Thirty-five Clostridial species are pathogenic [3], and the different strains in the genus make more different toxins than any other genus [3]. *C. perfringens* alone produces around sixteen different virulence factors, many of which are degradative enzymes that allow *C. perfringens* to gain nutrition from dead animals [2]. Its fourteen toxins is the highest number of toxins produced for any known species of microorganism [1].

C. perfringens, like other Clostridia, is an anaerobic chemoheterotroph which has no apparent genes coding for enzymes along the forward tricarboxylic acid cycle or electron transport chain [4]. Rather, it carries out many fermentations for energy. It can utilize a variety of carbohydrates in glycolysis, and then convert pyruvate to lactate via lactate dehydrogenase or to acetyl CoA via pyruvate ferridoxin oxidoreductase [4]. The conversion to acetyl CoA produces large amounts of hydrogen and carbon dioxide. It further metabolizes acetyl CoA to produce ethanol, acetate, or butyrate [4]. In addition to fermenting carbohydrates, it can ferment serine and threonine to propionate [4].

C. perfringens is naturally auxotrophic for eleven amino acids (arginine, glutamic acid, histidine, isoleucine, leucine, methionine, phenylalanine, threonine, tryptophan, tyrosine, valine) and two vitamins (pantothenic acid and pyridoxamine) and additionally requires either glycine or serine [5]. As a saprophytic bacterium, it would usually gain these nutrients from decaying organisms [2, 6].

Diseases of *C. perfringens* and relevant toxins.

Due to its abundant toxins, various strains of *C. perfringens* cause a range of diseases in people and animals, from mild food poisoning to potentially deadly gas gangrene. However, different *C. perfringens* strains only produce some of the fourteen toxins, and researchers have divided the strains into five types (A-E) based on the major toxin each produces. I discuss each type with the diseases it causes and relevant toxins below.

Food poisoning. Food poisoning is the most common disease caused by *C. perfringens*. It occurs when live *C. perfringens* type A cells that are positive for the enterotoxin gene *cpe* are ingested. The cells are stimulated to sporulate due to the low pH in the stomach [7], and sporulating cells release the CPE enterotoxin into the small intestine. This results in diarrhea and stomach pain that tend to subside within twenty-four hours [3]. The Center for Disease Control estimates that *C. perfringens* causes nearly a million cases of food-borne gastroenteritis per year in the United States [8]. In 2011, it was the third highest contributor to domestically acquired foodborne illness, below Norovirus and *Salmonella* [8].

Antibiotic-associated diarrhea. Antibiotic-associated diarrhea (AAD) is another *C. perfringens* type A disease frequently affecting children and the elderly in hospitals [9], particularly those that have recently taken antibiotics [3]. Based on indistinguishable strains infecting temporally-overlapping patients in hospitals and strains identified in the hospital environment and on patients' hands, it appears to be contagious, rather than just acquired via normal flora [10], hence its high frequency in hospital settings. According to one study, it is one fourth as frequent as AAD caused by *C. difficile* [10], and unlike *C. difficile*, no particular types of antibiotics were associated with higher risk factors. Rather, female gender and use of antacids were significant risk factors for *C. perfringens* AAD [10].

Clostridial myonecrosis. Clostridial myonecrosis, or gas gangrene, is a muscle tissue necrosis most commonly caused by *C. perfringens* type A. It is responsible for about 80% of traumatic gas

gangrene incidences [3]. It is characterized by rapid spreading into healthy tissue, the production of copious gas, and systemic shock due to bacterial toxins [3]. In order for a *C. perfringens* infection to go beyond a surface infection or cellulitis, there must be a situation causing anaerobic conditions. In a traumatic gangrene occurrence, which accounts for about 70% of gas gangrene incidences, there is a deep wound that destroys blood vessels, causing anaerobic conditions in the wound [3]. In other cases, there may be abdominal surgery, conditions related to childbirth such as a retained placenta, or an intramuscular epinephrine injection [3]. In individuals that have previously had a Clostridial infection, minor injuries may provide sufficient anaerobic conditions for spores from the previous infection to germinate [3].

The symptoms of Clostridial myonecrosis begin with severe pain at the sign of trauma, followed by a tissue color change, blister formation, and gas within the tissues. As the infection progresses, fever, tachycardia, and sweating occur, culminating in shock, organ failure, and death [3]. One unique characteristic of Clostridial infections is that no polymorphonuclear leukocytes (PMNLs) are present at the site of infection, but are present at the border between the necrotic and living tissue [3].

Early amputation or debridement of the necrotic tissue is required treatment, and when combined with antibiotic treatment (clindamycin, penicillin, and tetracycline are most common) and/or hyperbaric oxygen, the patient has a good chance of survival [3]. Patients already presenting with shock upon diagnosis are frequently too late for treatment to be effective [3]. Medscape estimates that 1,000 cases of Clostridial gas gangrene occur in the United States each year, and even when properly treated, at least 20–30% of these are fatal [11].

The two major toxins in the pathogenesis of Clostridial myonecrosis are alpha toxin and theta toxin. Alpha toxin, a phospholipase C and sphingomyelinase, is generally considered the most important in the pathogenesis of gas gangrene. When injected into mice, it causes a plethora of symptoms including bradycardia, myocardial failure, smooth muscle contractions, platelet aggregation, and inflammation [2]. Theta toxin, or perfringolysin O, forms large pores in cell membranes. Theta

toxin contributes to the development of shock by reducing vascular tone through various effects [3]. It also prevents PMNLs from interacting normally with endothelial cells and is responsible for the lack of PMNLs near the leading edge of *C. perfringens* in an infection [3].

Although not critical to the major symptoms of gas gangrene, several minor toxins possess degradative ability. Mu toxin is a hyaluronidase, which degrades hyaluronic acid, a component in connective tissue [2]. A protease, α-clostripain, has been shown to increase vascular permeability in mice, and its homologue in *Clostridium hisolyticum* aids in the apoptosis of neutrophils [12]. Other minor toxins include a collagenase, a nuclease, a hemolysin, and a caseinase [2].

Necrotizing enteritis in humans. *C. perfringens* Type C causes a rare necrotizing enteritis known as pigbel in Papua New Guinea. Beta toxin is secreted in type B and type C strains, and is responsible for this lethal disease, causing the intestinal wall to become crumbly and necrotic [3]. Beta toxin is both heat and trypsin sensitive, and is cleaved by trypsin in well-nourished persons, preventing its pathogenesis [2]. In Papua New Guinea, the patients have consumed contaminated meat and are malnourished due to low protein and high consumption of trypsin inhibitors such as sweet potato or soy beans [2, 3].

Symptoms of pigbel vary in severity, but always include diarrhea. Fluid and electrolyte replacement and antibiotic treatment are included in the treatment, which fifty percent of the time involves removal of the necrotic portion of the intestine [3]. Even then, mortality can be up to forty percent [3].

Enteric diseases in animals. *Clostridium perfringens* is the most important Clostridial pathogen in enteric disease of domestic animals [3]. Each toxin type can cause enterotoxemia or enteritis in various animals, including pigs, cows, fowl, dogs, horses, sheep, goats, or rabbits, and, by the time symptoms present, the animal is frequently close to death [3]. Necrotic enteritis in chickens can reduce the farmer's profit by about 33% in a flock with a higher incidence of enteritis, compared to a lower incidence [13].

Major toxins involved in animal diseases are epsilon toxin and iota toxin. Epsilon toxin causes

an enterotoxemia in hoofed mammals known as pulpy kidney disease in sheep. It aids in the bacteria's penetration of the intestine, allowing them to access the blood stream, and then appears to form pores on the membranes of kidney and brain cells [14]. It is secreted in an inactive form and activated by proteolytic cleavage [2]. Iota toxin causes necrosis and is produced by type E strains. It consists of two peptide chains, the smaller of which possesses ADP-ribosylating activity [2].

Type IV pili.

Type IV pili (TFP) are thin, polymeric filaments composed of a single protein, called pilin. A bacterial cell is able to extend a pilus via ATPase-based polymerization. They are present on most Gram-negative bacteria [15], and have been found to perform a variety of functions. Type IV pili's most significant function is attaching to host cells at the initiation of an infection [15]. TFP mutants of *Vibrio cholerae*, enteropathogenic *E. coli* (EPEC), *P. aeruginosa* and many other pathogens have shown a marked decrease in virulence *in vivo* due to the inability to establish an infection [16–18]. Type IV pili have been shown to be necessary for DNA binding and uptake in *Neisseria gonorrhoeae*, *Legionella pneumophila*, and many other Gram-negative bacteria [19]. *Myxococcus xanthus* uses pili to attach to secreted polysaccharide tails on neighboring bacteria in its social gliding motility [20]. *N. gonorrhoeae* and *P. aeruginosa*, among other Gram-negative bacteria, have a jerky twitching motility mediated by the extension and retraction of type IV pili [21]. Several researchers have shown TFP play a role in biofilm formation in *Pseudomonas aeruginosa* [22–24], and *V. cholerae* forms microcolonies by bundling toxin-coregulated pili [25].

TFP have been divided into two subclasses, Type IVa and Type IVb, based on characteristics of the pilin subunits, assembly systems and functions. Both types of pilins have an N-terminal alpha helix and a globular C-terminus, but Type IVa have a shorter leader sequence and a shorter mature sequence than Type IVb, and different N-terminal residues are N-methylated in each type [26]. *Neisseria*, *Pseudomonas*, and *Myxococcus* are examples of Type IVa. Type IVb pili have only

been studied in enteric pathogens, such as *V. cholerae* and EPEC, and are used to attach to the host and form microcolonies [15]. Type IVb pili will not be described further as *C. perfringens*' pili resemble the Type IVa pili [27].

A model has been proposed for the assembly and disassembly of Type IV pilins in Gram-negative bacteria. Below, the core proteins are described, and the nomenclature from *P. aeruginosa* is used, as it is the same as that used in *C. perfringens*. PilD is a peptidase which cleaves the leader sequence off the pilin monomer, usually called PilA [27, 28]. Across different species, the PilA monomers appear to be conserved in structure, with a short leader sequence, a hydrophobic alpha-helix at the N-terminus, and a globular C-terminus with beta-sheets [21, 29]. The C-terminus is less conserved than the N-terminus between species [21]. Within the pilus, the pilins are arranged in a helix, with five monomers per turn [21], their N-terminal helices twisted together to form a type of spine on the inside of the pilus [26]. PilQ and PilP respectively form and support the pore in the outer membrane of Gram-negative bacteria [21]. PilM, PilN, and PilO are inner membrane proteins that are present in all TFP systems, but whose functions have not yet been determined [28]. As PilM has an actin-like component, it is speculated that it may bind the TFP system to the cytoskeletal system, for polar localization [30]. There are also peptidoglycan-associated proteins, which putatively restructure the peptidoglycan to allow passage of the pilus. FimV in *P. aeruginosa* performs this function [30].

PilB is an ATPase which provides the energy to assemble the processed pilins into filaments. In most bacteria (*N. gonorrhoeae* perhaps excepted [31]), PilB requires PilC, a protein localized to the inner membrane region. PilC has been proposed to act as a piston, pushing pilins from the cytoplasmic membrane into the base of the pilus fiber, resulting in pilus extension [32]. It was required for the localization of PilB in *P. aeruginosa* [33]. PilT is an ATPase which disassembles pilin filaments, resulting in retraction [28]. PilB and PilT are hexameric ATPases belonging to the "secretion superfamily ATPases" which includes those involved in Type II and Type IV secretion systems [34].

A hypothetical model depicting the major proteins in a Gram-positive system is shown in Fig. 1.1. This model is based on the TFP system in Gram-negative bacteria.

Yellow fluorescent proteins have been used to localize PilB and PilT in *P. aeruginosa* cells and PilT in *M. xanthus* cells [33, 35]. In *M. xanthus*, immunofluorescence was used to localize PilB [35]. The proteins were predominately polar in both species, with PilB and PilT present at both poles in *P. aeruginosa*, although an additional retraction ATPase, PilU, was present at the piliated pole only [33]. PilT and PilU localized to the poles regardless of mutations in other TFP proteins, but PilB showed disperse localization in a PilC mutant [33]. In *M. xanthus*, where the cells undergo reversals in direction, PilB and PilT were found to move to alternating poles of the cell [35]. While PilQ, PilM, and PilC remained fixed at both poles, PilB and PilT alternated, with PilB at the piliated/leading pole, and PilT at the non-piliated/lagging pole [35].

Type II secretion systems.

A type II secretion system (TTSS) is a method of protein secretion in Gram-negative bacteria which transports folded proteins across the outer membrane [36]. It is known for transporting proteases, toxins, and other proteins important to virulence [37]. The proteins which the system transports can be large. For example, pullulanase, a protein exported by the *Klebsiella oxytoca* TTSS, is 117 kDa [37].

The components of TTSS are nearly the same as those of TFP. Mutation and complementation analysis showed it to require a minimum of twelve genes, depending on the individual bacteria [37]. These genes include a secretin like PilQ, and an ATPase and inner transmembrane protein, homologous to PilB and PilC in TFP systems. There is a leader peptidase similar to PilD, and one major and four minor pseudopilins, the major one being similar to Type IV pilins [38]. The TTSS pseudopilus is, however, much shorter and assembled into a left-handed helix, rather than right-handed as the pilus in TFP [6, 39]. Additionally, TTSS lack a retraction ATPase such as PilT [37].

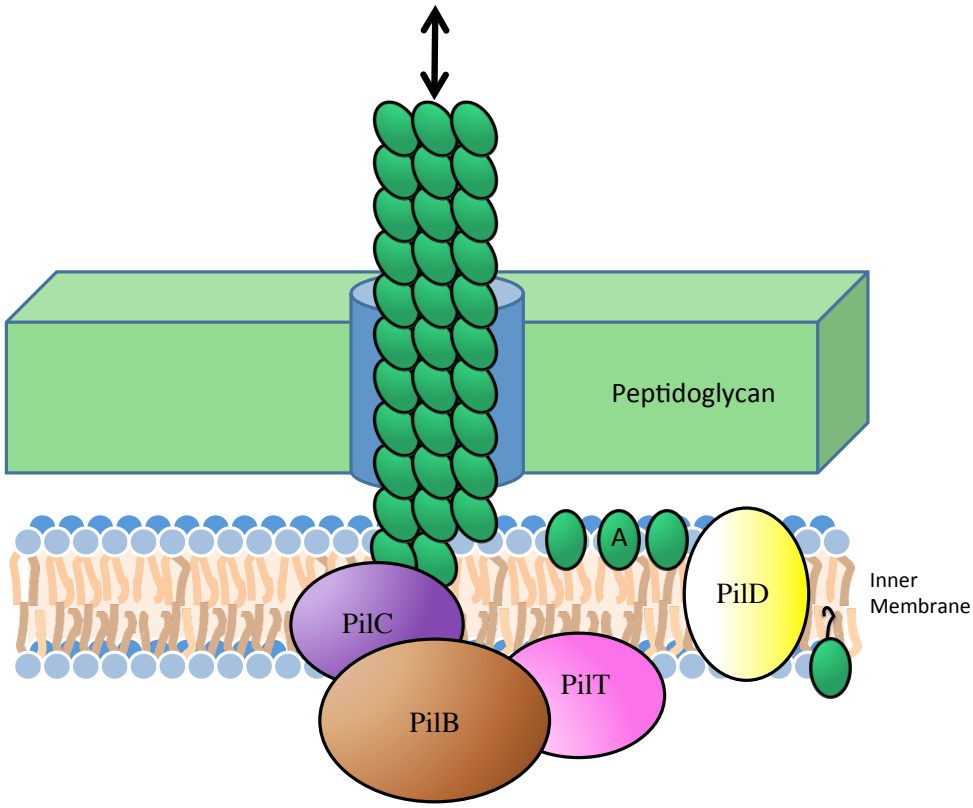

Figure 1.1: Model of TFP in Gram-positive bacteria. “A” equals PilA, and the channel through the peptidoglycan is formed by unknown proteins.

TFP genes in *C. perfringens*.

C. perfringens has four genes which, based on structural prediction models, appear to code for pilins. *C. perfringens* also has two proteins homologous to PilB, two to PilC, and one each for PilD, PilT, PilM, PilN, and PilO [27]. As *C. perfringens* seems to possess two copies of *pilB* and *pilC*, as well as four different pilins, some of these may be involved in TTSS, rather than in TFP-mediated motility.

ParM system for TFP localization.

The ATPase proteins MinD and ParA function in segregating and positioning bacterial chromosomes and plasmids during cell division. These proteins either organize themselves according to the curvature of the cell or position themselves based on a landmark protein [40]. Now, TadZ or CpaE, proteins in the same family as ParA but including a response regulator domain, have been shown to play a role in the positioning some Type IVb pili systems [40]. In these cases, TFP are found on the poles, and TadZ acts as a link between a polar landmark protein and the other pili proteins in that group [40]. However, Type IVa and other Type IVb pili systems have not been found to possess any homologue of TadZ, although their pili localize to the poles as well [40].

Study objectives.

The first objective in studying *C. perfringens* was the development of a usable inducible promoter system. As researchers of *C. perfringens* lacked many genetic tools, this promoter system would allow further research to involve expression of tagged proteins and complementation of mutants. We were able to construct and characterize a lactose-inducible promoter system that functioned in a gas gangrene strain, a food poisoning strain, and a strain that caused necrotic enteritis in chickens. The next objective was to apply this inducible promoter and other tools to determining the functions of PilA1, PilA2, PilA3, and PilA4, the *C. perfringens* proteins with

homology to pilin monomers. We planned to mutate each pilin gene individually and test these mutants and their complements in different assays which have known relevance to TFP or TTSS. In-frame deletion mutations of three of these pilin genes demonstrated that they did not play a role in spreading colony formation, but two of them may affect secreted proteins. Localizing the proteins by immunofluorescence allowed us to demonstrate the presence of three of these pilins on the poles of the cells, and western blot analysis revealed the protein expression levels. The final objective was to examine the localizations of PilB1, PilB2, and PilT, the pilin ATPase motors by tagging them with fluorescent proteins and tracking them in live cells. Results here led to testing each tagged protein in various mutant strains and sometimes in *B. subtilis*, a species lacking genes with homology to TFP genes. These results demonstrated that PilT controls PilB localization through association with cell division proteins.

Chapter 2

Construction and Characterization of a Lactose-Inducible Promoter System for Controlled Gene Expression in *Clostridium perfringens*

Andrea H. Hartman, Hualan Liu, Stephen B. Melville. 2011. Applied and Environmental Microbiology. (77)2: 471-478.

CO-AUTHORS' CONTRIBUTIONS

Hualan Liu performed half of the β-glucuronidase assays. Stephen Melville was the principal investigator and revised the manuscript.

ABSTRACT

Clostridium perfringens is a Gram-positive anaerobic pathogen which causes many diseases in humans and animals. While some genetic tools exist for working with *C. perfringens*, a tightly-regulated, inducible promoter system is currently lacking. Therefore, we constructed a plasmid-based promoter system that provided regulated expression when lactose was added. This plasmid (pKRAH1) is an *Escherichia coli-C. perfringens* shuttle vector containing the gene encoding a transcriptional regulator, BgaR, and a divergent promoter upstream of gene *bgaL* (*bgaR*-P_{bgaL}). To measure transcription at the *bgaL* promoter in pKRAH1, the *E. coli* reporter gene *gusA*, encoding β-glucuronidase was placed downstream of the P_{bgaL} promoter to make plasmid pAH2. When transformed into three different strains of *C. perfringens*, pAH2 exhibited lactose-inducible expression. *C. perfringens* strain 13, a commonly studied strain, has endogenous β-glucuronidase activity. We mutated gene *bglR*, encoding a putative β-glucuronidase, and observed an 89% decrease in endogenous activity with no lactose. This combination of a system for regulated gene expression and a mutant of strain 13 with low β-glucuronidase activity are useful tools for studying gene regulation and protein expression in an important pathogenic bacterium. We used this system to express the *yfp-pilB* gene, comprised of a yellow fluorescent protein (YFP)-encoding gene fused to an assembly ATPase gene involved in type IV pilus-dependent gliding motility in *C. perfringens*. Expression in the wild-type strain 13 showed that YFP-PilB localized mostly to the poles of cells, but in a *pilC1* mutant, it localized throughout the cell, demonstrating that the membrane protein PilC is required for polar localization of PilB.

INTRODUCTION

C. perfringens is an important bacterial pathogen, causing gas gangrene, food poisoning, necrotic enteritis, and other diseases in humans and many others in agriculturally important live-stock [2, 41–43]. Strains that are transformable by electroporation have been isolated and their genomes sequenced [2, 4, 44, 45], and many groups have developed effective methods to create site-directed and random mutants [46–49]. However, other genetic tools available for studying genes are limited or absent, including an inducible promoter system, although they have been developed for use in *Clostridium acetobutylicum* [50, 51]. A well-regulated promoter system would be a valuable tool in *C. perfringens* for complementing mutants, controlling the expression of fusion-tagged proteins, and modulating the intracellular levels of proteins to near physiological conditions.

There are several characteristics which would be desirable in an inducible promoter system. Ideally, a promoter system would work in a variety of *C. perfringens* strains, since different diseases are caused by strains that are genetically highly diverse [44]. It would be easy to induce, not requiring a temperature shift, expensive chemicals, or specific media. It would have a large range of activity based on the concentration of inducer added, and low activity in the absence of inducer. These characteristics would allow a protein to be highly expressed for potential purification or analysis of the effects of over-expression on the phenotype of the strain. Tight regulation allows the introduction of potentially lethal genes as well as observation of phenotypic changes that occur in the absence of expression of a gene that has been inactivated by mutation. Finally, a rapid response to the presence of the inducer would be desirable in studying short-term effects of the presence of the gene product on the cell. An example of a plasmid-based system that fulfills all of these criteria is the pBAD family of plasmids developed by Guzman and co-workers for use in *E. coli* [52]. The plasmids employ the AraC protein to provide arabinose inducible expression from the divergently transcribed promoter for the *araBAD* operon [52].

We used the genome sequence of *C. perfringens* strain 13 to identify regulators and promoters that, like the pBAD plasmids, would likely fulfill the desired requirements. We identified a lactose-

inducible regulatory system, consisting of a gene encoding a transcriptional regulator, *bgaR*, and the promoter of a divergently transcribed regulated gene, *bgaL* and constructed a plasmid-based system for controlled gene expression that functions in three different pathogenic strains of *C. perfringens*. We used the system in one of these strains to express a yellow fluorescent protein (YFP)-tagged type IV pilus-associated ATPase (PilB) and showed that cellular localization of this protein was dependent on a membrane-bound partner protein, PilC.

MATERIALS AND METHODS

Bacterial strains and growth conditions. Bacterial strains, plasmids, and primers used in this study are listed in Table 2.1. *E. coli* was grown in Luria Bertani (LB) medium supplemented with antibiotics as needed (400 μg/mL erythromycin, 100 μg/mL ampicillin, or 20 μg/mL chloramphenicol) and agar for plates. *C. perfringens* was grown in a Coy anaerobic chamber in brain heart infusion (BHI) media (Difco) or on BHI plates with appropriate antibiotics as indicated (30 μg/mL erythromycin or 20 μg/mL chloramphenicol). PY medium (30 g/L proteose peptone, 10 g/L yeast extract, 1 g/L sodium thioglycolate) was used to grow *C. perfringens* for β-glucuronidase assays.

Electroporation of *E. coli* and *C. perfringens*. Standard protocols were used for electroporation of plasmids into *E. coli* strain DH10B [53]. Electroporation of *C. perfringens* was done, based on a previously published method [54], as follows: cells (3 ml) were grown anaerobically overnight in BHI, resuspended and washed twice in sucrose electroporation buffer (333 mM sucrose, 6.7 mM $NaHPO_4$ [pH 7], 1 mM $MgCl_2$). Plasmid DNA and 400 μl of cell suspension were placed in a 4 mm cuvette on ice and electroporation was done in an anaerobic chamber using an ECM 630 Electro Cell Manipulator (BTX, Harvard Apparatus). After electroporation, cell suspensions were incubated in BHI anaerobically at 37°C for 3 hours, spread onto BHI plates with appropriate antibiotics and incubated anaerobically at 37°C until colony formation was observed.

Plasmid construction. To construct pAH2, we amplified the *bgaR*-P_{bgaL} region from strain 13 using the primers OAH1 and OAH2 by PCR using Phusion polymerase (New England Biolabs). Adenine residues were added to the ends of the PCR product using *Taq* polymerase and the PCR product was ligated to pGEM-T Easy (Promega) to create plasmid pAH7. The insert was sequenced to determine if any mutations had occurred during amplification. We digested pAH7 with XhoI and PstI and the *bgaR*-P_{bgaL} fragment was ligated to XhoI- and PstI-digested pSM240 [55] to create pAH2. Plasmid pAH1 was constructed in the same manner, but was discovered to have a frameshift mutation in *bgaR* (within codon 119 out of 279), causing translation to terminate after addition of 14 aberrant amino acids. As such, it provides a useful negative control for

Table 2.1: Strains, plasmids, and primers used in this study.

Strain, plasmid or primer	Description, relevant phenotype or genotype, or sequence (5' to 3')	Source
E. coli		
DH10B	F-*mcrA* Δ(*mrr-hsdRMSmcrBC*) F80d *lacZ* Δ*M15 lacX74 deoR recA1araD139* D (*ara, leu*)7697 *galU galK* Δ-*rpsL endA1 nupG*	Gibco/BRL
C. perfringens		
13	Gangrene strain	C. Duncan
SM101	Acute food poisoning strain	[45]
JGS4143	Chicken necrotic enteritis strain	J. G. Songer
AH1	*bglR*-:Erm^R, from strain 13	This study
AH2	*bgaR*-:Erm^R, from strain 13	This study
Plasmids		
pGEM-T Easy	Ampicillin resistance	Promega
pSM240	Contains *cpe-gusA*; chloramphenicol resistance	[55]
pAH1	Mutated *bgaR* with P_{bgaL} in pSM240	This study
pAH2	pSM240 with *bgaR* and P_{bgaL} upstream of *cpe-gusA*	This study
pKRAH1	Contains *bgaR*-P_{bgaL} and polylinker; chloramphenicol resistance	This study
pSM300	Suicide plasmid in *C. perfringens*; erythromycin resistance	[57]
pAH3	Contains a fragment of strain 13 *bglR* in pGEM-T Easy	This study
pAH4	Contains a fragment of strain 13 *bglR* in pSM300	This study
pAH5	Contains a fragment of strain 13 *bgaR* in pGEM-T Easy	This study
pAH6	Contains a fragment of strain 13 *bgaR* in pSM300	This study
pAH7	Contains strain 13 *bgaR* and P_{bgaL} in pGEM-T Easy	This study

Table 2.1: (continued)

Strain, plasmid or primer	Description, relevant phenotype or genotype, or sequence (5' to 3')	Source
Primers		
OAH1	GTTAACCTCGAGATGAAAAGTATTAGGGC	
OAH2	GCAGTTCTGCAGTATCTTCATGGTATTC	
OAH5	GGAGAGGTACCAGTTGAACATAAGGGAGG	
OAH6	CATGGAGCTCTCTTATCTCTAGAAACTAATTC	
OKR055	GAATCTAGAATCCGCGGTAGTCGACATCCATGGTTGAGCTCATGGATCCTAA	
OKR056	AGCTTTAGGATCCATGAGCTCAACCATGGATGTCGACTAC	
	CGCGGATTCTAGATTCTGCA	
OAH56	GGTACCCAAGTTGAGTATGTGGCTTCTATTGATG	
OAH57	GAGCTCTTCTGCTTAAGTTTACATAATCAGC	

experiments testing plasmid *bgaR* activity. To construct pKRAH1, we designed complementary primers (OKR055 and OKR056) that, when annealed, would contain several restriction recognition sequences rarely found in the *C. perfringens* chromosome and would have ends compatible with HindIII- and PstI-digested DNA. We ligated the annealed OKR055/OKR056 DNA to pAH2 digested with PstI and partially digested with HindIII to avoid cutting at a second HindIII site internal to the *bgaR* gene. To construct pKRAH-Y, the *yfp* gene in plasmid pSW4-YFP [56] was amplified using PCR with primers OAH13 and OAH14 which contain a SacI and SacII site, respectively, and ligated to SacI- and SacII-digested pKRAH1. To construct pKRAH-YB, the *yfp* gene in plasmid pSW4-YFP was amplified with primers OAH14 and OAH36, and we then amplified the *pilB* gene from strain 13 chromosomal DNA by using primers OAH37 and OAH38. Using these partially overlapping PCR products as the template, we amplified *yfp-pilB* using OAH14 and OAH38, and ligated the product into pGEM-T Easy as described above, creating plasmid pAH11. pAH11 and pKRAH1 with SacII and SacI and ligated together to form pKRAH-YB.

Mutation of the *bglR* and *bgaR* genes in strain 13. An 890 bp fragment internal to *bglR* was amplified from strain 13 using the primers OAH5 and OAH6 and Phusion polymerase. Adenine residues were added to the ends of the PCR product using *Taq* polymerase, and the PCR product ligated into pGEM-T Easy to create plasmid pAH3. Plasmid pAH3 was digested with KpnI and SacI to release the *bglR* gene fragment, which was ligated to pSM300, forming pAH4. Plasmid pSM300 is a suicide plasmid carrying an *ermBP* resistance gene [55]. Plasmid pAH4 was transformed into *C. perfringens* by electroporation and erythromycin-resistant (Erm^r) recombinants selected using BHI plates with erythromycin. An Erm^r transformant (strain AH1) was confirmed to have an insertion in the *bglR* gene by PCR amplification using primers that annealed within pAH4 and to an area of the chromosome outside of the homologous region used for integration. Strain 13 chromosomal DNA was screened as a negative control. PCR using primers designed to amplify the *bglR* wild-type gene produced a very faint band in the *bglR* mutant strain AH1, which did not disappear after several days of growth in BHI, which suggested there was a very small percentage of wild-type bacteria present, probably due to infrequent recircularization of the integrated plas-

mid via the regions of homology. A mutation was introduced into the *bgaR* gene in the same way, except a 389 bp fragment of *bgaR* was amplified from strain 13 with primers OAH56 and OAH57, cloned into PGEM-T Easy creating pAH5, and then ligated into pSM300, creating pAH6. The mutant (strain AH2) was constructed and screened as described above for strain AH1.

β-Glucuronidase assays and β-galactosidase assays. β-Glucuronidase assays were performed on mid-log-phase cells, and specific activity was calculated according to the protocol previously described by Melville et al [58]. β-Galactosidase assays were performed the same way, except that ortho-nitrophenyl-β-galactoside (ONPG) was used as the substrate. For the timed induction assays, the cells were sub-cultured into 500 ml of pre-warmed PY without inducer, and grown to mid-log phase. The inducer was then added and samples were removed at different time points and placed onto dry ice. The rest of the assay followed the same protocol as described in Melville et al. [58].

Fluorescence microscopy. For localization of YFP, 2% agarose pads with BHI, 0.1 mM lactose, and 20 μg/mL chloramphenicol were placed on slides as previously described [59]. The slides were placed into a Coy anaerobic chamber and bacteria were spread on them. After 2 h of growth,the slides were removed them from the chamber and exposed them to aerobic conditions for at least 20 min, and then a coverslip was placed on top and sealed with nail polish. Cells were viewed on an Olympus IX71 microscope using the Applied Precision deconvolution SoftWorx program. For localization of fluorescent proteins, images of more than 270 individual cells were examined.

RESULTS

Construction of a lactose-inducible promoter plasmid. We analyzed the genome of strain 13 for putative regulators of carbohydrate metabolism that were oriented in the opposite direction from the genes they regulated, similar to *araC* and the *araBAD* operon in *E. coli* [52]. An essential enzyme in most lactose metabolic pathways is β-galactosidase [60]. *C. perfringens* strain 13 possesses four genes that have been annotated to encode β-galactosidases (assigned gene designation): *CPE0167* (*pbg*), *CPE0771* (*bgaL*), *CPE0831* (also *bgaL*), and *CPE1266* (none) [4] . Of these β-galactosidase-encoding genes, only *CPE0771* (*bgaL*) had a divergently oriented transcriptional regulator associated with it, *CPE0770* (Fig. 2.1A).

CPE0770 was annotated as encoding an AraC-family transcriptional regulator [4]. Because *CPE0770* regulates *bgaL* in a lactose-dependent manner (see below), we renamed *CPE0770 bgaR* (i.e., regulator of *bgaL*). Also, because there are two genes named *bgaL* in strain 13, we recommend that *CPE0771* and *CPE0831* be renamed *bgaL* and *bgaM*, respectively. Upstream and divergent to *bgaR* is a gene named *gutA* (Fig. 2.1, which was annotated as a probable sugar transport protein [4] and may function as a transporter of lactose. The *gutA*, *bgaR* and *bgaL* genes and their synteny are highly conserved in all nine *C. perfringens* strains with completely sequenced [4, 44] and partially sequenced (NCBI database) genomes.

The entire *bgaR* gene and the putative promoter and N-terminal region of *bgaL* (*bgaR*-P_{bgaL}) were amplified by PCR and ligated into plasmid pSM240 to create plasmid pAH2 (Fig. 2.2).

This placed the *bgaL* promoter immediately upstream of a *cpe-gusA* reporter gene fusion present in pSM240 (Fig. 2.2), which consists of the *cpe* ribosomal binding site and first 13 codons fused in frame to the entire *gusA* gene of *E. coli* [58]. The *cpe* gene from *C. perfringens* strain SM101 encodes the enterotoxin (CPE) responsible for acute food poisoning and has a ribosome binding site that likely provides a high level of translation of the protein since it is expressed at very high levels in strain SM101 [58]. The *E. coli gusA* gene, encoding a β-glucuronidase [62] has been

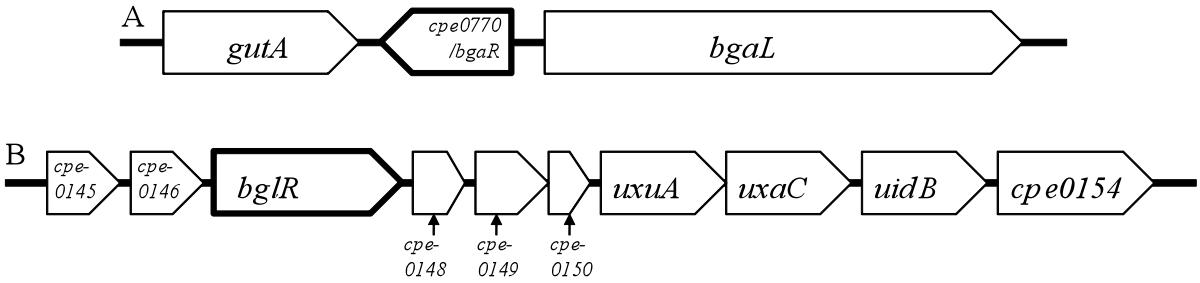

Figure 2.1: Gene orders surrounding the *bgaR* (CPE0770) and *bglR* (CPE0147) genes. (A) Gene order surrounding the *bgaR* (CPE0770) gene, an AraC family transcriptional regulator, in *C. perfringens* strain 13 (24). *gutA* encodes a probable sugar transport protein, and *bgaL* a β-galactosidase. (B) Genes in the operon that includes *bglR*, a probable β-glucuronidase in strain 13. Gene *CPE0145* is annotated as encoding a hypothetical protein, *CPE0146* a 2-keto-3-deoxygluconate kinase, *CPE0148* a putative transcriptional regulator, *CPE0149* a putative oxidoreductase, *CPE0150* a 2-dehydro-3-deoxyphosphogluconate/4-hydroxy-2-oxoglutarate aldolase, *uxuA* a D-mannonate dehydrolase, *uxaC* a glucuronate isomerase, *uidB* a glucuronide permease, and *CPE0154* a putative β-hexosamidase A.

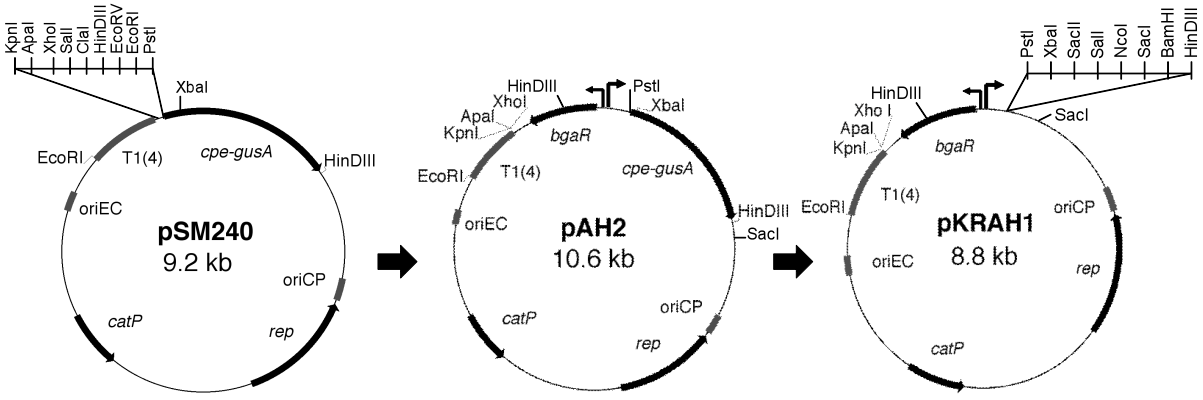

Figure 2.2: Relevant features of plasmids described in this report. Plasmid pSM240 was briefly described previously [55]. T1(4) denotes four tandem terminators [61].

used successfully as a reporter in *C. perfringens* [45, 58], *C. acetobutylicum* [50], *C. beijerinckii* [50], and *C. difficile*.

***bgaR*-P$_{bgaL}$ expression in three pathogenic strains of *C. perfringens*.** We transformed plasmid pAH2 into three different strains of *C. perfringens* and assayed β-glucuronidase activity at increasing concentrations of lactose (Fig. 2.3).

Strain SM101, an acute food poisoning-associated strain, has a low endogenous β-glucuronidase activity of ~4-8 U [58]. We observed about an 80-fold increase in expression at maximum induction (10 mM lactose) and just 2-fold expression above background levels in the absence of inducer (Fig. 2.3A). JGS4143, a strain isolated from an outbreak of chicken necrotic enteritis (G. Songer, personal communication), had 50 U of endogenous β-glucuronidase activity but showed lactose-inducible expression with pAH2 up to 10 times the background level (Fig. 2.3B). Strain 13, the source of *bgaR*-P$_{bgaL1}$, also has significant (45-70 U) background β-glucuronidase activity (Fig. 2.3C and [63]), but, with pAH1 present, we could detect about four-fold increased β-glucuronidase activity as the lactose concentration increased (Fig. 2.3C).

***bglR* in strain 13 encodes a β-glucuronidase.** Strain 13 is the most commonly used strain in *C. perfringens* pathogenesis and gene regulation studies [3, 43]. Due to endogenous β-glucuronidase activity (Fig. 2.3), it is difficult to gauge the precise levels of induction from the *bgaR*-P$_{bgaL}$ construct. Therefore, we located a gene that was annotated to encode a putative β-glucuronidase, *bglR*, in strain 13 [4]. The *bglR* gene is the second gene in a nine-gene region that likely forms an operon (Fig. 2.1B). Based on comparison to the *E. coli* genes involved in glucuronide metabolism [60], the *C. perfringens* strain 13 operon appears to encode enzymes involved in metabolizing β-glucuronides. Using NCBI BLAST analyses with genes from strain 13, the genes associated with β-glucuronide metabolism are conserved in *C. perfringens* strains F4969, JGS1721, JGS1495, JGS1987, and NCTC 8239, but absent in strains ATCC 13124, SM101, and ATCC 3626.

We introduced a mutation into the *bglR* gene of strain 13 via homologous recombination of a non-replicating plasmid (see Materials and Methods). The mutant strain, AH1, exhibited a 89%

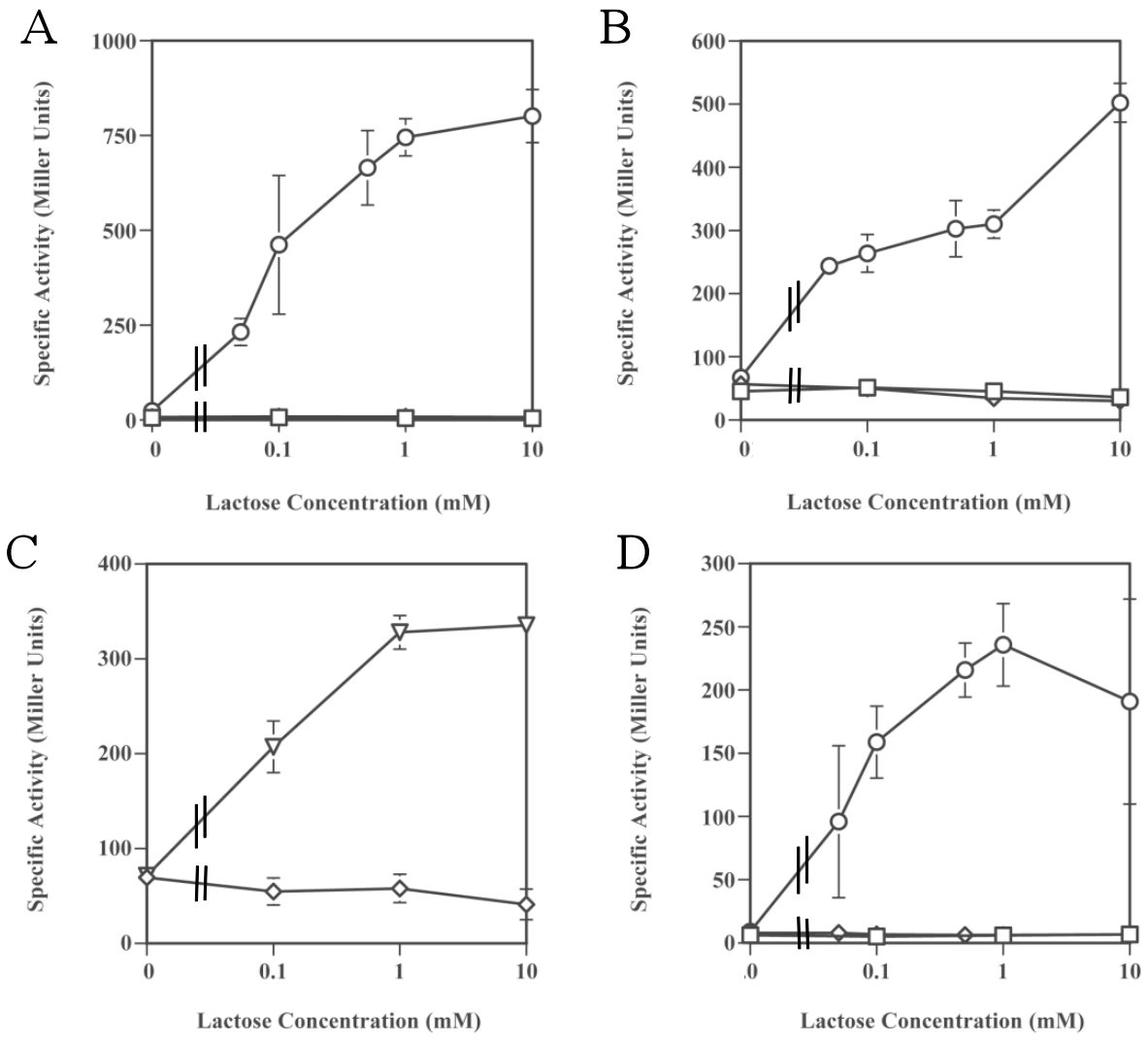

Figure 2.3: β-Glucuronidase activity in *C. perfringens* at different concentrations of lactose. (A) Strain SM101; (B) strain JGS4143; (C) strain 13; (D) strain AH1. Strains containing no plasmid (squares), pSM240 (diamonds), pAH2 (circles), and pAH1 (triangles). Except for the sample at 0 mM lactose, lactose concentrations are shown on a log scale.

decrease in the β-glucuronidase activity at 0 mM lactose (Fig. 2.3D), suggesting that *bglR* encoded an enzyme responsible for the majority of β-glucuronidase activity. In strain AH1, pAH2 produced lower activity in the absence of inducer than did pAH2 in strain SM101 (compare Fig. 2.3D to Fig. 2.3A).

Also, we tried substituting a 10 mM concentration of the gratuitous inducer isopropyl β-D-1-thiogalactopyranoside (IPTG) in place of lactose as an inducer of P_{bgaL}, but did not observe an increase in activity (data not shown), suggesting either IPTG is not an inducer or is not transported into the cell.

Expression from *bgaR*-P_{bgaL} begins 5-10 min after addition of inducer. To determine the kinetics of induction of the *bgaR*-P_{bgaL} construct, we added 1 mM lactose to two strains, AH1(pAH2) and SM101(pAH2) in mid-log phase and measured the induction of activity over time Fig. 2.4. The β-glucuronidase activity began to increase between 5 and 10 minutes after the addition of lactose and reached maximum levels between 1–2 hours after lactose was added Fig. 2.4.

Glucose has no significant effects on induction from *bgaR*-P_{bgaL}. We performed all our assays in PY, a low carbohydrate media, as carbohydrate-inducible promoters in *E. coli* have exhibited repression in the presence of glucose [52]. To determine if glucose has an effect on *bgaR*-P_{BgaL} expression, we tested the effects of adding 10 or 110 mM glucose (the amount present in PGY media [58] to strains AH1(pAH2) and SM101(pAH2). Neither 110 mM glucose nor 10 mM glucose had a significant effect on *bgaR*-P_{BgaL} expression (data not shown).

***bgaR* is the activator responsible for the lactose-induced activity.** It was possible that the results described above could be due to the activity of a transcriptional regulator other than BgaR on the *bgaL* promoter. To ensure that BgaR was the protein responsible for regulating the *bgaL* promoter, we introduced a mutation into the chromosomal copy of the *bgaR* gene (see Materials and Methods) to create strain AH2 . We then individually transformed pAH2 and pAH1 into this strain. Plasmid pAH1 has the same overall structure as pAH2, but the *bgaR* gene contains a frameshift mutation at residue 119 (out of 279) that leads to a prematurely terminated protein

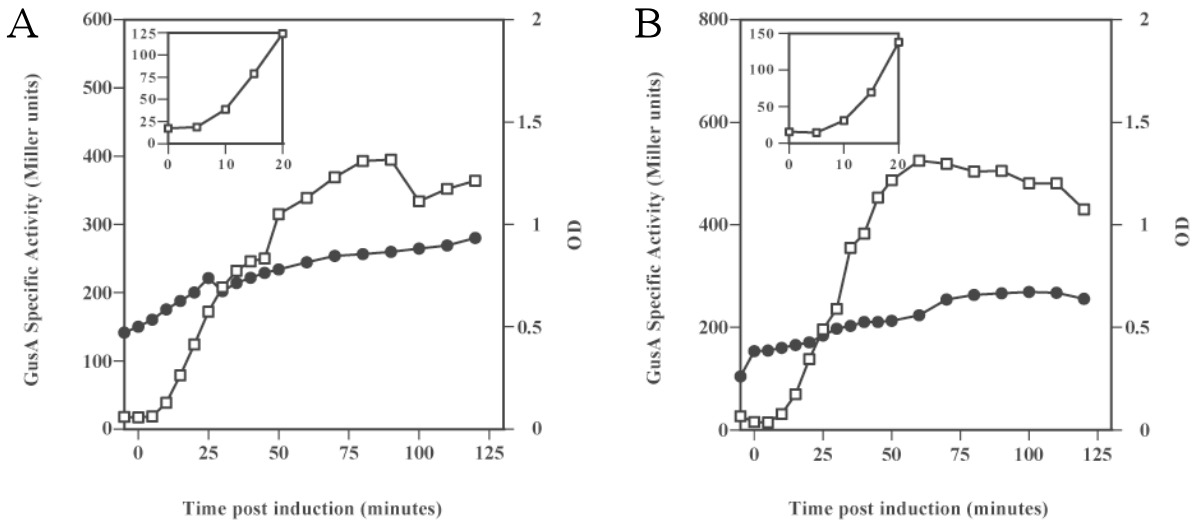

Figure 2.4: Timed induction of β-glucuronidase activity at 1 mM lactose in *C. perfringens*. Induction of β-glucuronidase activity (squares) at 1 mM lactose with strain AH1 (*bglR* mutant) (A) and SM101 (B) containing pAH2. OD (optical density at 600 nm) is shown as filled circles. Each chart shows a representative sample from two independent trials. The insets show an enlarged image of the first 20 min after induction.

of 133 residues in length that is inactive. The β-glucuronidase expression in strain AH2(pAH2) upon addition of lactose was similar to that seen with strain 13(pAH1) (Fig. 2.5). However, strain AH2(pAH1), which lacks any wild-type copy of the *bgaR* gene, showed a complete lack of induction in the presence of lactose, indicating BgaR is responsible for lactose-mediated induction. Since the absence of BgaR leads to loss of induction (Fig. 2.5), it is likely that BgaR functions as a transcriptional activator and not a repressor in response to lactose.

The *bgaR* mutant strain was examined to see if the mutation affected the total amount of the β-galactosidase activity, measured by hydrolysis of ONPG, in the cell. The level of β-galactosidase activity was relatively low in the wild-type strain (10-14 Units) and showed limited induction in the presence of lactose (Fig. 2.6). However, there was a significantly reduced level of enzyme activity in the *bgaR* mutant strain at each concentration of lactose except 0.1 mM and the limited amount of lactose-dependent induction was lost (Fig. 2.6). Because the activity of ONPG hydrolysis was relatively low, we performed a control where the *E. coli lacZ* gene, encoding β-galactosidase, under the control of the *cpe* gene promoter from strain SM101, was placed on a plasmid which was transformed into strain 13. This strain exhibited a significant increase in ONPG hydrolysis (data not shown), indicating there were no limitations to measuring ONPG hydrolysis in our assays.

Replacement of the *cpe-gusA* reporter with a multiple cloning site allows controlled expression of desired proteins. After determining that pAH2 works well for controlled induction, we replaced the *cpe-gusA* gene fusion with a multiple cloning site containing restriction enzyme recognition sites that are rarely found in *C. perfringens*. The resulting plasmid, pKRAH1 (Fig. 2.2), allows lactose-induced controlled expression of any gene desired.

YFP-PilB localizes in *C. perfringens* strain 13, but not in a *pilC* mutant strain. We previously showed that TFP have a role in *C. perfringens* gliding motility [27]. One of the gene clusters involved in TFP motility was an operon containing the genes *pilB*, *pilC*, *CPE1842*, and *CPE1841*. The *pilB* gene product is likely an ATPase responsible for assembly and extension of type IV pili (TFP) [27]. The *pilC* gene product is a membrane protein that we showed was necessary to

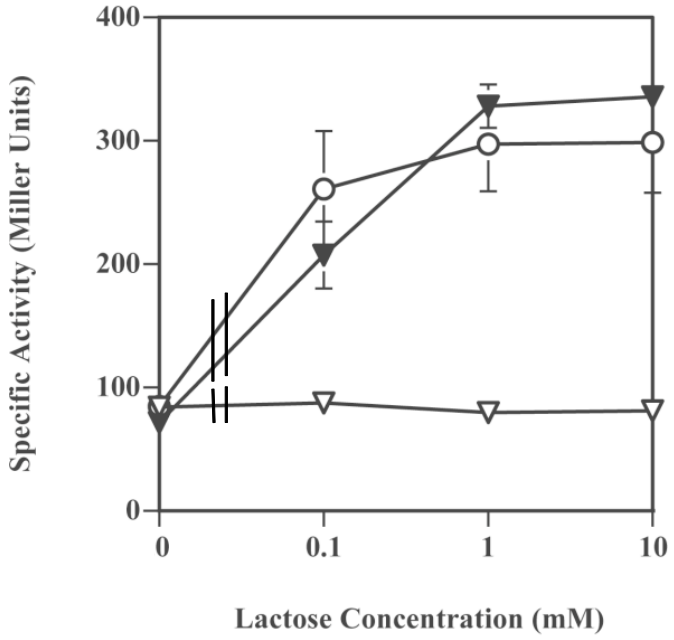

Figure 2.5: β-Glucuronidase activity in *bgaR*-mutated strains in response to lactose concentration. Strain AH2 (open symbols) with pAH1 (triangles) and pAH2 (circles). For comparison, strain 13 with pAH1 (same data as that shown in Fig. 2.3) is shown in filled triangles.

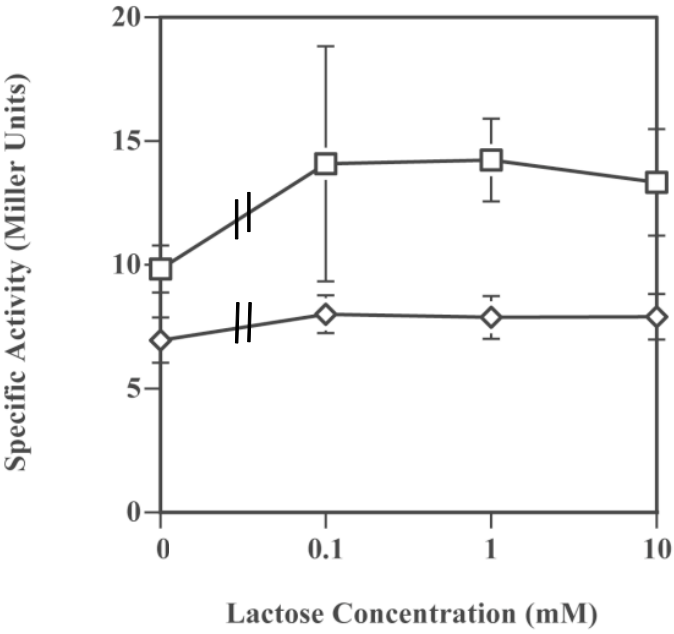

Figure 2.6: β-Galactosidase activity in response to lactose concentration. Strain 13 (squares) and strain AH2 (*bgaR* mutant) (diamonds).

TFP gliding motility in *C. perfringens* by mutagenesis of the gene [27]. PilC homologues have been shown to aid in localization of PilB to the poles of cells in Gram-negative bacteria with TFP, including *Pseudomonas aeruginosa* [33]. To determine whether PilC acted the same in Gram-positive *C. perfringens*, we inserted genes encoding TFP and a YFP-PilB fusion protein, in which YFP was attached to the N-terminus of PilB, into pKRAH1. In media without lactose, there was no visible fluorescence (data not shown). While expression of the *yfp* gene led to diffusion of the YFP protein throughout the cytoplasm of the bacteria (Fig. 2.7A), the YFP-PilB protein localized to the pole in 73% of fluorescent foci (Fig. 2.7B and C). In strain SM126, the previously constructed nonmotile *pilC* mutant derived from strain 13 [27], the fluorescence was still punctate, but only 42% was on cell poles, and those instances were less intense then the polar fluorescence in strain 13. (Fig. 2.7D) These results suggest that the PilC protein is at least partly responsible for polar localization of PilB in *C. perfringens*.

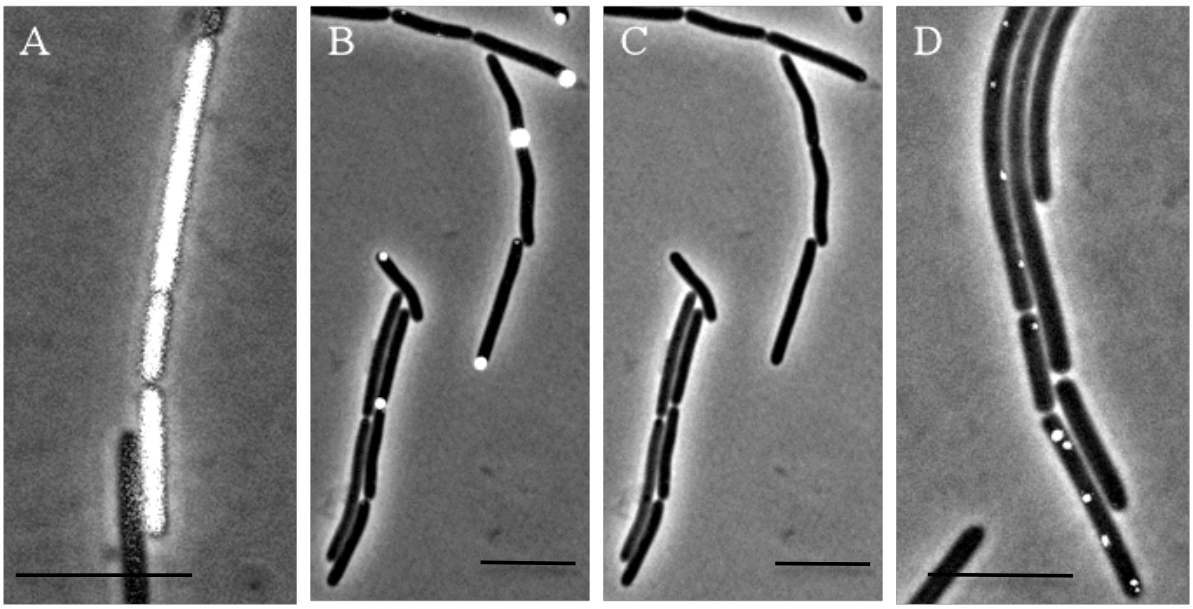

Figure 2.7: Cellular localization of the YFP-PilB fusion protein. Strains were grown on agarose pads with BHI and 0.1 mM lactose before images of cells were collected with phase-contrast microscopy and fluorescence microscopy (where indicated). (A) Strain 13 with pKRAH-Y, showing YFP fluorescence (white coloration in cells) distributed evenly throughout the cell. (B) Strain 13 with pKRAH-YB, in which the fluorescence (white spots) is distributed mostly to the poles. (C) Same image as that in panel B, but with phase contrast only to distinguish the location of cell poles. (D) Strain SM126, a *pilC* mutant derived from strain 13, with pKRAH-YB. Fluorescence intensity levels were adjusted to the same minimum and maximum levels for the images in panels B and D so they could be directly compared to each other.

DISCUSSION

Two gaps in the genetic tools available for *C. perfringens* were the absence of a vector in which promoters from genes of interest could be studied in the native *C. perfringens* host and a readily usable vector for highly controlled gene expression. Plasmid pSM240, which fulfills the first criterion, was briefly described previously, where it was used to analyze the expression patterns of promoters from the *sigK* and *spoIIGA* genes from strain SM101 [55], but a detailed description of its utility was not provided. Because it has a polylinker between a region containing four tandem terminators and the *cpe-gusA* reporter gene fusion (Fig. 2.2), it can be used to study the regulation of almost any promoter found in *C. perfringens*. The effectiveness of the terminators can be seen in Fig. 2.3A,B, and D, where the strains containing pSM240 show almost no additional β-glucuronidase activity over that of the wild-type strain lacking any plasmids. The *cpe-gusA* reporter in pSM240 is more useful in a *C. perfringens* strain 13 background if the *bglR* mutant strain, AH1, is used as the host. Since the endogenous β-glucuronidase activity was reduced from ~70 U to ~8 U in strain AH1, it will make possible the analysis of all but weak promoters.

We used a regulator of a putative β-galactosidase-encoding gene and its adjacent promoter as the basis for constructing a vector to fulfill the second need for highly controlled gene expression. We deliberately searched for sugar metabolism genes with a divergent regulator and promoter because this orientation is more likely to avoid read-through transcription from an upstream gene in the same orientation. This has been clearly demonstrated with the pBAD family of expression vectors developed by Guzman and co-workers [52]. In the case of the pBAD plasmids, the promoter could be repressed by the addition of glucose to the medium, giving a larger range of regulation [52], but the *bgaR*-P_{bgaL} in pAH2 could not. Although this may limit the range of transcriptional regulation, it can also be viewed as a positive feature since *C. perfringens* can be grown in rich medium with high levels of glucose without repression, which would be valuable for obtaining high levels of synthesis of a target protein for purification or other uses.

The *bgaR*-P_{bgaL} construct in pAH2 was regulated efficiently by lactose in three different strains

of *C. perfringens* that have three different pathogenesis profiles, gas gangrene (strain 13), acute food poisoning in humans (strain SM101), and necrotic enteritis in chickens (strain JGS4143) (Fig. 2.3). Since the *gutA-bgaR-bgaL* operon was found in all sequenced strains of *C. perfringens*, with GutA being the putative lactose permease, it suggests that this construct can be utilized in virtually any strain in this species. Although not tested yet, *bgaR*-P_{bgaL} may also provide regulated expression in other *Clostridium* species as long as they can transport lactose into the cell.

Sequence alignment of the four potential β-galactosidase proteins in strain 13 reveals a remarkable degree of divergence in the sequences, since the pair with the highest level of similarity, BgaM and CPE1266, exhibit only 24.2% sequence identity (Table 2.1). A search for homologues of the four β-galactosidase enzymes indicates they are found in all strains of *C. perfringens* with sequenced genomes (data not shown). Distinguishing characteristics of the β-galactosidases are listed in Table 2.2. For still unknown reasons, it appears that *C. perfringens* has evolved multiple mechanisms for facilitating the metabolism of lactose. Despite having multiple putative β-galactosidase enzymes, we detected a relatively low level of enzyme activity (10-14U) in strain 13 using ONPG as the substrate and this activity was only slightly affected by the presence of lactose (Fig. 2.6). Loss of *bgaR* function resulted in decreased activity, but 60% of the activity remained (Fig. 2.6). Since we have observed an 80-fold induction of the *bgaL* promoter by adding lactose (Fig. 2.3), it seems likely that the BgaL enzyme does not hydrolyze ONPG as a primary enzymatic activity.

Kobayashi et al suggested CPE0166 (ORF54) was a lactose transporter, likely a permease [64]. The *gutA* gene product, the putative lactose permease divergent to the *bgaR* gene (Fig. 2.1A) has little sequence similarity with CPE0166, and was likely given the *gutA* designation because it shows similarity to glucuronide transport proteins [4]. No obvious transporter was found nearby either the *bgaM* gene or *cpe1266*, the other two putative β-galactosidases in strain 13 (data not shown).

Another useful outcome of this study was the confirmation of the gene assignment that *bglR* encoded a β-glucuronidase in strain 13. This was done by mutagenesis of the *bglR* gene and show-

Table 2.2: Characteristics of four putative β-galactosidases in *C. perfringens* strain 13.

β-Galactosidases	% sequence similarity to:				Other bacteria with homology	Distinguishing characteristic(s)
	BgaL (CPE0771)	BgaM (CPE0831)	Pbg (CPE0167)	CPE1266		
BgaL (CPE0771)		17.3	10.4	15	*Firmicutes*	Homologous proteins are often annotated as glycoside hydrolases
BgaM (CPE0831)	17.3		10.2	24.2	*Agrobacterium-Sinorhizobium* *Firmicutes*	None
Pbg (CPE0167)	10.4	10.2		10.2	*Firmicutes*	Transcription shown to be induced by lactose [64] and cleaved X-gal when cloned into an *E.coli* plasmid and activated by ONPG [65]
CPE1266	15	24.2	10.2		*Bifidobacterium* and pathogenic members of the *Firmicutes*	Potential secretion signal sequence at the N terminus; homologous proteins are surface anchored and contribute to avoidance of phagocytosis by inhibiting complement deposition on the surface of the bacterium [66]

ing the mutant had a significant decrease in β-glucuronidase activity (Fig. 2.3D). However, the method used for mutagenesis, insertion of a non-replicating plasmid by homologous recombination, is likely to have polar effects on downstream genes in the locus, so we cannot exclude the possibility that one of these gene is also responsible for this phenotype. The remaining 11% of β-glucuronidase activity in the *bglR* mutant strain may be due to residual activity from another β-glucuronidase enzyme that cannot be detected by sequence homology to known β-glucuronidases or non-specific activity of another hexuronidase. Strain SM101 lacks the *bglR* gene, yet has low but detectable β-glucuronidase activity of 4-8 U (Fig. 2.3A), suggesting other enzymes with this activity exist in *C. perfringens*.

To demonstrate the utility of the expression system we used a pKRAH1-based vector to express a gene encoding a YFP-PilB protein fusion and showed that polar localization of PilB is due, at least in part, to the membrane-bound protein PilC (Fig. 2.7) This is similar to results seen in the Gram-negative bacterium *P. aeruginosa* and suggests that PilC functions as the membrane-bound partner for the PilB protein in *C. perfringens*. Expression of heterologous proteins, including the green fluorescent protein (GFP) family, in *C. perfringens* should provide the means to make significant discoveries related to gene and protein functions in this bacterium.

ACKNOWLEDGMENTS

We thank Katherine Rodgers for assistance in constructing plasmid pKRAH1 and Stephen Leppla for plasmid pSW4-YFP.

This work was supported by USDAA/NRICGP grant 2007=01543 and NIH grant 1R21AI088298-01 to S.B.M.

Chapter 3

The Expression, Location, and Function of Four Type IV Pilins of *Clostridium perfringens*

Andrea H. Hartman, Brittany A. Gianetti, Stephen B. Melville

CO-AUTHORS' CONTRIBUTIONS

Brittany Gianetti performed half of the microscopy and analysis, as well as conducting attachment and clumping assays. Stephen Melville was the principal investigator and revised the manuscript.

ABSTRACT

Clostridium perfringens, a Gram-positive pathogen, has four proteins homologous to pilins associated with Type IV pili or Type II secretion systems in Gram-negative bacteria. Localization and expression of each of these pilins was analyzed using immunofluorescence and western blots, respectively. PilA1 was not visible on the outside of the cell or expressed from the parent strain at levels discernible on a western blot. PilA2 localized to the poles of the cells. It was expressed from its native promoter during cell growth on plates, and appeared post-translationally modified. PilA3 and PilA4 localized to the poles also, but both were expressed at levels so low in the parent strain that they were undetectable on western blots. We mutated each of the genes coding for PilA1, PilA2, and PilA3, and we tested the mutants for various phenotypes including colony morphology, motility, secreted proteins, and clumping, to determine what role each pilin played in *C. perfringens*' pathogenesis. PilA3 was necessary for the secretion of a von Willebrand factor A domain-containing protein and contributed to keeping the cells suspended in culture. We have not yet found any significant differences between the other mutants and the parent strain, although we still need to confirm a stable, in-frame PilA4 mutant and carry out optimized attachment and DNA uptake assays with all the strains.

INTRODUCTION

Type IV pili (TFP) are retractable multimeric filaments commonly found in Gram-negative bacteria. They play roles in gliding or twitching motility [20, 21], host cell attachment in an infection [18], biofilm formation [24], and DNA uptake [19], among other functions. Varga et al. previously showed that *C. perfringens*, a Gram-positive, anaerobic pathogen, possessed genes for TFP [27]. *C. perfringens* also demonstrated a spreading colony formation on agar plates, and had a microscopic gliding motility defined by curvilinear social flares [27], two characteristics commonly correlated with TFP in Gram-negative bacteria.

Type II secretion systems (TTSS) are systems by which the cell secretes folded proteins, often virulence factors, outside of the cell [36, 37] . These proteins frequently look similar to TFP proteins, and contain many of the same core components [30]. *C. perfringens* was previously shown to possess multiple genes for these core components, including more than two genes with homology to pilins, two with homology to extension ATPases, and two with homology to PilC, the inner membrane platform protein [27]. Type II secretion systems have yet to be discovered in a Gram-positive bacteria, however.

To determine whether some of the core components were involved in TTSS and to identify what function(s) the TFP in *C. perfringens* possessed, we constructed insertion mutations and in-frame deletion mutations of *pilA1*, *pilA2*, and *pilA3* genes in *C. perfringens* strain 13 and examined the mutants for phenotypes associated with TFP and TTSS. This included colony morphology, social gliding motility, cell-cell attachment in cell culture media, and the presence of proteins secreted into liquid media. Biofilm assays, DNA uptake assays, and attachment to C2C12 mouse myoblasts (a cell type which a gas gangrene strain has affinity for in an actual infection) are other tests where the mutants could potentially reveal a phenotype.

METHODS

Bacterial strains and growth conditions. Bacterial strains, plasmids, and primers used in this study are listed in Table 3.1. *E. coli* was grown in Luria Bertani (LB) medium supplemented with antibiotics as needed (400 μg/mL erythromycin, 100 μg/mL ampicillin, or 20 μg/mL chloramphenicol) and 1.5% agar (Difco) for plates. *C. perfringens* was grown in a Coy anaerobic chamber in brain heart infusion (BHI) media (Difco) or on BHI plates with appropriate antibiotics as indicated (30 μg/mL erythromycin or 20 μg/mL chloramphenicol).

Construction of plasmids. To express the pilin proteins in *C. perfringens* using a regulated promoter, we amplified the genes of interest from strain 13 by PCR using Phusion polymerase (New England Biolabs) or Velocity polymerase (Bioline). Adenine residues were added to the ends of the PCR product using Taq polymerase (NEB) and the PCR product was ligated to pGEM-T Easy (Promega). Two restriction enzymes were used to remove the fragments containing the genes from pGEM-T Easy and ligate them to pKRAH1 [67] digested with the same two enzymes. This placed each gene under control of a lactose-inducible promoter in pKRAH1. We confirmed each clone was correct using PCR and DNA sequencing.

To construct the plasmids used to make the insertion mutants, we followed the above procedures, PCR-amplifying an internal fragment of the gene of interest, and inserting the final product into pSM300 [57]. Primers OAH103-OAH110 were used (Table 3.1).

To construct the plasmids used to make the in-frame deletion mutants, we used overlapping PCR [68] to amplify and join upstream and downstream regions flanking the gene and then proceeded with the above protocol for cloning into pGEM-T Easy and transferring the amplified DNA into its final vector, in this case pCM-galK [69]. Primers OAH129-OAH144 and OAH169-170 were used (Table 3.1).

Transformation of plasmids. Plasmids were introduced into *E. coli* and *C. perfringens* by electroporation as previously described [53, 67]. We typically made and screened the plasmids in *E. coli*

Table 3.1: Strains, plasmids, and primers used in this study.

Strain, plasmid or primer	Description, relevant phenotype or genotype, or sequence (5' to 3')	Source or Restriction site	Gene location
E. coli			
DH10B	F-*mcrA* Δ(*mrr-hsdRMSmcrBC*) F80d *lacZ* Δ*M15 lacX74 deoR recA1araD139* D (*ara, leu*)7697 *galU galK* Δ-*rpsL endA1 nupG*	Gibco/BRL	
C. perfringens			
13	Gangrene strain	C. Duncan	
HN13	*galK/galT* mutant derived from strain 13	[69]	
SM126	*pilC* mutant derived from strain 13	[27]	
AH4	*pilA1*-:Erm^R, from strain 13	this study	
AH5	*pilA2*-:Erm^R, from strain 13	this study	
AH6	*pilA3*-:Erm^R, from strain 13	this study	
AH7	Δ*pilA1*, from *HN13*	this study	
AH8	Δ*pilA2*, from *HN13*	this study	
AH9	Δ*pilA3*, from *HN13*	this study	
Plasmids			
pGEM-T Easy	Ampicillin resistance	Promega	
pKRAH1	Contains lactose-inducible promoter and polylinker; chloramphenicol resistance	[67]	
pCM-galK	Cm^R plasmid used for making in-frame deletions in *C. perfringens*	[69]	
pSM300	Suicide plasmid in *C. perfringens*; erythromycin resistance	[57]	
pAH12	contains a fragment of strain 13 *pilA1* in pGEM-T Easy	this study	
pAH13	contains a fragment of strain 13 *pilA1* in pSM300	this study	
pAH14	contains a fragment of strain 13 *pilA2* in pGEM-T Easy	this study	
pAH15	contains a fragment of strain 13 *pilA2* in pSM300	this study	
pAH16	contains a fragment of strain 13 *pilA3* in pGEM-T Easy	this study	
pAH17	contains a fragment of strain 13 *pilA3* in pSM300	this study	

Table 3.1: (continued)

Strain, plasmid or primer	Description, relevant phenotype or genotype, or sequence (5' to 3')	Source or Restriction site	Gene location
pAH18	contains a fragment of strain 13 *pilA4* in pGEM-T Easy	this study	
pAH19	contains a fragment of strain 13 *pilA4* in pSM300	this study	
pAH20	contains fragments around strain 13 *pilA1*in pGEM-T Easy	this study	
pAH21	contains fragments around strain 13 *pilA1* in pCM-galK	this study	
pAH22	contains fragments around strain 13 *pilA2* in pGEM-T Easy	this study	
pAH23	contains fragments around strain 13 *pilA2* in pCM-galK	this study	
pAH24	contains fragments around strain 13 *pilA3* in pGEM-T Easy	this study	
pAH25	contains fragments around strain 13 *pilA3* in pCM-galK	this study	
pAH26	contains fragments around strain 13 *pilA4* in pGEM-T Easy	this study	
pAH27	contains fragments around strain 13 *pilA4* in pCM-galK	this study	
A1-pKRAH	contains wildtype PilA1 in pKRAH1	this study	
A2-pKRAH	contains wildtype PilA2 in pKRAH1	this study	
A3-pKRAH	contains wildtype PilA3 in pKRAH1	this study	
A4-pKRAH	contains wildtype PilA4 in pKRAH1	this study	
Primers			
OAH11	GGCGATAAGTCGTGTCTTACCG		from within pSM300
OAH19	GTCGACTTAAAAAATATAAAAGGAGGACCATAAATG	SalI	*pilA1* RBS
OAH20	GGATCCTTAACAACAACCAGGACAACATACTATAGACACC GTAACTTTTCTTCCATTTTC	BamHI	reverse for *pilA1-Flash* (used for screening)
OAH21	GTCGACCATATTATTTTAAGGAGGAAAACCAATG	SalI	*pilA2* RBS
OAH22	GGATCCTTAACAACAACCAGGACAACATTGATTATTTCTT TCATTAGTTACTGATGCTG	BamHI	reverse for *pilA2-Flash* (used for screening)
OAH23	GTCGACCTATTAAGAGAAAGATGGTGATTAAATG	SalI	*pilA3* RBS
OAH24	GGATCCTTAACAACAACCAGGACAACATTTTTTATTTCTA AAAGTTAATATATTACTAACCTC	BamHI	reverse for *pilA3-Flash* (used for screening)
OAH53	GACAACTGGGAAAAACTGTGTTATTATAAATAC		forward for promoter of *pilA* region

Table 3.1: (continued)

Strain, plasmid or primer	Description, relevant phenotype or genotype, or sequence (5' to 3')	Source or Restriction site	Gene location
OAH93	CCGCGGTTTTAGTACCTACCTTTGAGGAGGAGAAATATG	SacII	*pilA4* RBS
OAH103	GGTACCCAAGTGCAATATGTGGAAAAGGAAATG	KpnI	*pilA1* internal
OAH104	GAGCTCCCATTACTTGAAGTTATTTTTATATTTGTAACAC TAC	SacI	*pilA1* reverse internal
OAH105	GGTACCGGGTTCACGCTAATTGAATTAATTATCGTTATAG C	KpnI	*pilA2* internal
OAH106	GAGCTCGCCTGAAACTTCTACTGCAAATACAC	SacI	*pilA2* reverse internal
OAH107	GGTACCGAATTAGTTGTAGCACTATCATTAATAACAATC	KpnI	*pilA3* internal
OAH108	GAGCTCCTTCATTTTCTAACCTAAAAGTAGTTTTTATATT ATTATC	SacI	*pilA3* reverse internal
OAH109	GGTACCCCCTTAGCGAAGTAATAATATACCTGG	KpnI	pilA4 internal
OAH110	GAGCTCCTTACTTTAACTGCATTTAACCTCAAAGAAG	SacI	*pilA4* reverse internal
OAH114	CCGCGGTTAATAAATATGCTTTTCTTTTTCTTTTTGCGGT TG	SacII	reverse *cpe1841* end
OAH121	GGATCCCTATTGATTATTTCTTTCATTAGTTACTGATGCT GA	BamHI	reverse *pilA2* end
OAH126	GGATCCGTATATTTATACTATAGACACCGTAACTTTTCTT CC	BamHI	reverse *pilA1* end
OAH127	GGATCCAACCCATCTTTTATTTTTTATTTCTAAAAG	BamHI	reverse *pilA3* end
OAH128	GAGCTCATAAATCACTTAACATTAATTTTCCATATGCC	SacI	reverse *pilA4* end
OAH129	GTCGACGTGATGCAGGTGTAGGATTTGATGC	SalI	Forward N-flanking of *pilA1*
OAH130	GTATATTTATACTATAGACACCGTAACTTTTCTTCCTGCT TTCAGTAATAACATTTATGGTCCTCC		Reverse N-flanking of *pilA1* with start of C-flanking
OAH131	GGAGGACCATAAATGTTATTACTGAAAGCAGGAAGAAAAG TTACGGTGTCTATAGTATAAATATAC		End of N-flanking with forward C-flanking of *pilA1*
OAH132	GGATCCGCTAATACTGCTATTATTCCACCAATAATAAATG	BamHI	Reverse C-flanking of *pilA1*
OAH133	GTCGACCAAACTTACTTACTAGCATGATTGATG	SalI	Forward N-flanking of *pilA2*

Table 3.1: (continued)

Strain, plasmid or primer	Description, relevant phenotype or genotype, or sequence (5' to 3')	Source or Restriction site	Gene location
OAH134	GATTATTTCTTTCATTAGTTACTGATGCGTTTTGTTTTTT TGTATTCATTGGTTTTCC		Reverse N-flanking of *pilA2* with start of C-flanking
OAH135	GGAAAACCAATGAATACAAAAAAACAAAACGCATCAGTAA CTAATGAAAGAAATAATC		End of N-flanking with forward C-flanking of *pilA2*
OAH136	GGATCCCACCAGATTTTGTAGTTTTTATAAGTATTAAC	BamHI	Reverse C-flanking of *pilA2*
OAH137	GTCGACCAAAAGATTTAGGCAATGGATCAAGTTTAG	SalI	Forward N-flanking of *pilA3*
OAH140	GGATCCGGCAAATGGTTAACATCGTAAGATCTAAATG	BamHI	Reverse C-flanking of *pilA3*
OAH141	GTCGACACTGTAAAAGATAAGAAATACAAAGAATCCC	SalI	Forward N-flanking of *pilA4*
OAH142	CCTCATAAATCACTTAACATTAATTTTCCATATGCCTCTT TTACTATACATATTTCATGCCCTCAAAGG		Reverse N-flanking of *pilA4* with start of C-flanking
OAH143	CCTTTGAGGGCATGAAATATGTATAGTAAAAGAGGCATAT GGAAAATTAATGTTAAGTGATTTATGAGG		End of N-flanking with forward C-flanking of *pilA4*
OAH144	GGATCCATAACAATAAATCCTTTCTTCTTGATTTTTAACC	BamHI	Reverse C-flanking of *pilA4*
OAH153	GTATTTAATATCTCTTTTAAGCATATTTAGCC		sequencing for pCM-galK forward
OAH154	CCCGAAAAGCAACACAACCAAG		sequencing for pCM-galK reverse
OAH165	GGAAATCCAGATTCTACTTACTTATTAGTG		forward for screening $\Delta PilA3$
OAH166	CATAAGTTACACTAACCTCTTCTCC		reverse for screening $\Delta PilA3$
OAH169	CACCTCCAACCCATCTTTTATTTTTTATTTCTATTTTTCA TTTAATCACCATCTTTCTC		Reverse N-flanking of *pilA3* with start of C-flanking
OAH170	GAGAAAGATGGTGATTAAATGAAAAATAGAAATAAAAAAT AAAAGATGGGTTGGAGGTG		End of N-flanking with forward C-flanking of *pilA3*
OKR32	GACACATTGCCTCCCAAATCATCCAA		reverse outside of *pilA1*
OKR37	GCAGATTTTTATGATGATGAACTAGAAAGAGAAATAC		Forward upstream of *pilA2*
OKR40	CAGAAGTGCTGTTTGTAGTAAAAATTACATTATC		Reverse downstream of *pilA2*

before transforming them into *C. perfringens*, but when making the plasmids expressing wildtpe PilA1, PilA3, and PilA4, we introduced the ligated plasmid directly into *C. perfringens* as the expressed protein appeared to be toxic to *E. coli*.

Construction of mutants. To construct the insertion mutants, suicide plasmids made with pSM300 were transformed into *C. perfringens* strain 13 and selected for erythromycin resistance. To confirm, a competition PCR was done with primers to each end of the gene, and primer to a site internal to the backbone of the suicide plasmid. The mutant band was the result of a segment amplifying from the plasmid through to one end of the gene, and the wildtype band was the result of the segment between both ends of the gene being amplified (data not shown).

The in-frame mutants were constructed according to the protocol by Nariya et al [69] with the following modification: we used chloramphenicol at 20 μg/ml. All the mutants were confirmed by PCR using primers from outside the gene to screen across the gene, so the mutant band is approximately the wildtype band length minus the length in base pairs of the gene of interest (data not shown).

Immunofluorescence. Immunofluorescence microscopy was done according to the protocol described previously [27]. Antibodies against PilA1 and PilA2 were obtained from Affinity Bioreagents. Yenzymes produced antibodies against PilA3 and PilA4. To do this, short peptides (one per pilin) that were predicted from structural models to be on the surface of the folded pilins were synthesized. Each of these peptides was injected into a rabbit for antibody production.

In order to view different fluorescent antibodies against PilA2 and PilA3 simultaneously, we labeled the cells with an antibody against PilA3 followed by a fluorescently-labeled secondary antibody as previously described [27]. After washing twice in 2.5 percent BSA (Bovine Serum Albumin) in DPBS (Dulbecco's phosphate- buffered saline without calcium and magnesium), we suspended the cells in 2.5 % BSA/DPBS with a 1:100 dilution of a FITC-labeled primary rabbit antibody against PilA2 and incubated at 37°C for 30 minutes. We then finished with the previously described protocol [27]. Additionally, controls were done to confirm that fluorescence from one

channel did not overlap wavelengths enough to appear as fluorescence from our second channel.

Membrane preparations, SDS-PAGE, and western blots. In order to prepare the cell membranes for western blots, we followed the following protocol: we either scraped the cells off an agar plate and resuspended in 1 ml resuspension buffer (20 mM $NaPO_4$ with 300 mM NaCl), or we centrifuged 1 ml of the liquid culture and resuspended in 1 ml resuspension buffer. We then added 1 μg lysozyme, and incubated at 37°C for 1 hour. We sonicated this solution until cell lysis was complete, then centrifuged on a tabletop centrifuge to pellet the cell crud. The supernatant was removed and centrifuged at 100,000 x g for 1 hour, and the resulting pellet resuspended in TRIS-Cl (pH 6.8).

Protein concentrations were determined using the BCA protein assay (Pierce) according to the manufacturer's instructions. The samples were boiled for 15 minutes with 4x SDS buffer (200 mM Tris-Cl [pH 6.8], 400 mM DTT, 8 % SDS, 0.4 % bromophenol blue, and 40 % glycerol) to result in a SDS buffer concentration of 1x. Amounts of the preparations corresponding to 20 μg protein were run on SDS-PAGE gels prepared using Thermo Scientific's EZ-Run solutions.

SDS-PAGE gels viewed for the secretome assay were stained with Ruby Sypro stain (Lonza) according to the manufacturer's instructions.

For Western blots, proteins were transferred from the gel onto the membrane according to the manufacturer's (Bio-Rad's) instructions. The membranes were then blocked with 5 % BSA in 1x TBST (Tris- buffered saline with Tween) from Santa Cruz Biotechnology for 2 hours, and then antibody serum was added at a ratio of 1:200. This was incubated at room temperature overnight on a shaker. The membrane was then washed 5 times for 5 minutes each with 1x TBST, before being incubated in a 1:15,000 ratio of Dylight 594-tagged goat-anti-rabbit antibody from Thermo Scientific with 5% BSA in TBST. The 5 washes were repeated as previously, and the membranes were then viewed on a Typhoon Fluorescent Scanner.

Data analysis of fluorescent microscopy. Wherever specific percentages are mentioned, the foci were analyzed according to human visualization and counting. For the analysis of PilA4 im-

munofluorescence, histograms were constructed using Matlab-based software programs MicrobeTracker and SpotFinderZ [70].

Video microscopy. Cells were viewed on an Olympus IX71 microscope using the Applied Precision SoftWorx program. BHI pads with 2% agarose on slides were made as previously described [59]. The slides were placed in an anaerobic chamber and cells from plates grown overnight streaked on them. After the cells grew at 37°C for two hours, coverslips were placed on the pads and sealed with nail polish while still inside the chamber. These sealed pads were placed in a heating chamber surrounding the microscope, the chamber being set to 37°C.

Clumping assays. Bacterial colonies were scraped off an agar plate, washed and resuspended in DPBS, and subcultured 1:250 into warm, anaerobic, heat-inactivated DMEM (Dulbecco's Modified Eagle Medium), with 4.5 g/l glucose and 10% fetal bovine serum, filter sterilized, in 50 ml culture flasks. They were incubated 3-5 hours anaerobically and viewed on an Olympus IX81 upright microscope linked to a Hamamatsu Model C4742 CCD camera.

Aggregation assays. Cultures were grown overnight. One milliliter was then removed from the top of the liquid and the OD_{600} measured as a control for growth, and the remainder of the cultures were centrifuged at 1046 x g for 4 minutes. One milliliter was removed from the top of the culture supernatant, and the OD_{600} was measured on a spectrophotometer.

Protein secretion profiles. The secreted proteins were prepared according to the protocol by Nariya et al [69], with the modification of adding 100 µl 10x aqueous solution of Complete Mini protease inhibitors (Roche) to 900 µl culture supernatant before filtering.

Viscosity test In order to measure the viscosity of overnight cultures, 300 µl of each culture was tested on the High Shear CAP-2000+ Viscometer from Brookfield Engineering Laboratories, Inc., a rotational viscometer. Biological duplicates were tested for each sample, and uninoculated BHI media was used as a control.

RESULTS

Structural analysis of Cpe2278 and Cpe1842. We previously showed that PilA2 had homology to major pilins from *P. aeruginosa* and *N. gonorrhoeae* [27], while PilA1 had homology to the PulG pseudopilin from *Klebsiella oxytoca* [27]. Later we discovered that genes *cpe2278* and *cpe1842* also coded for proteins with homology to pilins. The gene *cpe1842* is in an operon downstream of *pilB1* and *pilC1*, and *cpe2278* is downstream of *pilB2*, *pilC2*, *pilA2*, and *pilM*, *pilN*, and *pilO* [27].

We analyzed Cpe2278 and Cpe1842 by using the Fugue protein prediction program [71]. This program compares the sequence-predicted secondary and tertiary folds with other structures in the HOMSTRAD (Homologous Structural Alignment Database), which contains structures from the Protein Data Bank [71]. Cpe2278 had homology with 99% certainty to PulG from *Klebsiella pneumonia*, PilE from *N. meningitidis*, and pilins from *N. gonorrhoeae* and *P. aeruginosa*. Although PulG is a pseudopilin, we believe Cpe2278 is more similar to the major pilins, in part due to its larger size. Cpe1842 had homology with 50% certainty to pilins from *N. gonorrhoeae* and *P. aeruginosa*. Fugue used the crystal structures of the homologous proteins listed above as a template to create structural models of these proteins, and, using the program PyMOL, we displayed these structural models. In Fig. 3.1, the predicted model of Cpe2278 against the structure of PilE is shown (Fig. 3.1A) along with the predicted structure of Cpe1842 against the pilins from *N. gonorrhoeae* and *P. aeruginosa* (Fig. 3.1B). The structures of the proposed homologues of the latter are shown in our previous paper [27]. We propose renaming *cpe2278* as *pilA3* and *cpe1842* as *pilA4*.

Immunofluorescence on PilA2 and PilA3. We performed immunofluorescence (IF) microscopy on motile strain 13 cells, using the control serum as our negative control. The control serum was bled from the rabbit prior to antigen exposure. PilA2 was on one pole 23.5% of the time, both poles 4.8% of the time, and on neither pole 71.8% (n=1986). PilA3 was on one pole 24% of the time, both poles 8.8% of the time, and neither pole 67.1% (n=1243). Less than 1% of either group was in the center or between pole and center, and PilA2 and PilA3 co-localized in 89.6 (n=96) percent of cells with fluorescence (Fig. 3.2). Co-localization in a cell was defined as each

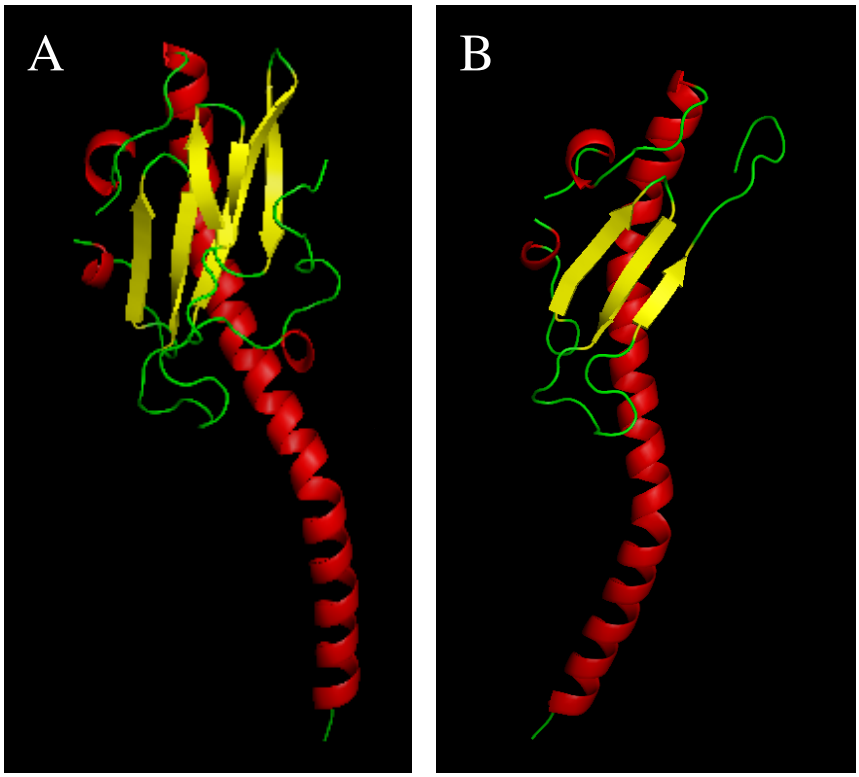

Figure 3.1: Structural models of Cpe2278 and Cpe1842. (A) Predicted 3-dimensional structure of the *C. perfringens* PilA3 protein from strain 13, based on PilE from *N. meningitidis*, assembled using the FUGUE structural comparison program. (B) Predicted 3-dimensional structure of PilA4 from strain 13, based on the pilins from *N. gonorrhoeae* and *P. aeruginosa*, assembled using FUGUE. All images created from the respective pdb files using the program PyMOL.

of that cell's foci in one fluorescent channel having a corresponding foci in the other fluorescent channel. Immunofluorescence using the control serum instead of the antiserum gave significantly lower signal.

Immunofluorescence on PilA1 and PilA4. Since PilA2 and PilA3 co-localized, we tested them in conjunction with PilA1. We had previously described PilA1 as appearing all over the cell [27], but we subsequently discovered that the cells had native green fluorescence at the same wavelength as our green fluorescent antibody. When the experiment was repeated with red antibodies, neither the control serum nor the antiserum yielded any signal (Fig. 3.3A-B). We treated the cells briefly (10 minutes at room temperature) with 1 mg/ml lysozyme before proceeding with the IF protocol. While this did result in signal from the antiserum, the control serum also yielded a signal not significantly different from the antiserum (Fig. 3.3C-D).

PilA4 yielded significantly higher fluorescence upon treatment with the antiserum compared with the control (Fig. 3.4A-B). We used the Matlab-based programs MicrobeTracker and SpotFinderZ to analyze the fluorescence on the cells treated with antiserum compared to the fluorescence on the cells treated with the control. While those treated with the control failed to show any particular localization, those treated with the antiserum had a higher percentage of fluorescence on the poles of the cell (Fig. 3.4C-D).

Colony morphology of insertion mutants. We constructed individual mutants of *pilA1* (strain AH4), *pilA2* (strain AH5), and *pilA3* (strain AH6) by inserting a suicide plasmid into each gene, but saw that the mutant strains appeared the same as the wildtype when grown on BHI agar plates (data not shown). The mutant strains were also examined by video microscopy for changes in their social gliding motility but displayed no obvious differences (data not shown). As these mutants were made by inserting a plasmid into the gene, we expected AH6 (the *pilA3* mutant) to be polar on the gene downstream of it. We expect AH4 and AH5, the *pilA1* and *pilA2* mutants, to be mutated in genes which are expected to be the last in an operon [27], although they may have unforeseen polarity. We were unable to construct an insertion mutant of PilA4. No further testing was done

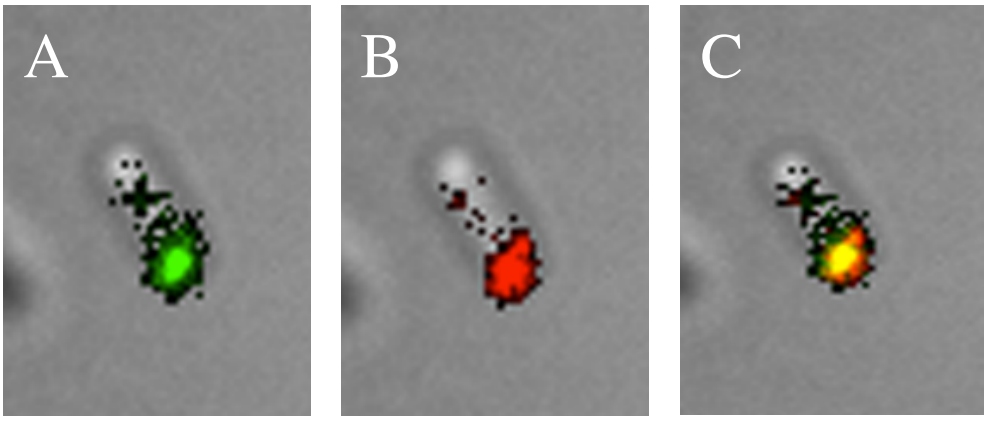

Figure 3.2: Immunofluorescence against PilA2 and PilA3 in strain 13. (A) FITC-labeled PilA3. (B) TRITC-labeled PilA2. (C) Both proteins shown together.

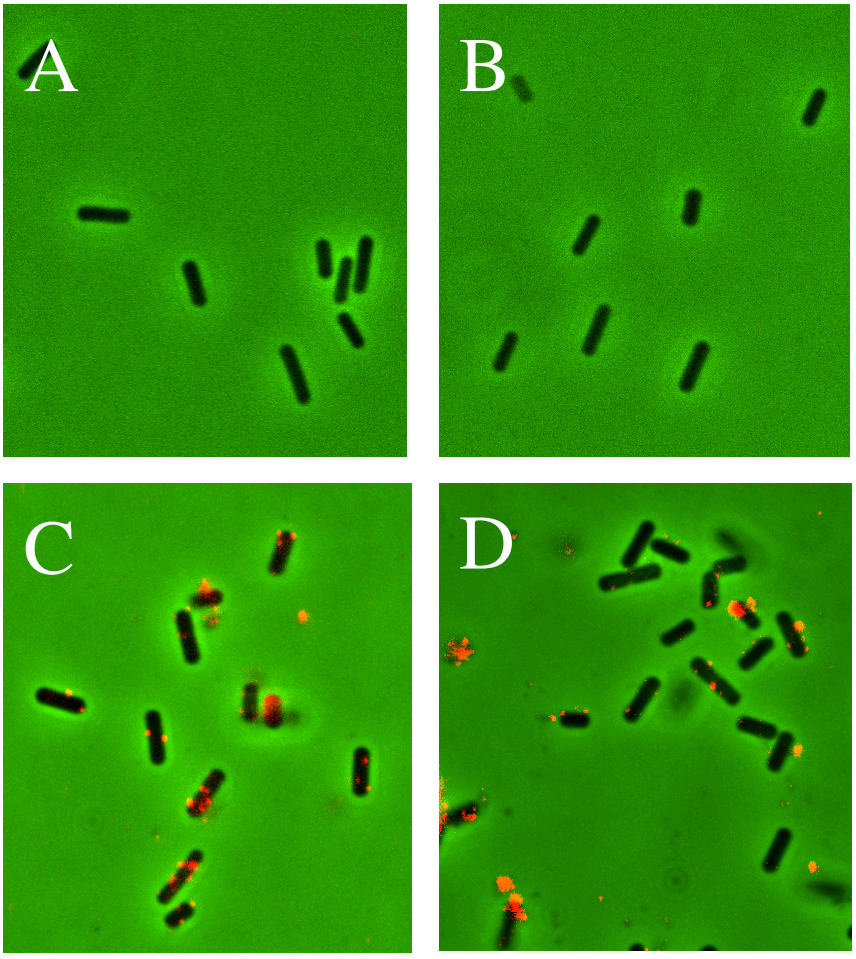

Figure 3.3: Immunofluorescence on PilA1. (A) Strain 13, treated with TRITC-labeled antibodies against control serum corresponding to PilA1. (B) Strain 13, treated with TRITC-labeled antiserum against PilA1. (C) Lysozyme-treated cells with control serum corresponding to anti-PilA1 antibodies. (D) Lysozyme-treated cells with antiserum against PilA1.

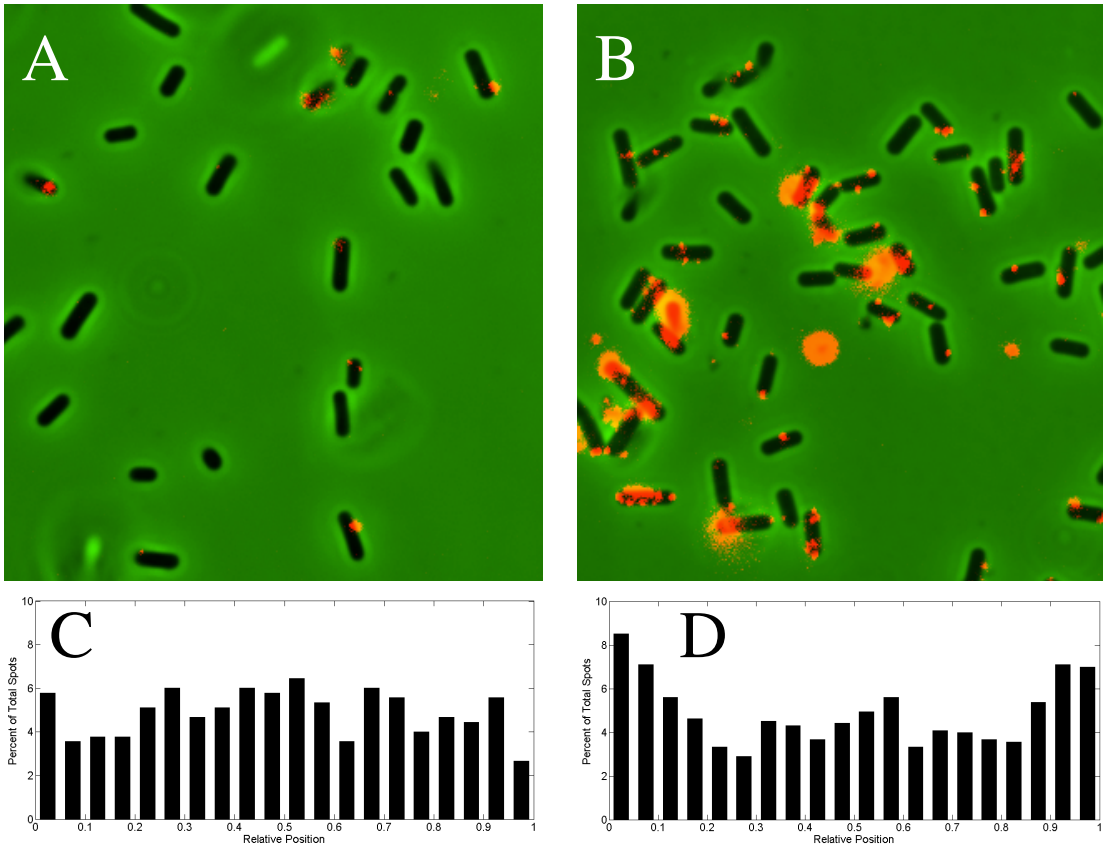

Figure 3.4: Immunofluorescence on PilA4. (A) Strain 13 cells with control serum corresponding to anti-PilA4 antibodies. (B) Cells with PilA4 antiserum. (C) Spot position histogram of strain 13 treated with PilA4 control serum. (D) Spot position histogram of strain 13 treated with PilA4 antiserum.

on these mutants as we gained the ability to construct in-frame mutants.

Western analysis of pilin mutants. We constructed an in-frame deletion mutation in *pilA1* (strain AH7), and we complemented it with plasmid A1-pKRAH. We then harvested strain HN13 and strain AH7 from growth on plates, growth in liquid at logarithmic phase, and growth in liquid at stationary phase, and did membrane preparations. We harvested the complemented mutant in liquid at logarithmic phase, and did a membrane preparation on those cells as well. When we viewed each of these samples on a western blot against PilA1 (Fig. 3.5A), we were able to see, in lane 6, the expressed complemented version at the predicted size of the processed protein (14.9 kDa unprocessed, 12.6 kDa processed). This is indicated with a white arrow. We could not detect any bands demonstrating protein in the wildtype or mutant strains. These results confirm that the antibodies to PilA1 work, but under these conditions, PilA1 appears not to be expressed or expressed at very low concentrations. We had previously determined that the pilins were most concentrated in the membrane preparation as opposed to preparations of the whole cell lysate or the supernatant (data not shown), hence why these are not mentioned.

We constructed plasmid A2-pKRAH with the wildtype *pilA2* gene behind an inducible promoter, using pKRAH1 as the backbone. When we performed a western blot on the membrane preparations from wildtype cells and HN13/A2-pKRAH cells grown under different conditions, the wildtype strain did not express the protein in noticeable quantities when grown in liquid, whether in logarithmic or stationary phase, but did express the protein in two different sizes when grown on agar plates. These bands are indicated with white arrows in lane 2 of (Fig. 3.5B). The bands appeared the expected sizes of 18.14 kDa and 19.56 kDa for processed and unprocessed pilin, respectively. However, as membrane proteins frequently do not run true to size, we find it more likely that these are both processed pilins, one having a post-translational modification. The reason we think this is because PilA2 induced from the plasmid ran as 4 bands, rather than two. These are indicated with gray arrows in lanes 3 and 5 of (Fig. 3.5B). The extra two bands are 4 and 5 kDa larger than the native pilin, at 22 and 25 kDa. We think these extra bands are unprocessed pilin modified and unmodified, as it is likely that PilD, the peptidase, was unable to process all

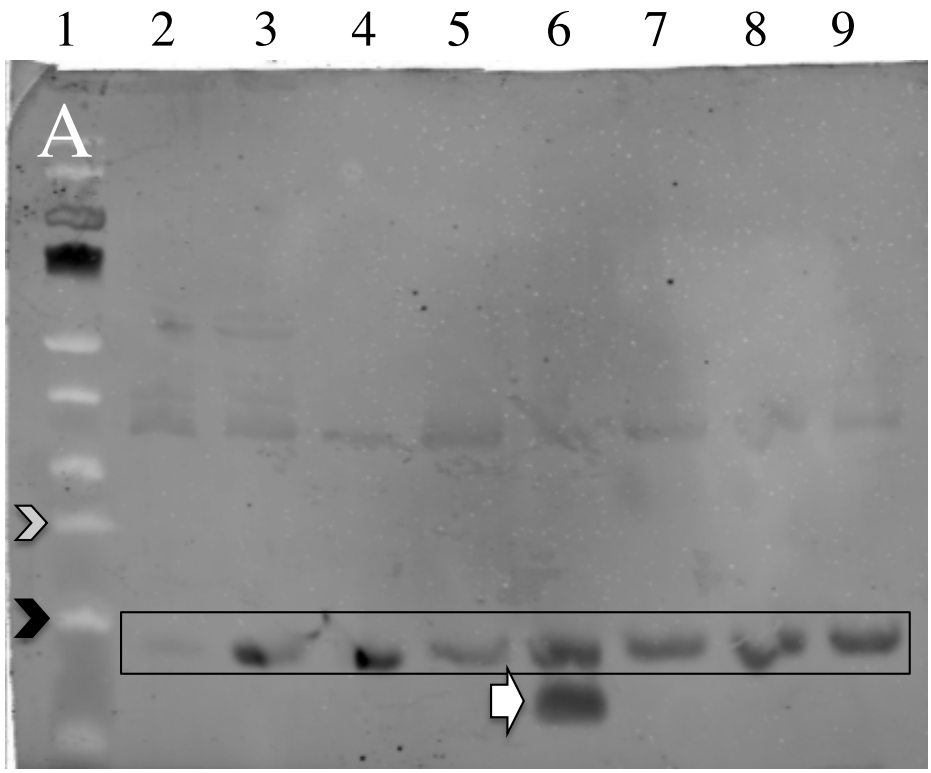

Figure 3.5: Western analysis of PilA1. On each western blot in lane 1, the Easy Run Protein ladder was used. The 26 kDa molecular weight (mw) marker is indicated with a gray chevron; the 17 kDa mw marker is indicated with a black chevron; and fluorescence from lysozyme (~14.7 kDa) is indicated by a box around it. This was from the preparation process, and is to be ignored. (A) Western against PilA1. Lane 2 is HN13 grown on plates. Lane 3 is AH7 (Δ*pilA1*) grown on plates. Lane 4 is HN13 grown in liquid at logarithmic phase. Lane 5 is AH7 grown in liquid at logarithmic phase. Lane 6 is AH7/A1-pKRAH induced. A white arrow indicates PilA1 in this lane. Lane 7 is HN13 from an overnight culture, and lanes 8 and 9 are AH7 from an overnight culture.

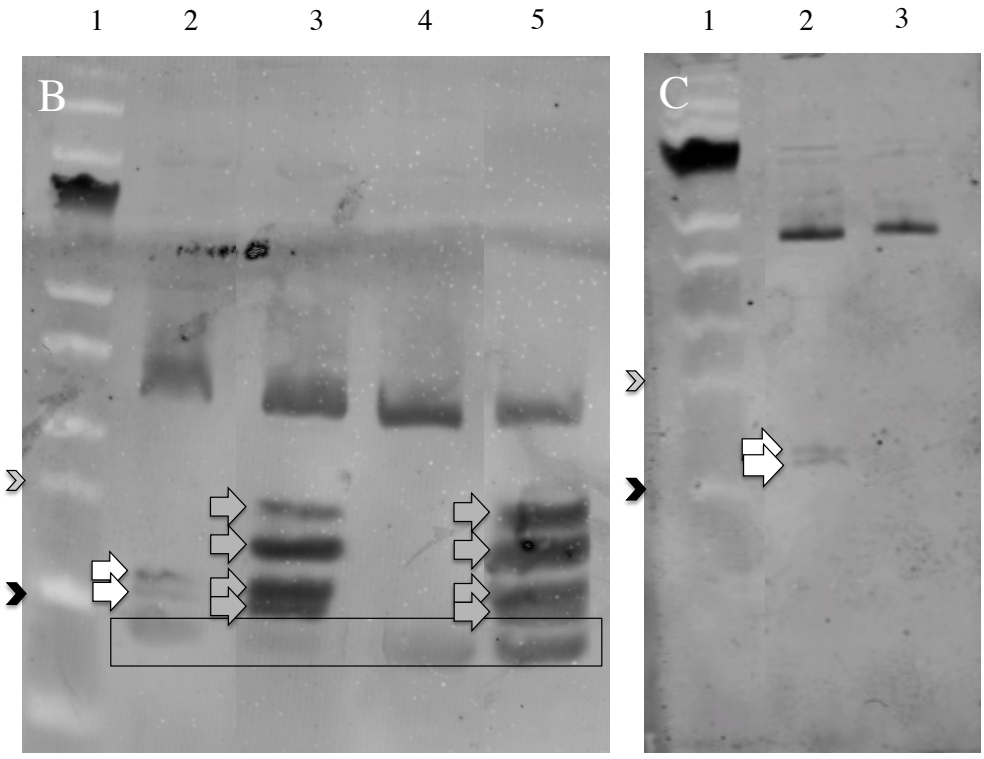

Figure 3.5: (continued) Western analysis of PilA2. (B) Western blot against PilA2. Lane 2 shows HN13 grown on plates. Lane 3 shows HN13/A2-pKRAH induced, grown on plates. Lane 4 shows HN13 grown in liquid at logarithmic phase. Lane 5 shows HN13/A2-pKRAH induced, grown in liquid at logarithmic phase. (C) Western blot against PilA2. Lane 2 shows HN13 grown on plates. Lane 3 shows the AH8 (Δ*pilA2*) grown on plates. White arrows are indicating PilA2 bands in the wildtype strain. Light gray arrows are indicating lactose-induced PilA2 bands.

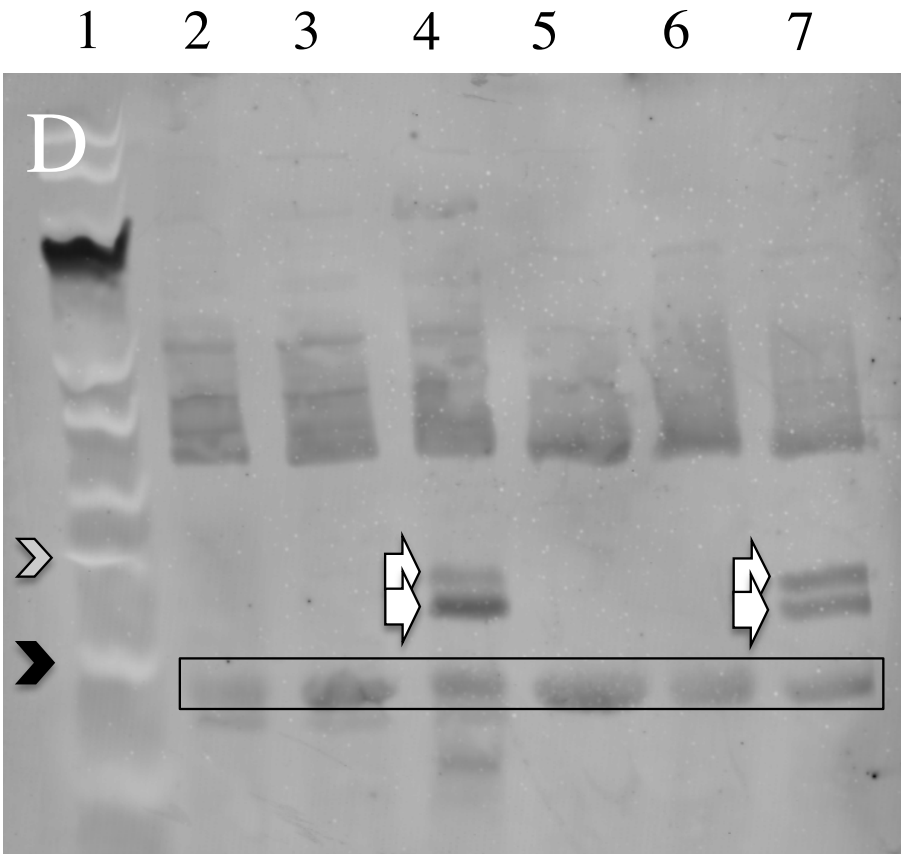

Figure 3.5: (continued) Western analysis of PilA3. (D) Western blot against PilA3. Lane 2 shows HN13 grown on plates. Lane 3 shows AH9 (Δ*pilA3*) grown on plates. Lane 4 shows AH9/A3-pKRAH induced, grown on plates. Lane 5 shows HN13 grown in liquid at logarithmic phase. Lane 6 shows AH9 grown in liquid at logarithmic phase. Lane 7 shows AH9/A3-pKRAH induced, grown in liquid at logarithmic phase. White arrows are pointing out PilA3 bands.

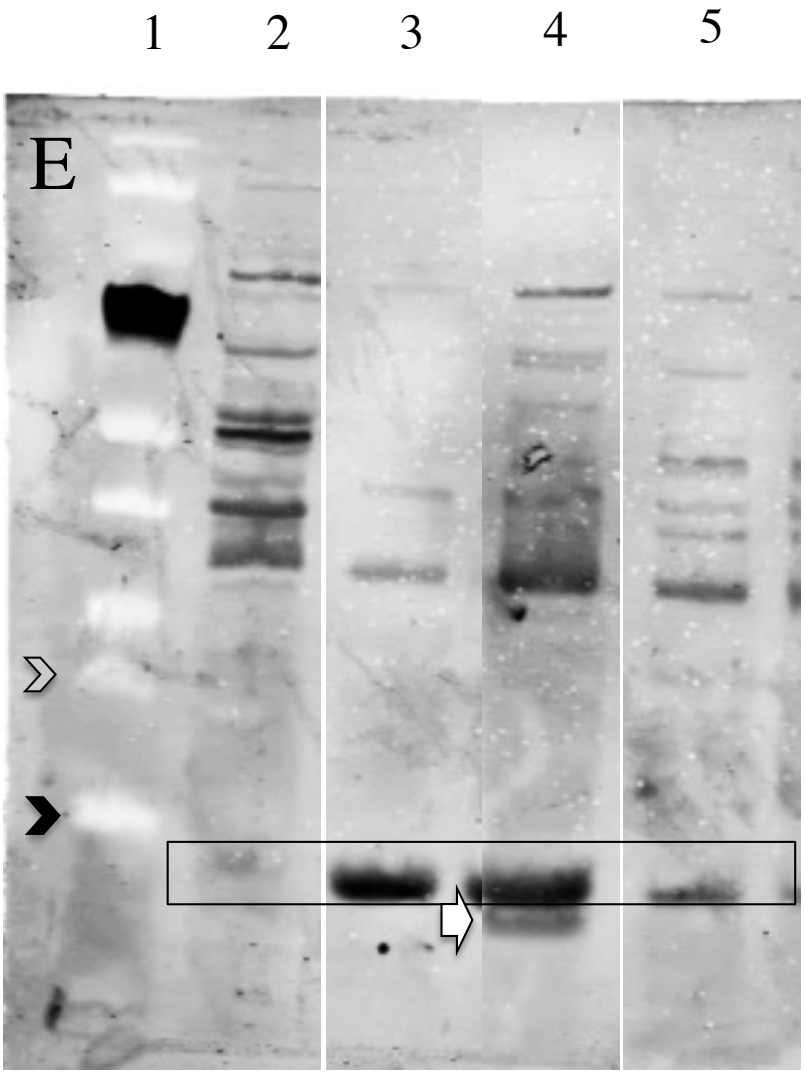

Figure 3.5: (continued) Western analysis of PilA4. (E) Western blot against PilA4. Lane 2: from HN13 grown on plates. Lane 3: from HN13 grown in liquid at logarithmic phase. Lane 4: from HN13/A4-pKRAH induced. Lane 5: from HN13 from an overnight culture. The white arrow is pointing out the PilA4 band.

the artificially expressed PilA2. We have not, as of yet, determined the modifications. Later, we constructed an in-frame deletion mutation in *pilA2* (strain AH8) and confirmed by western blot (Fig. 3.5C).

We were able to construct an in-frame deletion mutation in *pilA3* (Strain AH9) and complement it with plasmid A3-pKRAH. When we viewed a western blot of PilA3 in wildtype, mutant, and complement, it was only visible in the complemented strain at the expected unprocessed size of 21.26 kDa and processed size of 20.03 kDa. These bands are indicated with white arrows in (Fig. 3.5D). We made western blots of preparations from plates, liquid at logarithmic phase, and liquid at stationary phase, but in none of them was wildtype PilA3 visible. Although PilA3 appears not to be expressed under these conditions, we believe it is expressed in very low concentrations, due to phenotypes possessed by the Δ*pilA3* mutant strain. The ribosome binding site (RBS) at the beginning of *pilA3* shows low similarity to the *C. perfringens* RBS consensus sequence, while the *pilA2* consensus sequence is nearly identical (AGGAGGA compared to AAGGAGGT). This is likely a reason PilA3 is expressed so much less than PilA2.

We performed a western blot against PilA4 from HN13 and HN13/A4-pKRAH. The band is not visible in preparations from HN13 grown on plates or in liquid at logarithmic phase, but is present in the lane containing the preparation from HN13/A4-pKRAH. It is indicated with a white arrow in (Fig. 3.5E). Although we expect the protein to be in processed (15.36 kDa) and unprocessed portions (16.2 kDa), there is only one apparent band. This may be because the bands are so close together they are indistinguishable, or because the majority is the same conformation. We have not yet confirmed an in-frame deletion mutant of *pilA4*, but based on the results from immunofluorescence microscopy we believe PilA4 to be expressed at very low concentrations, similar to PilA3.

Secretome analysis of the PilA mutants. Because TFP proteins bear similarity to TTSS proteins, we wanted to examine the proteins secreted by both strain HN13 and the strains in which the pilins had in-frame deletion mutations. When the secretome of the wildtype grown in BHI medium

was compared on an SDS-PAGE gel with that of the PilA1 and PilA3 deletion mutants grown in BHI medium, mutant strain AH7 (Δ*pilA1*) looked identical to the wildtype. However, one band was consistently missing in AH9 (Δ*pilA3*)(Fig. 3.6A). This area is indicated with a white arrow in each location it is missing. We cut that band out in the lane with proteins from the wildtype and the corresponding place in the lane with proteins from the mutant, and had them analyzed by mass spectrometry. The band in the wildtype lane was determined to be Cpe0517, a von Willebrand factor type A domain-containing protein. When plasmid A3-pKRAH was introduced into the *pilA3* deletion mutant, it complemented this phenotype, whether induced or uninduced (Fig. 3.6B). The promoter P_{bgaL} on plasmid pKRAH1 is a little leaky when uninduced [67], and apparently the amount of PilA3 necessary for the functioning phenotype is small.

When secretome profiles of strain AH8 (Δ*pilA2*) and HN13 grown in BHI were compared, AH8 appeared to have an additional band at 72 kDa compared to the wildtype (Fig. 3.7). Its absence is indicated with a white arrow. However, when these areas were analyzed by mass spectrometry, no differences in proteins could be determined.

Additional phenotypic testing of the PilA deletion mutants. We tested strains AH7 (Δ*pilA1*) and AH9 (Δ*pilA3*) for phenotypes in colony morphology, microscopic motility, clumping, host cell attachment, biofilm and capsule production, DNA uptake, and aggregation. In the aggregation assay, AH9 failed to remain suspended in the media, although we are unsure of the cause of this phenotype (Fig. 3.8). Measuring the viscosity of the cultures showed there to be no significant difference between AH9 culture and HN13, and prior to centrifugation, cells from each strain appeared the same under the microscope. Aggregation was restored to wildtype levels when the plasmid expressing the wildtype protein was introduced into the mutant strain, both when induced and uninduced with lactose. We were also unable to find any other significant differences between AH7 or AH9 compared with wildtype, although in the attachment and DNA uptake assays, we were unable to get a stable baseline from our wildtype strain, so these need to be repeated.

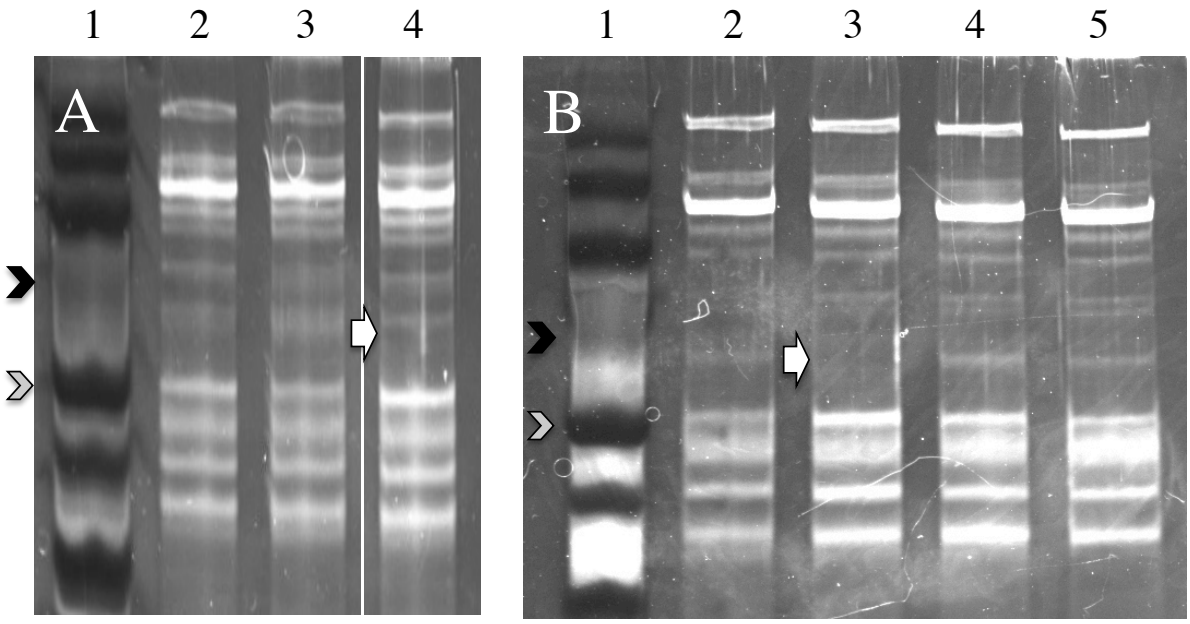

Figure 3.6: Secretome analysis of the PilA3 mutant. In each gel, the black chevron indicates the 72 kDa band, and the light gray chevron indicates the 55 kDa band. White arrows are indicating the absence of a band that is present in the wildtype. In both A and B, lane 1 shows the Easy Run protein ladder. (A) SDS-PAGE gel showing secretome profiles of HN13 (lane 2), AH7 (Δ*pilA1*) (lane 3), AH9 (Δ*pilA3*) (lane 4). (B) SDS-PAGE gel showing secretome profiles of HN13 (lane 2), AH9 (Δ*pilA3*) (lane 3), AH9/PilA3-pKRAH induced (lane 4), AH9/A3-pKRAH uninduced (lane 5).

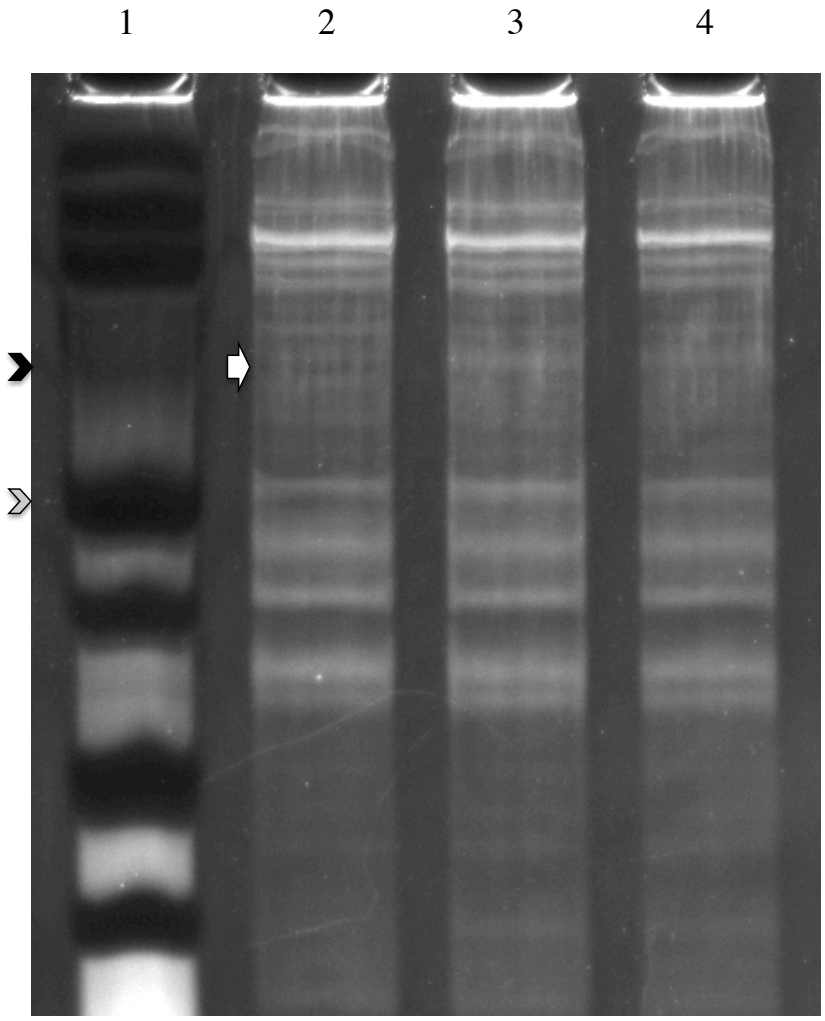

Figure 3.7: Secretome analysis of the PilA2 mutant. The black chevron indicates the 72 kDa band, and the light gray chevron indicates the 55 kDa band. A white arrow indicates the absence of a band that is present in the mutants. Lane 1 contains the Easy Run protein ladder. Lane 2 contains the secreted proteins from HN13. Lanes 3 and 4 contain secreted proteins from biological replicates of AH8 (Δ*pilA2*).

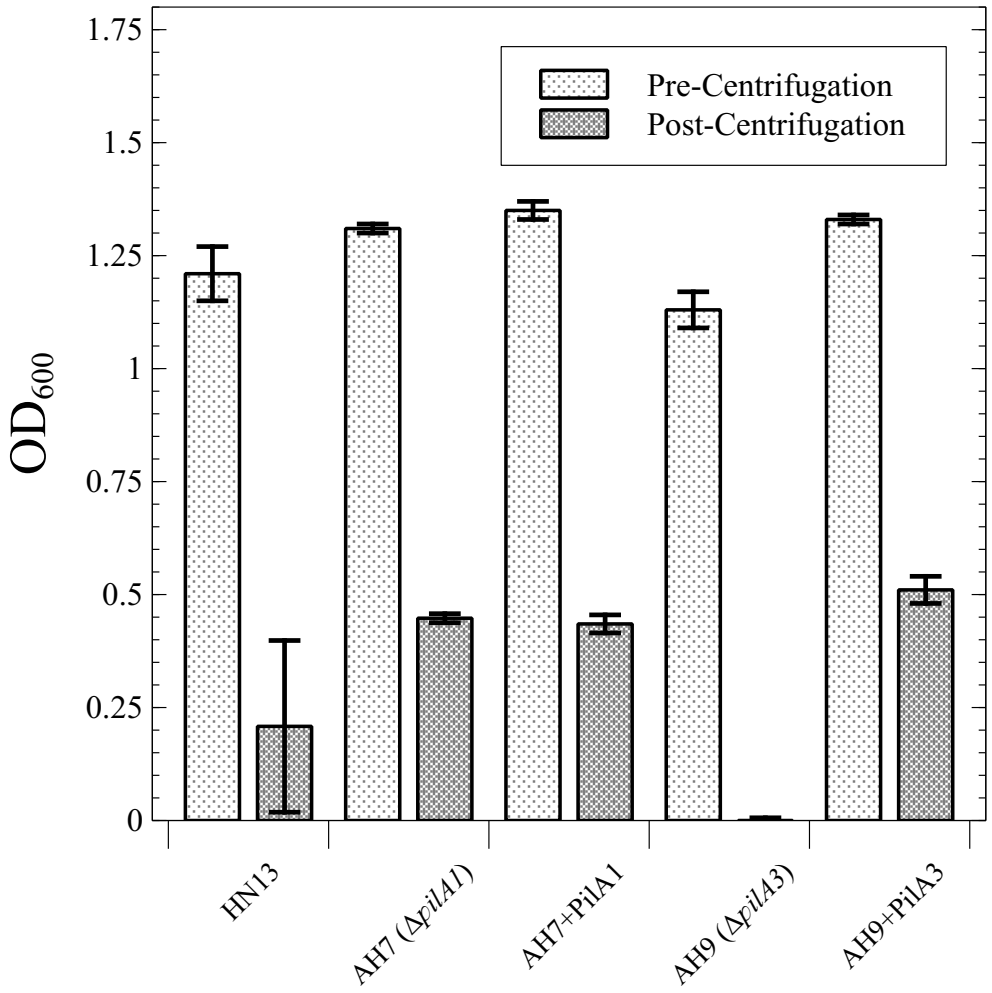

Figure 3.8: Results of aggregation assay. Each column is the average of three replicates. Error bars show the sample standard deviation.

DISCUSSION

The functions of the four pilin homologues in *C. perfringens* have been difficult to determine, due to difficulties making mutants, difficulties getting consistent data from our wildtype strain in a variety of tests, and lack of obvious phenotypes. In tests that would determine effects on the most suspected of TFP functions: host cell attachment and DNA uptake, we could not get our wildtype to yield consistent data, perhaps because expression of the TFP system was not consistently turned on in the wildtype. Strain AH9 (Δ*pilA3*) was the only mutant to yield consistent differences in any assay, and, unfortunately, we do not know what the function is of the Von Willebrand Factor A domain-containing protein. Nor do we know why the wildtype cells stay suspended in the aggregation assay, as both appearance of the cells and viscosity of the cultures had no significant differences (data not shown).

Previously, Rodgers et al. found that *N. gonorrhoeae* expressing *C. perfringens*' PilA2 changed its adherence from vulval cells to mouse muscle cells [72], but as we were not able to obtain a stable PilA2 mutant until later, we were not able to test strain AH8 (Δ*pilA2*) in many of the assays. Due to the difficulty making a mutant, the data by Rodgers et al, the location in the chromosome and the predicted structure of PilA2, we still suspect this to be the dominant Type IV pilin. We also suspect that attachment and uptake of DNA may be key functions, but we need to optimize these assays and get a consistent baseline from the wildtype strain.

ACKNOWLEDGMENTS

We would like to thank Sean Mury for his advice and technical help with the microscope, Dr. W. Keith Ray for analyzing our protein bands with a mass spectrometer, and Elizabeth Pickering for providing the MicrobeTracker/SpotFinderZ analysis.

Chapter 4

PilT is Critical for Localization of Other Type IV Pili ATPases in *Clostridium perfringens*

Andrea H. Hartman, Brittany A. Gianetti, Stephen B. Melville

CO-AUTHORS' CONTRIBUTIONS

Andrea Hartman conducted the research and drafted the manuscript. Brittany Gianetti did half of the microscopy and analysis. Stephen Melville was the principal investigator and revised the manuscript.

ABSTRACT

The Gram-positive anaerobic pathogen *Clostridium perfringens* possesses genes homologous to Type IV pili (TFP) and Type II Secretion System (TTSS) genes in Gram-negative bacteria [27]. We used variants of green fluorescent protein (GFP) to tag the ATPases involved in TFP assembly and retraction, and visualized their locations in cells, using both still shots and video. PilB1 and PilB2, ATPase extension motors, co-localized at the poles and what appear to be future division sites. PilT, an ATPase retraction motor, also localized to poles and division sites, but was sometimes independent of the PilB proteins, and was shown to move within a small area in the cell. We viewed PilB1 and PilB2 in an in-frame deletion PilT mutant. PilB1 failed to localize to the poles, but localization was restored when PilT was co-expressed with PilB1 in the mutant. We viewed *C. perfringens*' PilT in *Bacillus subtilis*, a species lacking any genes with homology to TFP, and PilT continued to localize and move in a similar pattern to that seen in *C. perfringens*. *C. perfringens*' PilT was expressed in *B. subtilis* strain AH93, which contains an inducible inhibitor of cell division protein FtsZ. PilT continued to localize to poles and sites of future division unless the function of FtsZ was inhibited 30 minutes before expression of PilT. When division in *C. perfringens* was inhibited by cephalexin, PilT localized to evenly spaced points throughout the cell. We believe PilT may be a protein responsible for mediating interactions between cell division or cytoskeletal proteins and the TFP assembly apparatus.

INTRODUCTION

Clostridium perfringens is a Gram-positive anaerobe able to cause a variety of diseases, including gas gangrene, food poisoning, necrotic enteritis, and intestinal diseases in livestock [2]. It possesses genes with homology to Type IV pili (TFP) and Type II Secretion System (TTSS) genes in Gram-negative bacteria [27]. TFP have been discovered in several Gram-negative species but only a few Gram-positive species, and TTSS have so far only been discovered in Gram-negative bacteria [73].

The model for the Type IV pilin assembly apparatus in *P. aeruginosa* includes PilA, the pilin, the leader sequence of which is cleaved by PilD, a peptidase [28]. The ATPase motor protein PilB is responsible, with PilC, for extending the pilus [32, 34], while PilT is the ATPase responsible for retracting the pilus [34]. *C. perfringens* has been found to have two PilB homologues, two PilC homologues, one PilD, one PilT and four PilA homologues [27]. It also has PilM, PilN, and PilO, structural proteins whose function remains unclear [30].

In several Gram-negative bacteria the pili mediate motility by extending a pilus to attach to a surface and then retracting to pull toward the point of attachment [21]. Several laboratories have viewed fluorescently-tagged PilB and PilT proteins while cells are moving to try to determine when extension and retraction of pili were occurring. PilT in *Myxococcus xanthus* has been documented switching from one end of the cell to the other in order to cause a reversal in direction [35]. PilT and PilB in *Pseudomonas aeruginosa* were documented as having bipolar localization [33].

C. perfringens demonstrates a motility that may be due in part to Type IV pili. The cells are unable to move on their own, as *M. xanthus* or *Neisseria gonorrhoeae* can, but they can extend away from the colony rapidly by maintaining a head-to-tail and side-to-side attachment in straight chains aiming away from the colony (Video 4.1).

As *C. perfringens* has two PilB homologues and only one PilT, we sought to determine the roles of PilB1, PilB2, and PilT in *C. perfringens* by labeling each of these proteins with fluorescent

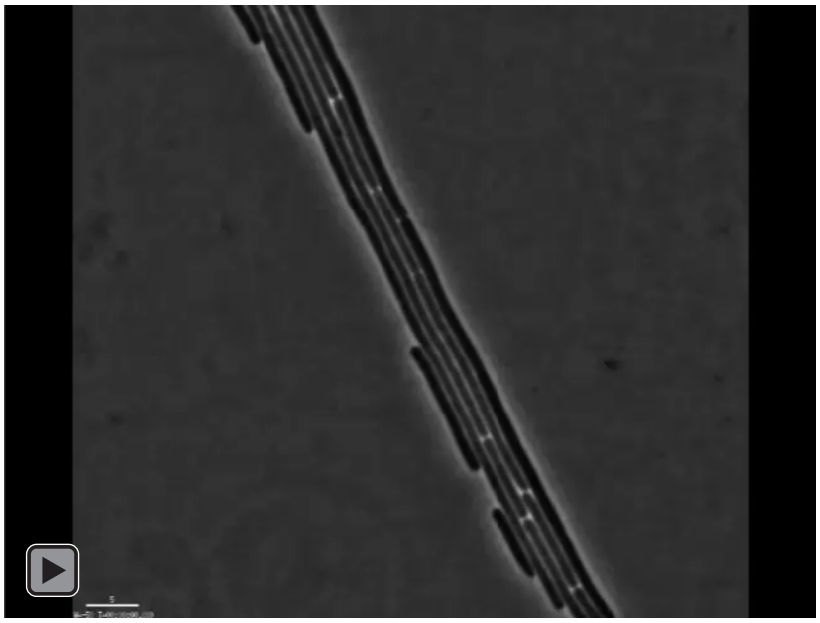

Video 4.1: Motile strain 13. *C. perfringens* strain 13 growing on BHI agarose pads under anaerobic conditions.

proteins and viewing them alone, in combinations, and in strains deficient in various TFP proteins.

METHODS

Bacterial strains and growth conditions. Bacterial strains, plasmids, and primers used in this study are listed in Table 2.1. *E. coli* and *B. subtilis* were grown in Luria Bertani (LB) medium supplemented with antibiotics as needed (400 μg/mL erythromycin, 100 μg/mL ampicillin, or 20 μg/mL chloramphenicol, 100 μg/mL spectinomycin) and agar for plates. *C. perfringens* was grown in a Coy anaerobic chamber in brain heart infusion (BHI) media (Difco) or on BHI plates with appropriate antibiotics as indicated (30 μg/mL erythromycin or 20 μg/mL chloramphenicol). All were grown at 37°C.

Construction of plasmids. To construct the tagged proteins for expression, we amplified the genes of interest from pSW4-YFP (yellow fluorescent protein), pSW4-CFP (cyan fluorescent protein), or *C. perfringens* strain 13 chromosomal DNA by PCR using Phusion polymerase (New England Biolabs). We then fused the two genes as previously described [68], positioning the fluorescent gene on the N-terminus of the ATPase gene. We included restriction sites in the primers. Adenine residues were added to the ends of the PCR product using Taq polymerase and the PCR product was ligated to pGEM-T Easy (Promega). We then used two restriction enzymes to remove the fragment containing the gene and ligated it to pKRAH1 [67], pCM-GalK [69] or pDR111 [74] digested with the same two enzymes. (pDR111 was a gift from Kumaran Ramamurthy at the NIH.)

Electroporation and transformation of plasmids. Electroporations into *E. coli*, and electroporation into *C. perfringens* were done as previously described [53, 67]. Transformation into *B. subtilis* was done as described [75].

Construction of mutants. In-frame deletion mutants in *C. perfringens* were made according to the protocol by Nariya et al [69].

Fluorescent microscopy. Cells were viewed on an Olympus IX71 microscope using Applied Precision SoftWorx program. We made BHI pads with 2% agarose on slides as previously described [59]. This media also contained 0.1 mM lactose, and 20 μg/mL chloramphenicol. We placed these

Table 4.1: Strains, plasmids, and primers used in this study.

Strain, plasmid or primer	Description, relevant phenotype or genotype, or sequence (5' to 3')	Source
[1em] *E. coli*		
DH10B	F-*mcrA* Δ*(mrrhsdRMSmcrBC)* F80d *lacZ* Δ*M15 lacX74 deoR recA1araD139* D (*ara, leu*)7697 *galU galK* Δ*rpsL endA1 nupG*	
C. perfringens		
13	Gangrene strain	
HN13	*galK*$^-$ *galT*$^-$ from strain 13	[69]
SM1300	Δ*pilT*, from strain HN13	This study
AH11	Δ*pil*B, from strain HN13	This study
AH12	Δ*pilB2*, from strain HN13	This study
AH13	Δ*pilB1/B2*, from strain HN13	This study
B. subtilis		
PS832		Popham lab
AH93	*amyE::Pxyl-mciZ cat*	[76]
Plasmids		
pGEM-T easy	Ampicillin resistance	Promega
pKRAH1	Contains *bgaR*-P$_{bgaL}$ and polylinker Chloramphenicol resistance	[67]
pKRAH-YB	pKRAH1 with the *yfp-pilB1* fusion gene	[67]
pKRAH-YB2	pKRAH1 with the *yfp-pilB2* fusion gene	This study
pKRAH-CBYB2	pKRAH1 with the *cfp-pilB1* and *yfp-pilB2* fusion gene	This study
pKRAH-CTYB	pKRAH1 with the *cfp-pilT* and *yfp-pilB1* fusion genes	This study
pKRAH-CTYB2	pKRAH1 with the *cfp-pilT* and *yfp-pilB2* fusion genes	This study
pCM-galK	Suicide plasmid for *C. perfringens*, chloramphenicol resistance	[69]
pDR111	Suicide plasmid for *B. subtilis*, ampicillin and spectinomycin resistance	K. Ramamurthy
pKRAH-YT	pKRAH1 with the *yfp-pilT* fusion gene	This study
pDR111-YT	pDR111 with the *yfp-pilT* fusion gene	This study
pKRAH-ACYT	pKRAH1 with the *ftsA-cfp* and *yfp-pilT* fusion genes	This study

Table 4.1: (continued)

Strain, plasmid or primer	Description, relevant phenotype or genotype, or sequence (5' to 3')	Source
pAH8	pGEM-T Easy with *yfp-pilB1*	This study
pAH9	pGEM-T Easy with *yfp-pilB2*	This study
pAH10	pGEM-T Easy with *cfp-pilB1*	This study
pAH11	pGEM-T Easy with *cfp-pilT*	This study
pAH12	pGEM-T Easy with *yfp-pilT*	This study
pAH13	pGEM-T Easy with *ftsA-cfp*	This study
pAH14	pGEM-T Easy with *yfp-pilT* for pDR111	This study
pAH15	pCM-galK with crossover fragments for making strain SM1300	This study
pAH16	pCM-galK with crossover fragments for making strain AH11	This study
pSW4-YFP	Contains *yfp* codon specific to low GC bacterial strains	[56]
pSW4-CFP	Contains *cfp* codon specific to low GC bacterial strains	[56]
pAH17	pGEM-T Easy with crossover fragments for making strain SM1300	This study
pAH18	pGEM-T Easy with crossover fragments for making strain AH11	This study
pAH19	pGEM-T Easy with crossover fragments for making strain AH12	This study
pAH20	pCM-galK with crossover fragments for making strain AH12	This study
Primers		
OAH14	CCGCGGTAAATAACAAAAAGGAGAACGCATAATGTCAAAAGGAG	*yfp* or *cfp* start with SacII
OAH36	CACACGGAATGGATGAATTATATAAGATGAAATATACCAT TAAAGATATAGATATGAAGC	*yfp* end with *pilB* start
OAH37	CTTCATATCTATATCTTTAATGGTATATTTCATCTTATAT AATTCATCCATTCCGTGTGTAATTCC	reverse complement of oAH36
OAH38	GAAGCGAGCTCTTTAAACCCAAACATCTAAC	*pilB* end with SacI
OAH39	CACACGGAATGGATGAATTATATAAGTTGATTAGTTATCA GAAAAAGCGTTTAGGAG	*yfp* end with *pilB2* start
OAH40	CTAAACGCTTTTTCTGATAACTAATCAACTTATATAATTC ATCCATTCCGTGTGTAATTCC	reverse complement of OAH39
OAH41	CTTTCGAGCTCTTACATATCATAAGTTATATTTAAC	*pilB2* end with SacI

Table 4.1: (continued)

Strain, plasmid or primer	Description, relevant phenotype or genotype, or sequence (5' to 3')	Source
OAH42	CACACGGAATGGATGAATTATATAAGATGCAAAGTTTAGC AGAACTTTTAGAG	forward *yfp* end with *pilT* start
OAH43	CTCTAAAAGTTCTGCTAAACTTTGCATCTTATATAATTCA TCCATTCCGTGTGTAATTCC	reverse complement of OAH42
OAH44	GAGCTCTATATTTAATACATCAATAATCGAC	reverse *pilT* end with SacI
OAH58	CCGCGGCTTTAAACCCAAACATCTAACCCC	reverse *pilB* end with SacII
OAH59	CACACGGAATGGATGAATTATATAAGGGAGGAGGAGGAGG AGGAATGAAATATACCATTAAAGATATAGATATGAAGC	forward *yfp* end with linker and *pilB* start (used for CB)
OAH60	CATATCTATATCTTTAATGGTATATTTCATTCCTCCTCCT CCTCCTCCCTTATATAATTCATCCATTCCGTGTGTAATTC	reverse complement of OAH59
OAH67	CTGCAGAATTTTTAGATAGGGAGGTACACATAGAAAAAATG	*ftsA* start and RBS with PstI
OAH68	GCGTTCTTAGAGGAGCTTTTTGGAGGAGGAATGTCAAAAG GAGAAGAATTATTTACAGGG	*ftsA* end and *cfp* start
OAH69	CCTGTAAATAATTCTTCTCCTTTTGACATTCCTCCTCCAA AAAGCTCCTCTAAGAACGCC	Reverse *ftsA* end and *cfp* start
OAH70	GCCGCGGTCTTACCCCCCGGGATC	*cfp* end with Sac II
OAH182	GTCGACAAAAAGGAGAACGCATAATGTCAAAAG	forward *yfp* with SalI
OAH183	GCATGCTCTATATTTAATACATCAATAATCGAC	reverse *pilT* with SphI
OBG1	CTGCAGTAAATAACAAAAAGGAGAACGCATAATGTCAAAAGGAG	forward *cfp* start with PstI
OBG2	CCGCGGTATTTAATACATCAATAATCGACTTAAAATC	Reverse *pilT* end with Sac II
OAH146	CAAATTACCTCTATATTTAATACATCAATAATCGTGCTAA ACTTTGCATAAATCTCCTCC	Reverse N-term of *pilT* with start of C-term
OAH147	GGAGGAGATTTATGCAAAGTTTAGCACGATTATTGATGTA TTAAATATAGAGGTAATTTG	End of N-term with forward C-term of *pilT*
OAH148	GAGCTCCATGAATTAAATAGGTATCCAATATGTGTTCCTC	Reverse C-term of *pilT* with SacI
OAH153	GTATTTAATATCTCTTTTAAGCATATTTAGCC	sequencing primer for pCM-galK forward

Table 4.1: (continued)

Strain, plasmid or primer	Description, relevant phenotype or genotype, or sequence (5' to 3')	Source
OAH154	CCCGAAAAGCAACACAACCAAG	sequencing primer for pCM-galK reverse
OAH155	TAGCCTAGGCCATGGTCGACGGGGCATATGGAAGTTTATAGTGAG	Forward N-term of *pilB1* with SalI
OAH156	GTAAAACATGCCTTTAATAGTTCTTCTCCGGTATATTTCA TATATCAACCTCCTCATCAG	reverse N-term of *pilB1* with C-term of *pilB1*
OAH157	GATGAGGAGGTTGATATATGAAATATACCGGAGAAGAACT ATTAAAGGCATGTTTTACC	Forward N-term of *pilB1* with C-term of *pilB1*
OAH158	GATCTAGACTCGAGCTCCCCTATACTACTGCTTAAAGTAGTCCC	Reverse C-term of *pilB* with SacI
OAH159	CCATGGCATATGGACGTCGACGAGTAATTCATTTTTGGATGATTTGGGAG	Forward N-term of *pilB2* with SalI
OAH160	CATTTCTTCAACTGTGGTATTCCCCTCCTGATAACTAATC AAAGAAAATACCTCC	reverse N-term of *pilB2* with C-term of *pilB2*
OAH161	GGAGGTATTTTCTTTGATTAGTTATCAGGAGGGGAATACC ACAGTTGAAGAAATG	Forward N-term of *pilB2* with C-term of *pilB2*
OAH162	GATCTAGACTCGAGCTCAGACATTCCACTTGATGATACTATTCCC	Reverse C-term of *pilB2* with SacI
OAH163	GTCGACCGACATGTTCATGTTACAATACTTATTAGAATTAG	Forward N-term of *pilT* with SalI site

slides into a Coy anaerobic chamber and streaked the cells on them. After letting them grow for two hours, we removed them from the chamber and exposed them to aerobic conditions for at least twenty minutes. To take images, we put a coverslip on top, sealed the coverslips with nail polish and viewed on the microscope at room temperature. To make videos, we returned them to the anaerobic chamber, and put coverslips on inside the chamber, sealing them with nail polish. We viewed them on the microscope at 37°C. In strains co-expressing two fluorescent proteins, controls were done to determine that neither emission from YFP nor CFP could be viewed in emissions filtered for the other.

Data analysis. Wherever specific percentages are mentioned, the foci were analyzed according to human visualization and counting. Histograms were constructed using Matlab-based software programs MicrobeTracker and SpotFinderZ [70].

RESULTS

Localization of PilB1 and PilB2. Because *C. perfringens* has two genes with homology to PilB, the TFP or TTSS ATPase extension motor [27], we sought to determine how these proteins localized. Two fluorescently-labeled constructs, CFP-PilB1 and YFP-PilB2, were expressed from pKRAH-CBYB2 in *C. perfringens* strain 13. This plasmid contains a lactose-inducible promoter which was characterized previously [67]. In bacteria growing under aerobic conditions on a solid surface, individual foci of CFP-PilB1 and YFP-PilB2 co-localized 89.8% of the time, and the spots that did not co-localize (5% per protein) were all very small (Fig. 4.1A-C).

CFP-PilB1 and YFP-PilB2 were on the poles 73% of the time (n=293). Images with both expressed proteins and with individually expressed YFP-PilB and YFP-PilB2 from pKRAH1 in strain 13 were also analyzed using MATLAB-based programs, MicrobeTracker and SpotFinderZ [70]. Histograms show in Fig. 4.1D-E the results of the individual analysis of YFP-PilB1 and YFP-PilB2, which also demonstrate polar localization.

In order to make videos of cells growing in anaerobic conditions, the cells were exposed to aerobic conditions in order to allow the GFPs to fluoresce, and were returned to anaerobic conditions prior to video microscopy. Therefore, we were unable to see the localization of newly-synthesized protein, but could see previously-synthesized proteins. This was, in effect, equivalent to a pulse-chase experiment.

In addition to being present on the poles of the cell, the fluorescent foci also appeared at internal points which are likely future division septa. Cells divided at these internal points in videos of anaerobically growing cells (Fig. 4.1F-G and Video 4.2). These future division septa are not necessarily in the center of the cell, as *C. perfringens* strain 13 makes very long cells when grown on surfaces, and is able to divide in several places along the length of the cell (Video 4.1).

Another observation from the videos of expressed GFP-tagged PilB proteins was that they remained stationary relative to the cell rather than alternating between poles such as PilT in *M.*

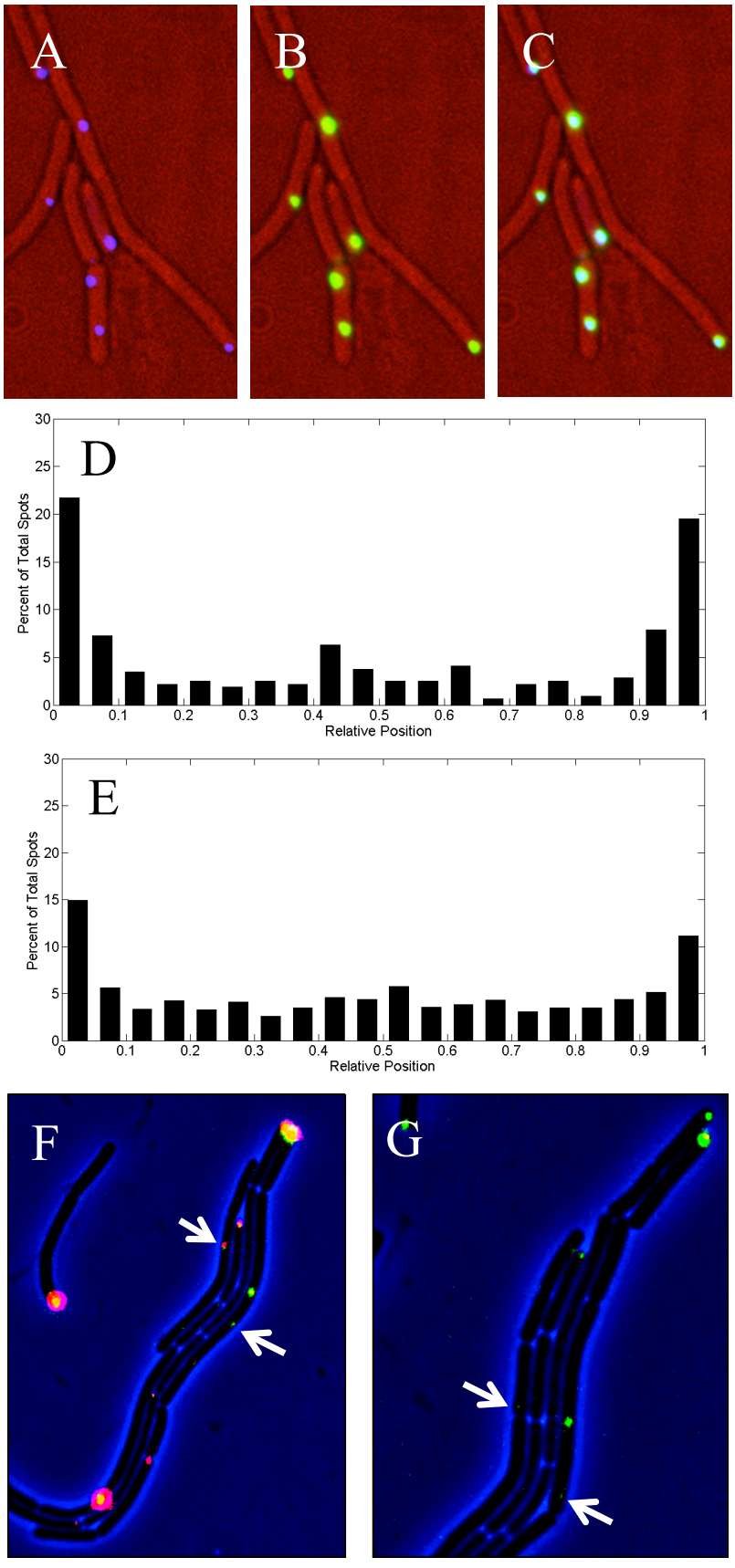

Figure 4.1: Localization of PilB1 and PilB2. Colors were altered in pictures with blue background to show fluorescence better. In blue pictures, CFP appears green and YFP appears pink. Both together appear yellow. Phase contrast channel appears blue. Fluorescent proteins were induced with 0.1 mM lactose. (A) CFP-PilB1 in *C. perfringens* strain 13 pKRAH-CBYB2 (B) YFP-PilB2 in strain 13 pKRAH-CBYB2 (C) Both CFP-PilB1 and YFP-PilB2 shown together in strain 13 pKRAH-CBYB2 (D) Histogram of YFP-PilB distance from poles in strain 13 pKRAH-YB. (n [fluorescent foci] = 318). Assignment of leading pole in this and all following histograms was arbitrary. (E) Histogram of YFP-PilB2 distance from poles in strain 13 pKRAH-YB2. (n = 1186) (F) CFP-PilB1 and YFP-PilB2 in growing strain 13 pKRAH-CBYB2 at time point 00:00. (G) CFP-PilB1 and YFP-PilB2 in growing strain 13 pKRAH-CBYB2 at time point 20:00 min:sec. Arrows indicated proteins' presence at sites where the cell divided.

xanthus has been shown to do [35] (Video 4.2).

Localization of PilT by fluorescent tags. We wanted to determine how the retraction ATPase PilT localized in relation to PilB1 and PilB2. In *M. xanthus*, these two ATPases are in opposite poles of the cell, doing opposite functions by spatial or temporal separation [35]. As *C. perfringens* possesses only one PilT homologue and two PilB homologues, the PilT may be associated with only one of the PilB proteins, while the other could be involved in Type II secretion systems. Alternatively, the PilB proteins may form a hetero-hexamer and work together.

We expressed a fluorescently-tagged PilT in combination with each of the tagged PilB proteins (see Table 4.1) in *C. perfringens* strain 13. In a study of CFP-PilT and YFP-PilB2 in chains of cells on an aerobic solid surface, the proteins appeared at a pole 70.2% of the time, at the center of the cell 13.2% of the time, and between center and end 16.7% of the time. 82% of these proteins co-localized; 14% were PilT alone; and 3% were PilB2 alone (Fig. 4.2A-C). The combination of PilB1 and PilT gave similar results (data not shown).

In summary, 14% of PilT protein was independent of PilB2. A histogram is shown of the MicrobeTracker/SpotFinderZ analysis of YFP-PilT from strain 13 pKRAH-YT (Fig. 4.2D).

In videos with PilT and PilB2, wherever PilT co-localized with PilB2, it remained in the same position in the cell throughout growth. Where PilT was independent, it moved in what may have been a helical pattern throughout the cell, or in a circular revolution around the poles (Fig. 4.2E, Video 4.3). We know this movement is not due to rotation of the cells, because in one of the cells, the PilT co-localized with PilB2 does not move from the left side of the cell (Fig. 4.2E, Video 4.3).

Localization of tagged PilB1 and PilB2 in a PilT mutant. We constructed an in-frame PilT mutant (strain SM1300), and expressed YFP-PilB1 and YFP-PilB2 from pKRAH-YB or pKRAH-YB2, respectively. We had previously shown that PilB1 did not localize normally in SM126 (a PilC insertion mutant) [67]. In that case, 40% of spots still localized to the poles as opposed to 70%. In SM1300, YFP-PilB1 appeared in faint foci all over the cell (Fig. 4.3A), and failed to localize to the poles (Fig. 4.3B). This is in contrast to YFP-PilB1 expressed in strain 13, which

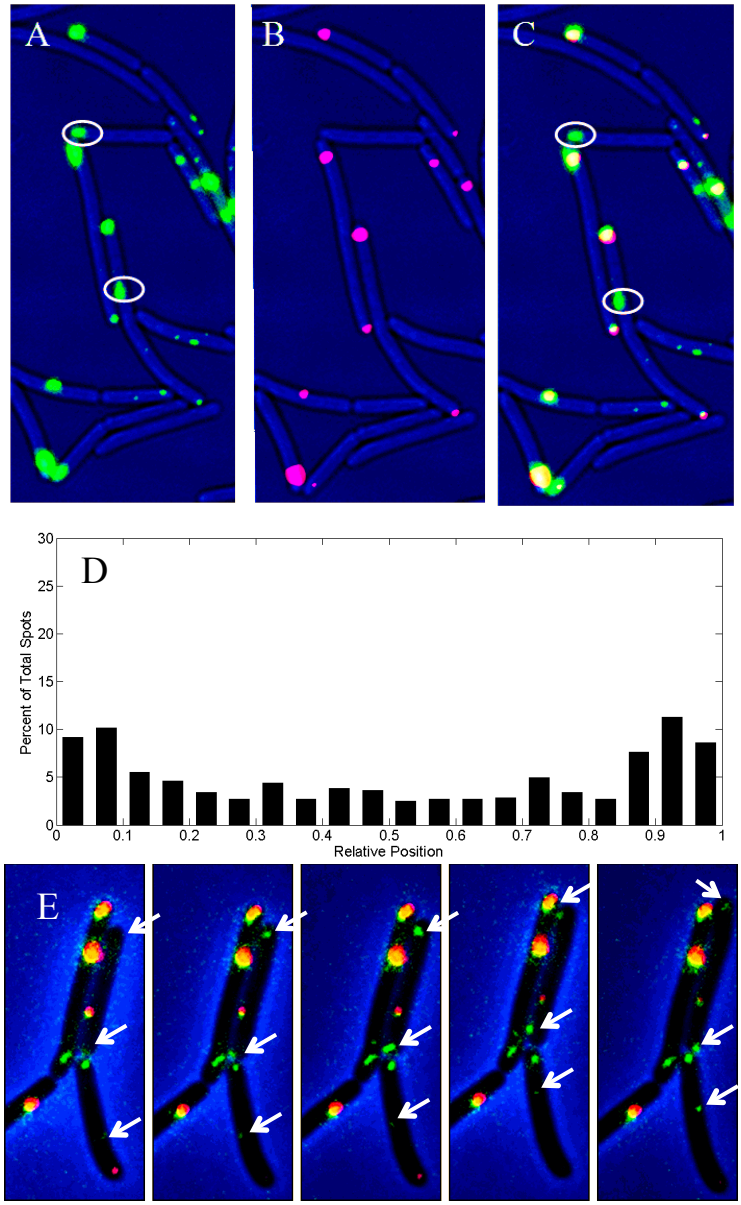

Figure 4.2: Localization of PilT. Colors were altered in pictures with blue background to show off fluorescence better. In blue pictures, CFP appears green and YFP appears pink. Both together appear yellow. Phase contrast channel appears blue. Fluorescent proteins were induced with 0.1mM lactose. (A) CFP-PilT in strain 13 pKRAH CTYB (B) YFP-PilB2 in strain 13 pKRAH CTYB2 (C) Both CFP-PilT and YFP-PilB2 shown together in strain 13 pKRAH CTYB2. Circles are identifying independent foci of CFP-PilT. (D) Histogram of YFP-PilT distance from poles in strain 13 pKRAH YT. (n = 523) (E) sequential images of CFP-PilT with YFP-PilB2 in Strain 13. Arrows are indicating location of moving foci of CFP-PilT. Images are shown in sequential order at 0, 10, 14, 24, and 30 minutes.

Video 4.2: Motile strain 13 with CFP-PilB1 and YFP-PilB2. Strain 13 with CFP-PilB1 and YFP-PilB2 growing on BHI agarose pads under anaerobic conditions. CFP appears blue and YFP appears green. Both together appear teal. Phase contrast channel appears red. Fluorescent proteins were induced with 0.1 mM lactose.

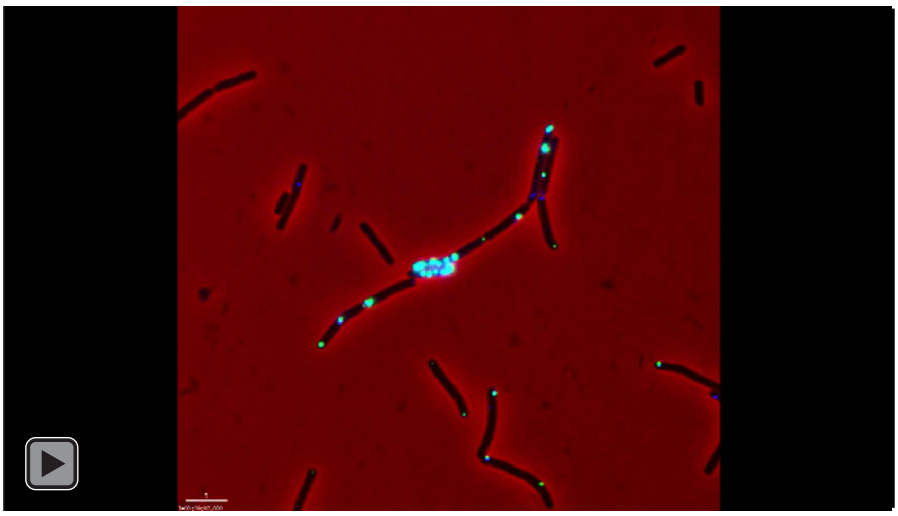

Video 4.3: Motile strain 13 with CFP-PilT and YFP-PilB2. Strain 13 with CFP-PilT and YFP-PilB2 growing on BHI agarose pads under anaerobic conditions. CFP appears blue and YFP appears green. Both together appear teal. Phase contrast channel appears red. Fluorescent proteins were induced with 0.1 mM lactose.

showed an obviously polar pattern (Fig. 4.1D). YFP-PilB2 appeared to have normal polar localization (Fig. 4.3C-D). When the *pilT* mutation was complemented by expression of CFP-PilT, the localization of YFP-PilB returned to the poles (Fig. 4.3E-F). These results demonstrate that PilT is responsible for the localization of PilB1, but not PilB2.

Localization of fluorescently-tagged PilT in PilB mutants and *B. subtilis*. As PilT seemed important for the localization of YFP-PilB1, and had an independent motile fraction, we wanted to determine if PilT localization was dependent on other pilin proteins. We tested it in in-frame PilB1, PilB2, and PilB1/PilB2 mutants. Expression in the double mutant is shown in Fig. 4.4A-B. PilT localized normally in each mutant strain.

Blast analysis of each of *C. perfringens*' TFP related proteins against *B. subtilis* strain 168 revealed that competence protein ComGA bears significant homology to both PilB1 and PilB2. Other TFP proteins from *C. perfringens* lacked significant homology to any protein from *B. subtilis* strain 168. This would indicate that *B. subtilis* lacks a TFP system, and thus the mechanism by which the motile pool of PilT localizes and moves is distinct from Type IV pili. Based on gene annotation, *B. subtilis* has the same type of *minCD* and *divIVA* genes as *C. perfringens* (http://www.xbase.ac.uk/). These are genes that control the location of the cell division machinery [77], suggesting that the method of positioning cell division machinery is very similar between *B. subtilis* and *C. perfringens*. Using the plasmid pDR111 (a gift from Kumaran Ramamurthy at the NIH), we expressed YFP-PilT from an integrated site in the *B. subtilis'* chromosome, inducing it with 0.5 mM IPTG (Isopropyl B-D-1-thiogalactopyranoside) in liquid and viewing it on BHI agarose pads with 0.5 mM lactose. YFP-PilT localized the same way in *B. subtilis* as observed in *C. perfringens* (Fig. 4.4C-D, Fig. 4.2D), although with more localization in the center than in *C. perfringens*, perhaps because *B. subtilis* divided symmetrically more consistently. Additionally, most of the fluorescent spots moved, either around the poles or up into the cell and back (Video 4.4).

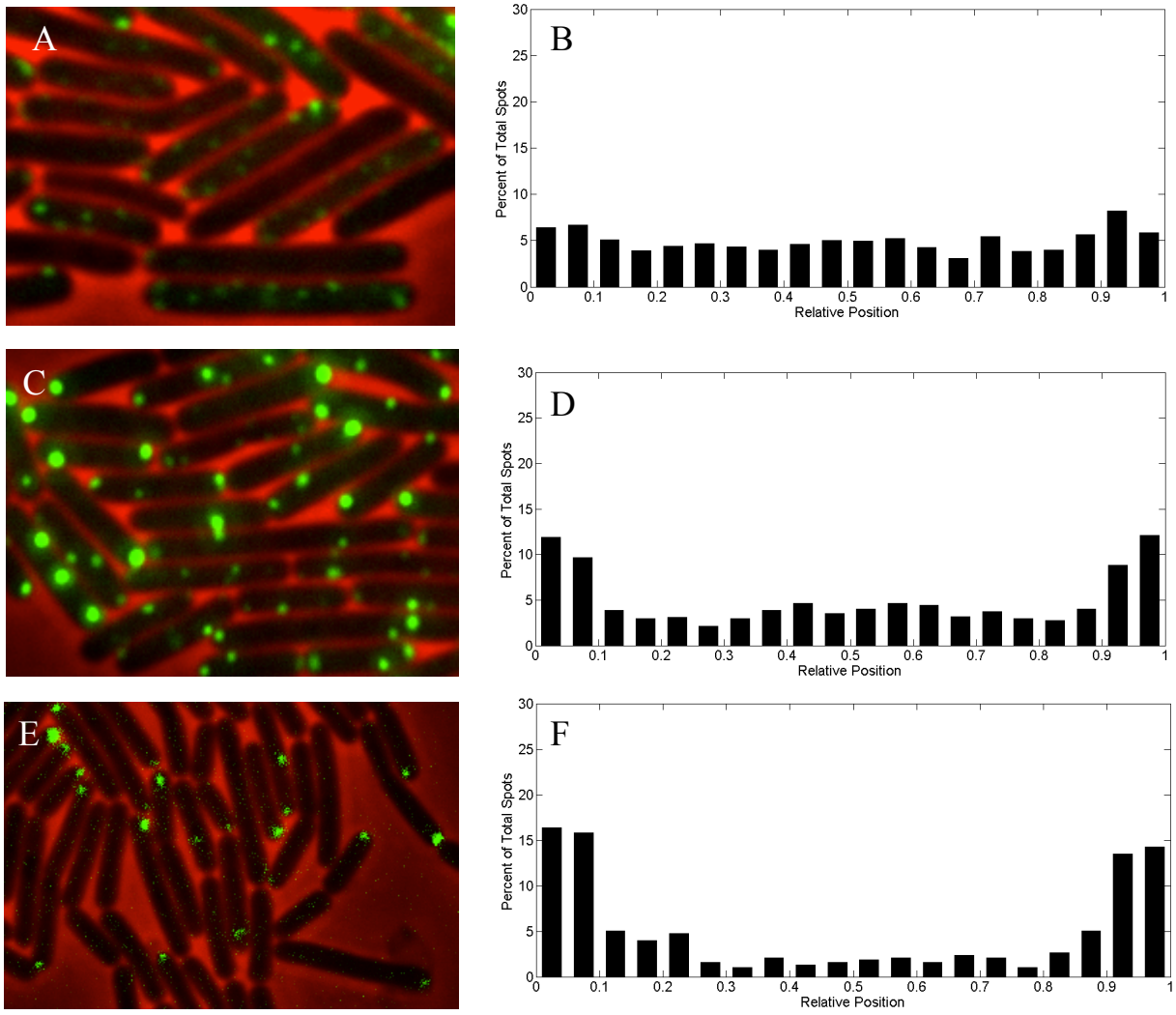

Figure 4.3: Localization of tagged PilB1 and PilB2 in a PilT mutant. (A) YFP-PilB1 in strain SM1300 pKRAH-YB(B) Histogram of YFP-PilB1 distance from poles in SM1300 pKRAH-YB (n=1331). (C) YFP-PilB2 in strain SM1300 pKRAH-YB2 (D) Histogram of YFP-PilB2 distance from poles in SM1300 pKRAH-YB2 (n = 973) (E) YFP-PilB1 from CTYB in strain SM1300 pKRAH-CTYB (F) Histogram of YFP-PilB1 from CTYB in strain SM1300 pKRAH-CTYB (n = 708).

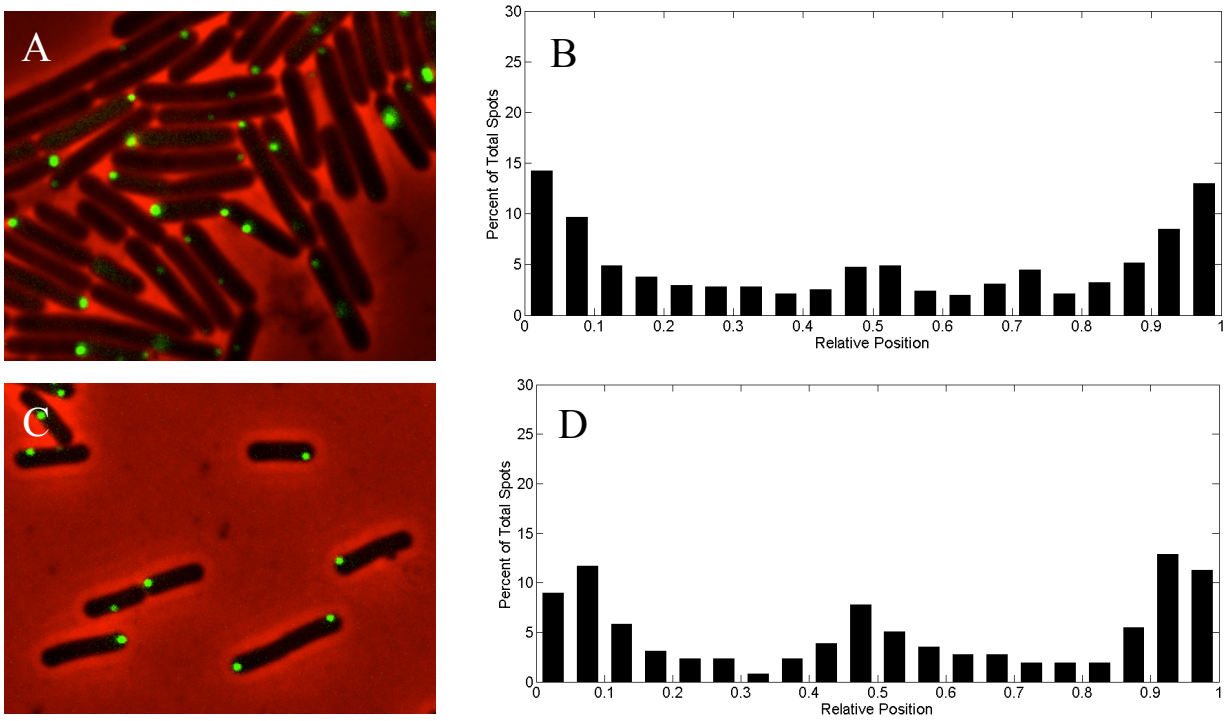

Figure 4.4: Localization of PilT in PilB mutant strains and *B. subtilis*. (A) YFP-PilT in strain AH13 pKRAH-YT (B) Histogram of YFP-PilT distance from poles in strain AH13 pKRAH-YT (n = 716) (C) YFP-PilT in *B. subtilis* strain PS832 pDR111-YT (D) Histogram of YFP-PilT distance from poles in PS832 pDR111-YT. (n = 257)

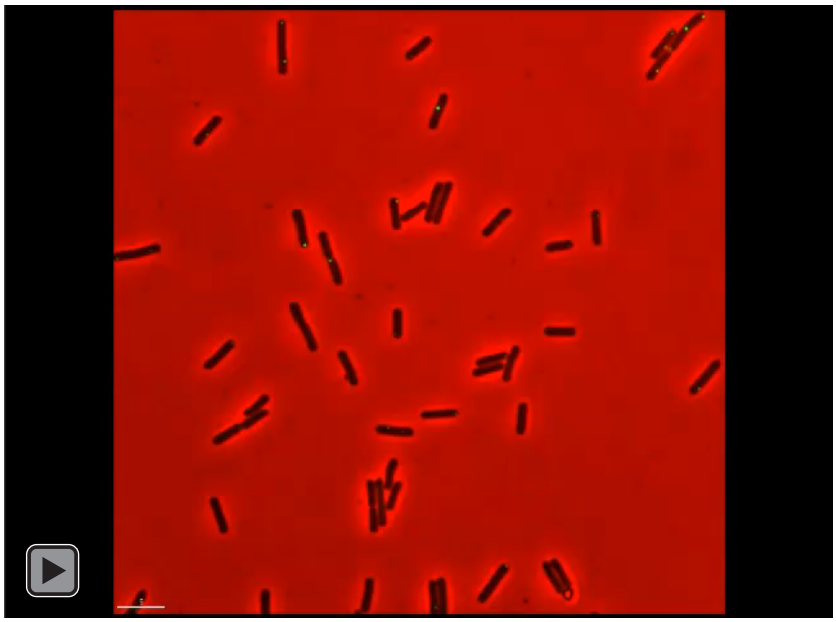

Video 4.4: Localization of YFP-PilT in *B. subtilis* PS832. *B. subtilis* cells were grown in liquid media to early log phase, expression of YFP-PilT being induced with 0.5 mM IPTG. An aliquot was then applied to agarose pads containing 0.5 mM lactose.

Localization of PilT in relation to cell division proteins. In five sequenced *C. perfringens* strains, (SM101, ATCC13124, 13, F4969, JGS1987), *pilT* is located on the chromosome next to *ftsA* and *ftsZ*, two major cell division proteins. However, an in-frame mutation in *pilT* does not appear to affect cell division (data not shown). Other proteins involved in Type IV pili are clustered together on the *C. perfringens* chromosome [27]. We treated the *C. perfringens* cells expressing CFP-PilT and YFP-PilB1 with 10 μg/ml cephalexin, an antibiotic that inhibits FtsI, producing a late block in the cell division cycle, and saw that PilT and PilB1 localized at evenly spaced points throughout the lengthened cells (Fig. 4.5A). This seems to indicate that PilT and PilB1 localize to the future septa before cell division is complete.

We tagged FtsA with CFP and co-expressed it with YFP-PilT from pKRAH. We saw that FtsA appeared in patches throughout the cell, and while PilT appeared much less, the places where PilT appeared were co-localized with FtsA (Fig. 4.5B). This patchy conformation of FtsA corresponds with what Sulius and Jensen found to be the arrangement of MreB, a cytoskeletal protein in rod-shaped cells [78].

B. subtilis strain AH93 contains a xylose-inducible MciZ, which blocks the polymerization and GTPase activity of FtsZ [76]. When we expressed YFP-PilT in *B. subtilis* strain AH93 with 0.5 mM IPTG, and simultaneously expressed MciZ with 0.05% xylose, PilT continued to move and localize fairly normally (Fig. 4.5C-D, Video 4.5). However, when we induced MciZ 30 minutes before inducing YFP-PilT, PilT lost polar localization (Fig. 4.5E-F, Video 4.6). As it localizes normally when the inhibitor is expressed at the same time as PilT, it is difficult to determine if it requires a protein downstream or upstream of FtsZ in the division process. However, as it failed to localize normally when MciZ was previously induced, this may indicate PilT relies on division machinery in order to localize.

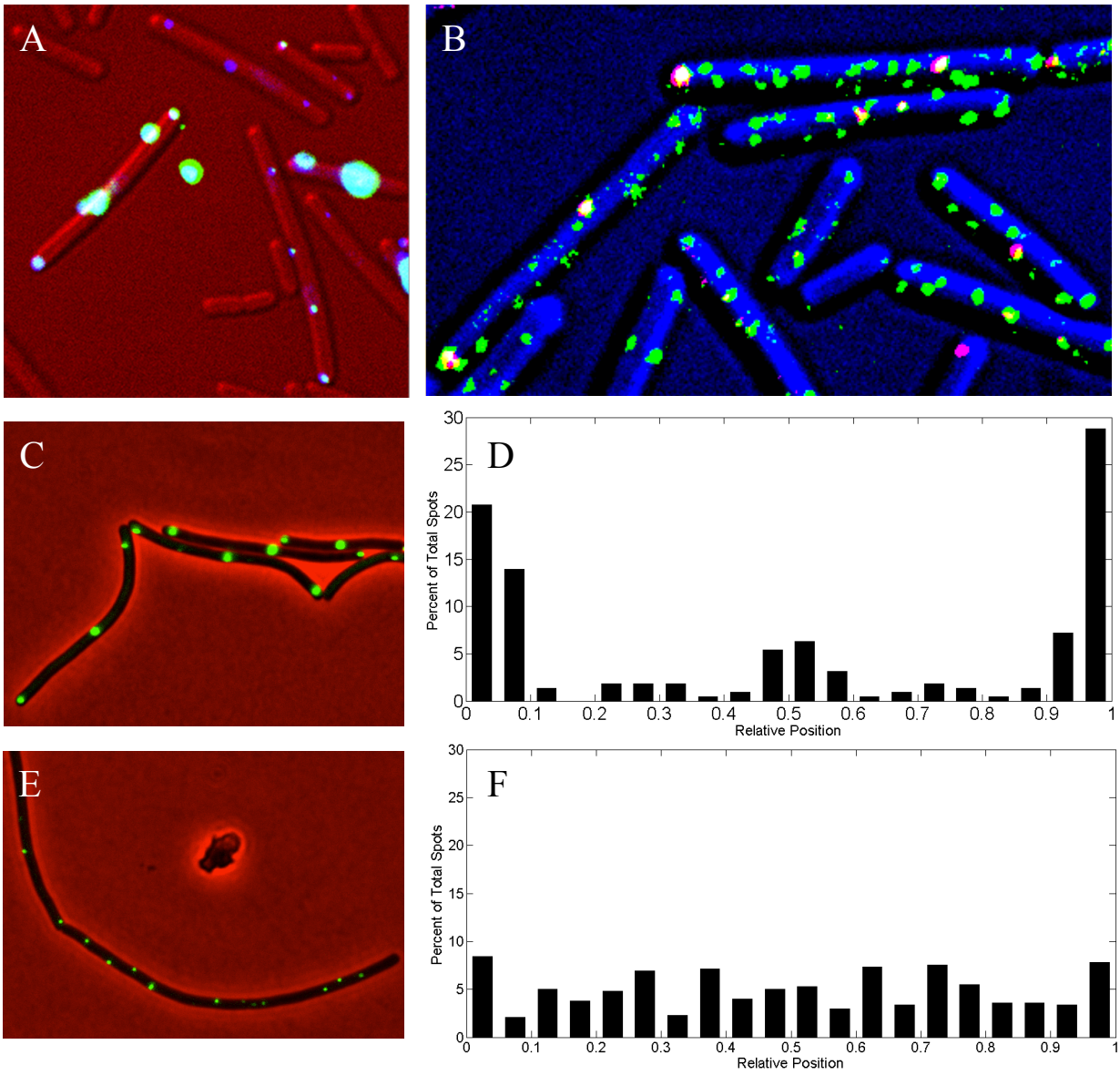

Figure 4.5: Localization of PilT in relation to cell division proteins. (A) CFP-PilT and YFP-PilB in strain 13 pKRAH-CTYB, treated with 10 μg/ml cephalexin. (B) FtsA-CFP (shown in green) and YFP-PilT (shown in pink) expressed in strain 13 pKRAH-ACYT (C) YFP-PilT in *B. subtilis* strain AH93 in which MciZ was induced the same time as YFP-PilT (D) Histogram of YFP-PilT distance from poles in AH93 with induced MciZ as in 5C (n = 222) (E) YFP-PilT in *B. subtilis* strain AH93 in which MciZ was induced 30 minutes prior to YFP-PilT (F) Histogram of YFP-PilT distance from poles in AH93 with induced MciZ as in 5E (n =476).

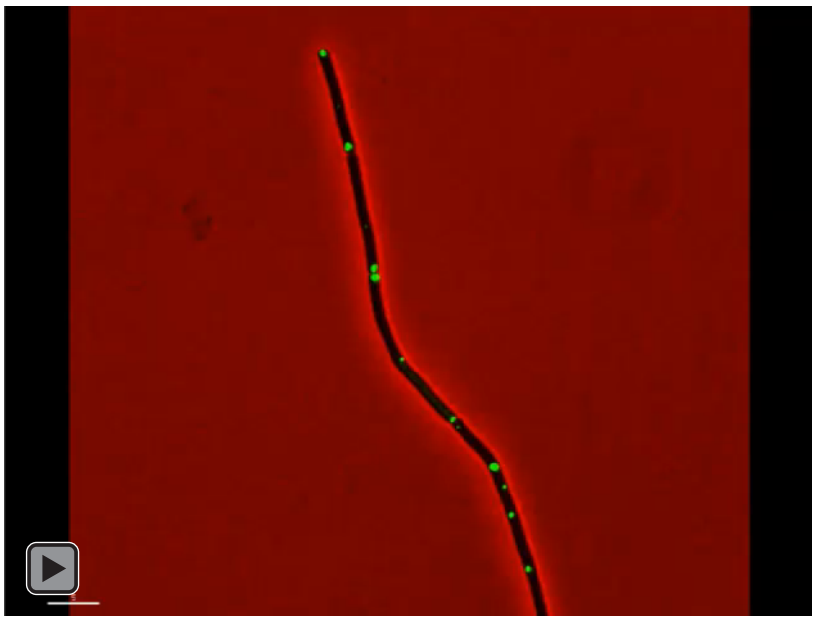

Video 4.5: Localization of YFP-PilT in *B. subtilis* strain AH93. MciZ and YFP-PilT were induced at the same time.

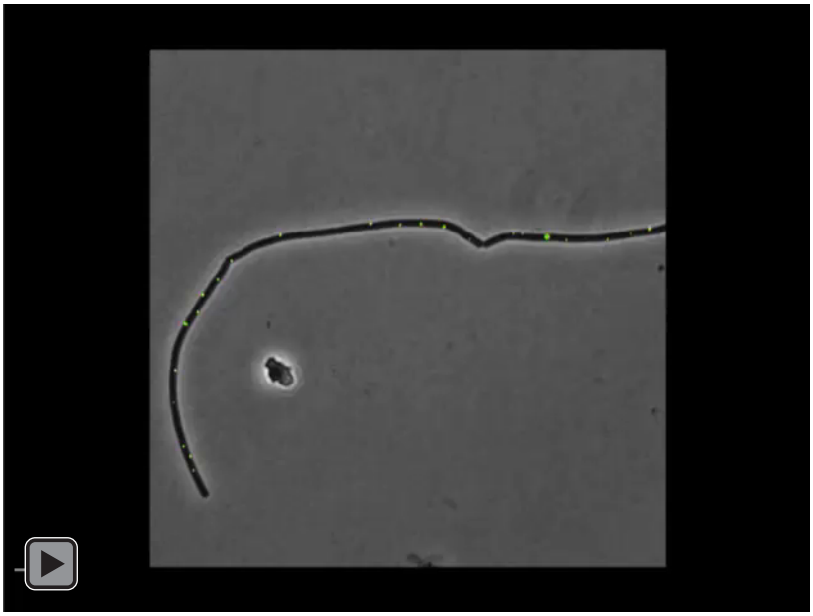

Video 4.6: Localization of YFP-PilT in *B. subtilis* strain AH93 with early inhibition. MciZ was induced 30 minutes prior to YFP-PilT

DISCUSSION

Until this point, PilT's only suspected role has been that of TFP retraction. Because the gene coding for it has a conserved place on the chromosome next to cell division proteins, and it localized normally in the absence of other TFP proteins when expressed in *B. subtilis*, it appears it may additionally play a role associated with cell division proteins. This role may be localizing the TFP apparatus to the poles. TadZ/CpaE has been shown to do this in a subset of Type IVb pili families, but no homologues of this protein have been found in the Type IVa pili families [40]. The MreB cytoskeletal protein has been shown to have a role in positioning the pilus apparatus [79], and it was hypothesized that PilM, with an actin-like domain, was the intermediary [80]. However, in the absence of PilM, *C. perfringens*' PilT localized normally in *B. subtilis*, and appeared to move in a circular or helical pattern. PilB1 required the presence of PilT in order to localize to the poles, although PilB2 did not. This suggests that PilT may be a linking protein between the cytoskeletal and division proteins and the type IV pili assembly.

In order to better confirm PilT's effect on PilB1, we need to express PilB1 and co-express PilB1 and PilT in *B. subtilis*. PilB1 alone should not localize to the poles, while the co-expressed proteins should.

These observations do not explain what the independent, moving portion of PilT is doing in *C. perfringens*, but it suggests it may be connected with cell division proteins which are known to be dynamic [81]. Nor do these observations explain how or why PilB2 localizes to the poles in the absence of PilT even though it typically co-localizes with PilB1. Determining the answers to these questions will require further research.

ACKNOWLEDGMENTS

We would like to thank Sean Mury for his advice and technical help with the microscope. Elizabeth Pickering helped with the use of Microbe Tracker and data analysis. The David Popham lab contributed PS832, and Casey Bernhards aided in the transformation of *B. subtilis*.

Chapter 5

Final Discussion

Type IV pili (TFP) and Type II secretion (TTS) systems are important and frequent topics of study in microbiology due to their impact on bacterial pathogenesis. However, despite their popularity in research, their function is still not fully understood. *Clostridium perfringens* is an excellent candidate in which to study these systems. In addition to being an important pathogen, it is a Gram-positive bacteria, having a simple TFP system due to the fact that only one membrane needs to be spanned by the pilus. The genomes of several strains of *C. perfringens* have been sequenced, and these strains are easily transformable. Studying the TFP system and the TTS system in *C. perfringens* had some problems, though. There was a lack of genetic tools with which to work, *C. perfringens*' DNA did not recombine easily, and, although aerotolerant, the majority of the manipulations needed to be performed within an anaerobic chamber.

The first problem to be solved was the lack of a protein expression system in which expression could be easily controlled. As promoters for sugar-metabolism genes are commonly regulated by their respective sugars, we tried several predicted promoters and regulating genes with the putative sugars that induced them. In one case, addition of the sugar altered the level of expression of the reporter gene in direct correlation with the amount of sugar added. This was *bgaR* and P_{bgaL}, which are characterized in Chapter 2.

Another genetic tool became available when a lab in Japan developed a system for creating in-frame deletion mutations in *C. perfringens* using positive and negative selections to screen. We were able to use that system to construct several deletion mutations in TFP genes, including *pilA1*, *pilA2*, and *pilA3*, described in Chapter 3, and *pilB1*, *pilB2*, and *pilT*, described in Chapter 4.

Upon the development of these techniques, one of our goals was to identify what functions the putative TFP pilin homologues were performing. TFP can be involved in many different roles of pathogenesis, and genes for proteins involved in the TTS system look similar to TFP genes. As *C. perfringens* has multiple genes with homology to TFP core proteins, we wanted to determine what system each pilin was involved in, which were the major pilins, and what roles they played in the pathogenesis of *C. perfringens*.

The inducible promoter system constructed in Chapter 2 allowed us to complement deletion mutants and overexpress the pilins. We expressed wildtype copies to view the pilins' locations on western blots. This was especially valuable, as two of the four pilins (PilA1 and PilA3) were not expressed at high enough concentrations, under the conditions used, for us to detect them in the wildtype strain using western blots. These expressed proteins provided a positive control, such that we were able to determine where they would run on SDS-PAGE gels. One protein that was expressed in higher concentrations was PilA2, and it appeared to be modified, although we have yet to determine what these modifications were. I hypothesize that PilA2 is the major pilin involved in TFP, based on the amount of protein synthesized in the wildtype. Large amounts of PilA2 were only expressed when the cells were grown on solid surfaces, which implies involvement in TFP.

We were unable to fuse the pilin proteins with fluorescent proteins, as the pilins are very small and are assembled into pili that transverse the cell membrane and peptidoglycan. We tried smaller tags, SNAP and FlAsH, but were unable to find one that worked anaerobically, could be applied specifically to the pilin proteins, and was small enough and in an unobtrusive place that the machinery could still assemble the pilins into pili.

We were able to use antibodies to tag the pilins, although due to the process of fixing and washing cells, were not able to view them in their natural state on solid surfaces. Using these antibodies, we were able to ascertain that three of the four pilins were on the exterior of the cells, at the poles, and that the final pilin (PilA1), does not appear to be assembled to the exterior of the cell (Chapter 3).

We constructed deletion mutations in *pilA1* (AH7), *pilA2* (AH8), and *pilA3* (AH9). We determined that AH9 (Δ*pilA3*) failed to remain suspended in liquid as the wildtype did and, by using mass spectrometry to analyze proteins, that AH9 failed to secrete a von Willebrand factor A domain-containing protein. For mutants lacking PilA1 or PilA2, we were unable to determine any phenotypes significantly different from that of the wildtype, but we expect that attachment and DNA uptake assays may yield interesting results.

Our next focus was the ATPase motors, of which *C. perfringens* contained two extension motors, and only one copy of the retraction motor. As TFP systems possess only one extension ATPase in other bacteria studied so far [30], we suspected that one of them may be involved in the TTS system, or that they may be functioning in different locations of the cell.

In this case, we were able to use the inducible promoter system from Chapter 2 to express YFP- and CFP-tagged constructs of both the PilB proteins and the PilT alone or in pairs, and view them in live cells on surfaces. This revealed that the PilB proteins co-localized with each other and with PilT, predominantly at the cell poles. A fraction of PilT localized and moved independent of PilB1 and PilB2. More interestingly, YFP-PilB1 failed to localize to the poles in the PilT mutant, but localization was restored in the PilT mutant when CFP-PilT was co-expressed with YFP-PilB1. YFP-PilB2 was unaffected in the PilT mutant. In Chapter 2, we had shown that, in similar fashion, PilB1 had not localized normally in the insertion mutant of *pilC1* [67].

Additionally, YFP-PilT localized in a polar pattern in *B. subtilis*, which, based on gene homology, appears to lack a TFP system. Localization of YFP-PilT in *B. subtilis* was only disrupted when, prior to expression of PilT, the GTPase and polymerization functions were inhibited for FtsZ, a major and early cell division protein.

Based on PilB1's distributed localization in the PilT mutant and PilA2's high level of expression on plates, and ignoring gene location in the chromosome, a one possible model is that PilB1, PilC1, PilA2 and PilT are involved together in TFP production, while PilB2, PilC2, and PilA3 are involved in TTSS. Another possible model, taking into account the location of genes on the chromosome, is that PilA2, PilB2, and PilC2 are involved in TFP production, and do not need PilT to localize. PilB1, PilC1, PilA4, and PilA3 are involved in the TTSS, and its localization depends on the TFP assembly apparatus, including PilT, being in position.

Future work in characterizing these genes and their involvement in TFP or TTSS, would be to construct and confirm a deletion mutation of *pilA4*, optimize the attachment and DNA uptake assays and test each mutant against the wildtype in these and the other assays described in Chapter

3. Additionally, the PilB mutants could be tested in the same assays as the pilin mutants in an attempt to match each pilin with its respective assembly ATPase.

The fluorescently-tagged PilB proteins need to be viewed in *B. subtilis* to confirm that they require TFP proteins in order to localize, and that PilB1 localizes to the poles in the presence of PilT alone. Based on previous data, it may require PilC as well.

Ultimately, the goal is characterizing TFP and developing an understanding of them that presents a method for blocking their function. This could potentially aid treatment or prevent infections via a plethora of microbes, including *N. meningitidis* and *N. gonorrhoeae*, *Pseudomonas*, and *Clostridium*.

References

[1] **P. Dürre**. *Handbook on clostridia*. CRC Press, 2005.

[2] **J. I. Rood** and **S. T. Cole**. "Molecular Genetics an Pathogenesis of *Clostridium perfringens*". In: *Microbiological Reviews* 55.4 (1991), p. 28.

[3] **J. Rood** et al., eds. *The Clostridia: Molecular Biology and Pathogenesis*. Cambridge: Academic Press, 1997.

[4] **T. Shimizu** et al. "Complete genome sequence of *Clostridium perfringens*, an anaerobic flesh-eater". In: *Proc Natl Acad Sci U S A* 99.2 (2002), pp. 996–1001.

[5] **M. Sebald** and **R. N. Costilow**. "Minimal Growth Requirements for *Clostridium perfringens* and Isolation of Auxotrophic Mutants". In: *Applied Microbiology* 29.1 (1975), pp. 1–16.

[6] **D. White**. *The Physiology and Biochemistry of Prokaryotes*. 3rd. Oxford University Press, 2007, p. 628.

[7] **J. Novak** and **V. Juneja**. "*Clostridium perfringens*: hazards in new generation foods". In: *Inovative Food Science and Emerging Technologies* 3 (2002), pp. 127–32.

[8] *CDC 2011 Estimates: Findings*.

[9] **R. J. Carman** et al. "*Clostridium perfringens* toxin genotypes in the feces of healthy North Americans". In: *Anaerobe* 14.2 (2008), pp. 102–8.

[10] **N. J. Asha**, **D. Tompkins**, and **M. H. Wilcox**. "Comparative analysis of prevalence, risk factors, and molecular epidemiology of antibiotic-associated diarrhea due to *Clostridium difficile*, *Clostridium perfringens*, and *Staphylococcus aureus*". In: *J Clin Microbiol* 44.8 (2006), pp. 2785–91.

[11] **D. R. Revis**. *Clostridial Gas Gangrene*.

[12] **S. Manabe** et al. "Purification and characterization of a clostripain-like protease from a recombinant *Clostridium perfringens* culture". In: *Microbiology* 156.Pt 2 (2010), pp. 561–9.

[13] **A. Lovland** and **M. Kaldhusdal**. "Severely impaired production performance in broiler flocks with high incidence of *Clostridium perfringens* -associated hepatitis". In: *Avian Pathology* 30.1 (2001), pp. 73–81.

[14] **A. R. Cole** et al. "*Clostridium perfringen*s e-toxin shows structural similarity to the pore-forming toxin aerolysin". In: *Nature Structural & Molecular Biology* 11.8 (2004), pp. 797–798.

[15] **K. T. Forest**. "Structure and Assembly of Type IV Pilins". In: *Structural Biology of Bacterial Pathogens*. Ed. by **G. Waksman**, **M. Caparon**, and **S. Hultgren**. Washington, D.C.: ASM Press, 2005. Chap. 6, pp. 81–100.

[16] **H. Sato**, **K. Okinaga**, and **H. Saito**. "Role of pili in the pathogenesis of *Pseudomonas aeruginosa* burn infection". In: *Microbiol Immunol* 32.2 (1988), pp. 131–9.

[17] **D. Bieber** et al. "Type IV pili, transient bacterial aggregates, and virulence of enteropathogenic *Escherichia coli*". In: *Science* 280.5372 (1998), pp. 2114–8.

[18] **D. A. Herrington** et al. "Toxin, toxin-coregulated pili, and the *toxR* regulon are essential for *Vibrio cholerae* pathogenesis in humans". In: *J Exp Med* 168.4 (1988), pp. 1487–92.

[19] **F. E. Aas** et al. "Competence for natural transformation in *Neisseria gonorrhoeae*: components of DNA binding and uptake linked to type IV pilus expression". In: *Mol Microbiol* 46.3 (2002), pp. 749–760.

[20] **Y. Li** et al. "Extracellular polysaccharides mediate pilus retraction during social motility of *Myxococcus xanthus*". In: *Proceedings of the National Academy of Sciences* 100.9 (2003), pp. 5443–5448.

[21] **J. S. Mattick**. "Type IV pili and twitching motility". In: *Annu Rev Microbiol* 56 (2002), pp. 289–314.

[22] **G. O'Toole** and **R. Kolter**. "Flagellar and twitching motility are necessary for *Pseudomonas aeruginosa* biofilm development". In: *Mol Microbiol* 30.2 (1998), pp. 295–304.

[23] **K. B. Barken** et al. "Roles of type IV pili, flagellum-mediated motility and extracellular DNA in the formation of mature multicellular structures in *Pseudomonas aeruginosa* biofilms". In: *Environmental Microbiology* 10.9 (2008), pp. 2331–2343.

[24] **M. Klausen** et al. "Biofilm formation by *Pseudomonas aeruginosa* wild type, flagella and type IV pili mutants". In: *Mol Microbiol* 48.6 (2003), pp. 1511–24.

[25] **T. J. Kirn** et al. "Delineation of pilin domains required for bacterial association into microcolonies and intestinal colonization by *Vibrio cholerae*". In: *Mol Microbiol* 35.4 (2000), pp. 896–910.

[26] **L. Craig**, **M. E. Pique**, and **J. A. Tainer**. "Type IV Pilus Structure and Bacterial Pathogenicity". In: *Nature Reviews (Microbiology)* 2 (2004), p. 16.

[27] **J. J. Varga** et al. "Type IV pili-dependent gliding motility in the Gram-positive pathogen *Clostridium perfringens* and other Clostridia". In: *Mol Microbiol* 62.3 (2006), pp. 680–94.

[28] **E. Nudleman** and **D. Kaiser**. "Pulling Together with Type IV Pili". In: *Journal of Molecular Microbiology and Biotechnology* 7 (2004), p. 11.

[29] **D. W. Keizer** et al. "Structure of a pilin monomer from *Pseudomonas aeruginosa*: implications for the assembly of pili". In: *J Biol Chem* 276.26 (2001), pp. 24186–93.

[30] **M. Ayers**, **P. L. Howell**, and **L. L. Burrows**. "Architecture of the type II secretion and type IV pilus machineries". In: *Future Microbiol* 5.8 (2010), pp. 1203–18.

[31] **E. Carbonnelle** et al. "A systematic genetic analysis in *Neisseria meningitidis* defines the Pil proteins required for assembly, functionality, stabilization and export of type IV pili". In: *Mol Microbiol* 61.6 (2006), pp. 1510–22.

[32] **L. Craig** et al. "Type IV pilus structure by cryo-electron microscopy and crystallography: implications for pilus assembly and functions". In: *Mol Cell* 23.5 (2006), pp. 651–62.

[33] **P. Chiang**, **M. Habash**, and **L. L. Burrows**. "Disparate subcellular localization patterns of *Pseudomonas aeruginosa* Type IV pilus ATPases involved in twitching motility". In: *J Bacteriol* 187.3 (2005), pp. 829–39.

[34] **V. Jakovljevic** et al. "PilB and PilT are ATPases acting antagonistically in type IV pilus function in *Myxococcus xanthus*". In: *J Bacteriol* 190.7 (2008), pp. 2411–21.

[35] **I. Bulyha** et al. "Regulation of the type IV pili molecular machine by dynamic localization of two motor proteins". In: *Mol Microbiol* 74.3 (2009), pp. 691–706.

[36] **M. Sandkvist**. "Type II secretion and pathogenesis". In: *Infect Immun* 69.6 (2001), pp. 3523–35.

[37] **M. Russel**. "Macromolecular assembly and secretion across the bacterial cell envelope: type II protein secretion systems". In: *J Mol Biol* 279.3 (1998), pp. 485–99.

[38] **C. R. Peabody** et al. "Type II protein secretion and its relationship to bacterial type IV pili and archaeal flagella". In: *Microbiology* 149.Pt 11 (2003), pp. 3051–72.

[39] **T. L. Johnson**. "Type II Secretion: from Structure to Function". In: *FEMS* 255 (2006), p. 12.

[40] **J. Lutkenhaus**. "The ParA/MinD family puts things in their place". In: *Trends in Microbiology* (2012).

[41] **R. Collie**, **J. Kokai-Kun**, and **B. McClane**. "Phenotypic characterization of enterotoxigenic *Clostridium perfringens* isolates from non-foodborne human gastrointestinal diseases". In: *Anaerobe* 4 (1998), pp. 69–79.

[42] **C. Hogenauer** et al. "Mechanisms and management of antibiotic-associated diarrhea". In: *Clin Infect Dis* 27.4 (1998), pp. 702–10.

[43] **J. I. Rood**. "Virulence genes of *Clostridium perfringens*". In: *Annu Rev Microbiol* 52 (1998), pp. 333–60.

[44] **G. S. Myers** et al. "Skewed genomic variability in strains of the toxigenic bacterial pathogen, *Clostridium perfringens*". In: *Genome Res* 16.8 (2006), pp. 1031–40.

[45] **Y. Zhao** and **S. B. Melville**. "Identification and characterization of sporulation-dependent promoters upstream of the enterotoxin gene (*cpe*) of *Clostridium perfringens*". In: *J Bacteriol* 180.1 (1998), pp. 136–42.

[46] **I. Guillouard**, **T. Garnier**, and **S. T. Cole**. "Use of site-directed mutagenesis to probe structure-function relationships of alpha-toxin from *Clostridium perfringens*". In: *Infect Immun* 64.7 (1996), pp. 2440–4.

[47] **J. T. Heap** et al. "The ClosTron: a universal gene knock-out system for the genus *Clostridium*". In: *J Microbiol Methods* 70.3 (2007), pp. 452–64.

[48] **A. Lanckriet** et al. "Generation of single-copy transposon insertions in *Clostridium perfringens* by electroporation of phage mu DNA transposition complexes". In: *Appl Environ Microbiol* 75.9 (2009), pp. 2638–42.

[49] **J. Vidal** et al. "Use of an EZ-Tn5-based random mutagenesis system to identify a novel toxin regulatory locus in *Clostridium perfringens* strain 13". In: *PLoS One* 4.7 (2009), e6232.

[50] **L. Girbal** et al. “Development of a sensitive gene expression reporter system and an inducible promoter-repressor system for *Clostridium acetobutylicum*”. In: *Appl Environ Microbiol* 69.8 (2003), pp. 4985–8.

[51] **S. B. Tummala**, **N. E. Welker**, and **E. T. Papoutsakis**. “Development and characterization of a gene expression reporter system for *Clostridium acetobutylicum* ATCC 824”. In: *Appl Environ Microbiol* 65.9 (1999), pp. 3793–9.

[52] **L. M. Guzman** et al. “Tight regulation, modulation, and high-level expression by vectors containing the arabinose PBAD promoter”. In: *J Bacteriol* 177.14 (1995), pp. 4121–30.

[53] **W. J. Dower**, **J. F. Miller**, and **C. W. Ragsdale**. “High efficiency transformation of *E. coli* by high voltage electroporation”. In: *Nucleic Acids Res* 16.13 (1988), pp. 6127–45.

[54] **S. P. Allen** and **H. P. Blaschek**. “Factors involved in the electroporation-induced transformation of *Clostridium perfringens*”. In: *FEMS Microbiol Lett* 58 (1990), p. 4.

[55] **K. H. Harry** et al. “Sporulation and enterotoxin (CPE) synthesis are controlled by the sporulation-specific sigma factors SigE and SigK in *Clostridium perfringens*”. In: *J Bacteriol* 191.8 (2009), pp. 2728–42.

[56] **I. Sastalla** et al. “Codon-optimized fluorescent proteins designed for expression in low-GC Gram-positive bacteria”. In: *Applied and Environmental Microbiology* 75.7 (2009), p. 12.

[57] **J. Varga**, **V. L. Stirewalt**, and **S. B. Melville**. “The CcpA protein is necessary for efficient sporulation and enterotoxin gene (*cpe*) regulation in *Clostridium perfringens*”. In: *J Bacteriol* 186.16 (2004), pp. 5221–9.

[58] **S. B. Melville**, **R. Labbe**, and **A. L. Sonenshein**. “Expression from the *Clostridium perfringens cpe* promoter in *C. perfringens* and *Bacillus subtilis*”. In: *Infect Immun* 62.12 (1994), pp. 5550–8.

[59] **P. T. Tran**, **A. Paoletti**, and **F. Chang**. “Imaging green fluorescent protein fusions in living fission yeast cells”. In: *Methods* 33.3 (2004), pp. 220–5.

[60] **F. Neidhardt**, ed. Escherichia coli *and Salmonella cellular and molecular biology*. 2nd ed. Washington D.C.: ASM Press, 1996.

[61] **J. Sussman** et al. “Vectors for constructing kan gene fusions: direct selection of mutations affecting IS10 gene expression”. In: *Gene* 90.1 (1990), pp. 135–140.

[62] **R. A. Jefferson**, **S. M. Burgess**, and **D. Hirsh**. “beta-Glucuronidase from *Escherichia coli* as a gene-fusion marker”. In: *Proc Natl Acad Sci U S A* 83.22 (1986), pp. 8447–51.

[63] **M. Mendez** et al. “Carbon catabolite repression of type IV pilus-dependent gliding motility in the anaerobic pathogen *Clostridium perfringens*”. In: *J Bacteriol* 190.1 (2008), pp. 48–60.

[64] **T. Kobayashi**, **T. Shimizu**, and **H. Hayashi**. “Transcriptional analysis of the beta-galactosidase gene (pbg) in *Clostridium perfringens*”. In: *FEMS Microbiol Lett* 133.1-2 (1995), pp. 65–9.

[65] **T. Shimizu** et al. “Sequence analysis of flanking regions of the *pfoA* gene of *Clostridium perfringens*: beta-galactosidase gene (pbg) is located in the 3’-flanking region”. In: *Microbiol Immunol* 39.9 (1995), pp. 677–86.

[66] **A. B. Dalia**, **A. J. Standish**, and **J. N. Weiser**. "Three surface exoglycosidases from *Streptococcus pneumoniae*, NanA, BgaA, and StrH, promote resistance to opsonophagocytic killing by human neutrophils". In: *Infect Immun* 78.5 (2010), pp. 2108–16.

[67] **A. H. Hartman**, **H. Liu**, and **S. B. Melville**. "Construction and characterization of a lactose-inducible promoter system for controlled gene expression in *Clostridium perfringens*". In: *Appl Environ Microbiol* 77.2 (2011), pp. 471–8.

[68] **S. N. Ho** et al. "Site-directed mutagenesis by overlap extension using the polymerase chain reaction". In: *Gene* 77.1 (1989), pp. 51–59.

[69] **H. Nariya** et al. "Development and application of a method for counterselectable in-frame deletion in *Clostridium perfringens*". In: *Appl Environ Microbiol* 77.4 (2011), pp. 1375–82.

[70] **E. C. Garner**. "MicrobeTracker: quantitative image analysis designed for the smallest organisms". In: *Mol Microbiol* 80.3 (2011), pp. 577–579.

[71] **J. Shi**, **T. L. Blundell**, and **K. Mizuguchi**. "FUGUE: sequence-structure homology recognition using environment-specific substitution tables and structure-dependent gap penalties". In: *J Mol Biol* 310.1 (2001), pp. 243–57.

[72] **K. Rodgers**, **C. G. Arvidson**, and **S. Melville**. "Expression of a *Clostridium perfringens* type IV pilin by *Neisseria gonorrhoeae* mediates adherence to muscle cells". In: *Infect Immun* 79.8 (2011), pp. 3096–105.

[73] **N. P. Cianciotto**. "Type II secretion: a protein secretion system for all seasons". In: *Trends in Microbiology* 13.12 (2005).

[74] **R. A. Britton** et al. "Genome-Wide Analysis of the Stationary-Phase Sigma Factor (Sigma-H) Regulon of *Bacillus subtilis*". In: *J Bacteriol* 184.17 (2002), pp. 4881–4890.

[75] **C. Anagnostopoulos** and **J. Spizizen**. "Requirements for transformation in *Bacillus subtilis*". In: *Journal of Bacteriology* 81 (1961), pp. 74–76.

[76] **A. A. Handler**, **J. E. Lim**, and **R. Losick**. "Peptide inhibitor of cytokinesis during sporulation in *Bacillus subtilis*". In: *Mol Microbiol* 68.3 (2008), pp. 588–599.

[77] **I. Barak** et al. "Lipid spirals in *Bacillus subtilis* and their role in cell division". In: *Mol Microbiol* 68.5 (2008), pp. 1315–27.

[78] **M. Swulius** and **G. Jensen**. "The helical MreB cytoskeleton in E. coli MC1000/pLE7 is an artifact of the N-terminal YFP tag". In: *Journal of Bacteriology* (2012).

[79] **K. N. Cowles** and **Z. Gitai**. "Surface association and the MreB cytoskeleton regulate pilus production, localization and function in *Pseudomonas aeruginosa*". In: *Mol Microbiol* (2010).

[80] **C. L. Kirkpatrick** and **P. H. Viollier**. "Poles Apart: Prokaryotic Polar Organelles and their Spatial Regulation". In: *Cold Spring Harbor Perspectives in Biology* (2010).

[81] **P. C. Peters** et al. "A new assembly pathway for the cytokinetic Z ring from a dynamic helical structure in vegetatively growing cells of *Bacillus subtilis*". In: *Mol Microbiol* 64.2 (2007), pp. 487–99.

Appendix

A. Copyright Permissions

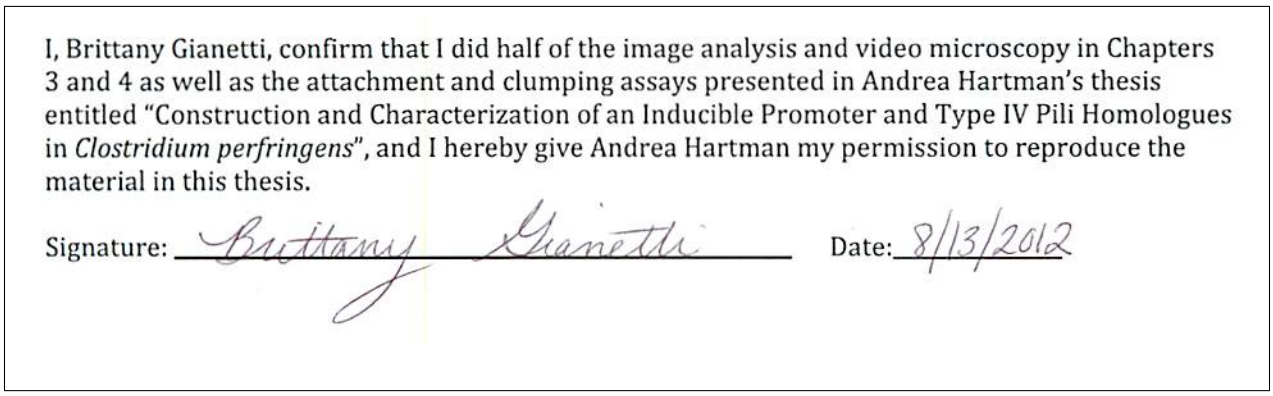
I, Brittany Gianetti, confirm that I did half of the image analysis and video microscopy in Chapters 3 and 4 as well as the attachment and clumping assays presented in Andrea Hartman's thesis entitled "Construction and Characterization of an Inducible Promoter and Type IV Pili Homologues in *Clostridium perfringens*", and I hereby give Andrea Hartman my permission to reproduce the material in this thesis.

Signature: Brittany Gianetti Date: 8/13/2012

Figure A.1: Permission from Brittany A. Gianetti.

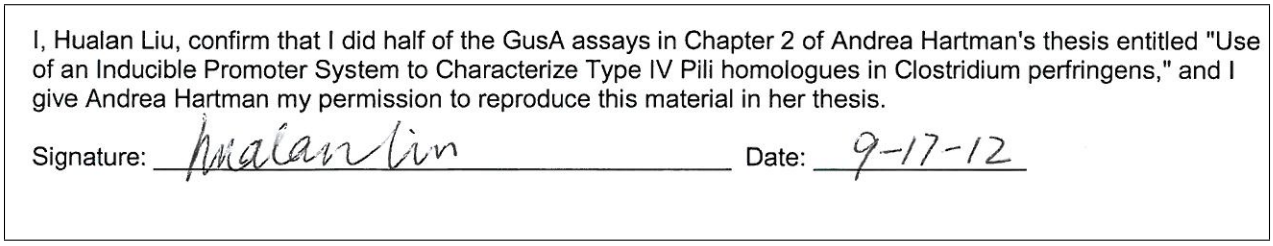
I, Hualan Liu, confirm that I did half of the GusA assays in Chapter 2 of Andrea Hartman's thesis entitled "Use of an Inducible Promoter System to Characterize Type IV Pili homologues in Clostridium perfringens," and I give Andrea Hartman my permission to reproduce this material in her thesis.

Signature: Hualan Liu Date: 9-17-12

Figure A.2: Permission from Hualan Liu.

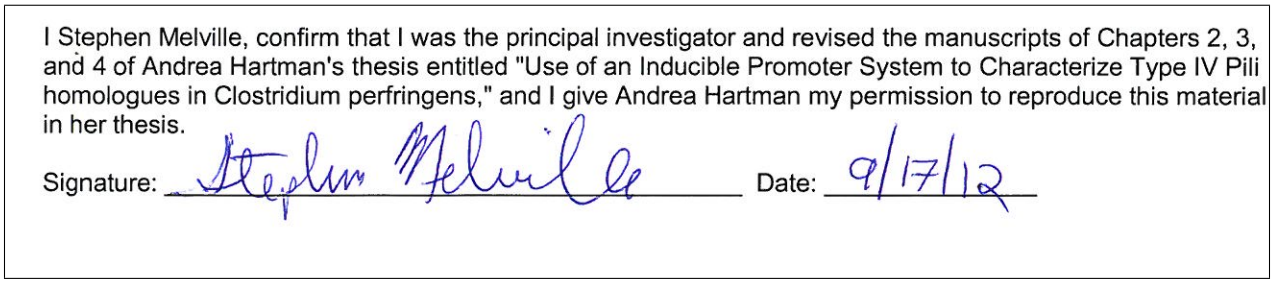
I Stephen Melville, confirm that I was the principal investigator and revised the manuscripts of Chapters 2, 3, and 4 of Andrea Hartman's thesis entitled "Use of an Inducible Promoter System to Characterize Type IV Pili homologues in Clostridium perfringens," and I give Andrea Hartman my permission to reproduce this material in her thesis.

Signature: Stephen Melville Date: 9/17/12

Figure A.3: Permission from Steven B. Melville.

.

LAST UPDATED: November 5, 2009

ASM Journals Statement of Authors' Rights

Authors may post their articles to their institutional repositories

ASM grants authors the right to post their accepted manuscripts in publicly accessible electronic repositories maintained by funding agencies, as well as appropriate institutional or subject-based open repositories established by a government or non-commercial entity. Since ASM makes the final, typeset articles from its primary-research journals available free of charge on the ASM Journals and PMC websites 6 months after final publication, ASM recommends that when submitting the accepted manuscript to PMC or institutional repositories, the author specify that the posting release date for the manuscript be no earlier than 6 months after the final publication of the typeset article by ASM.

Authors may post their articles in full on personal or employer websites

ASM grants the author the right to post his/her article (after publication by ASM) on the author's personal or university-hosted website, but not on any corporate, government, or similar website, without ASM's prior permission, provided that proper credit is given to the original ASM publication.

Authors may make copies of their articles in full

Corresponding authors are entitled to 10 free downloads of their papers. Additionally, all authors may make up to 99 copies of his/her own work for personal or professional use (including teaching packs that are distributed free of charge within your own institution). For orders of 100 or more copies, you should seek ASM's permission or purchase access through Highwire's Pay-Per-View option, available on the ASM online journal sites.

Authors may republish/adapt portions of their articles

ASM also grants the authors the right to republish discrete portions of his/her article in any other publication (including print, CD-ROM, and other electronic formats) of which he or she is author or editor, provided that proper credit is given to the original ASM publication. "Proper credit" means either the copyright lines shown on the top of the first page of the PDF version, or "Copyright © American Society for Microbiology, [insert journal name, volume number, year, page numbers and DOI]" of the HTML version. You may obtain permission from Rightslink. For technical questions about using Rightslink, please contact Customer Support via phone at (877) 622-5543 (toll free) or (978) 777-9929, or e-mail Rightslink customer care at **customercare@copyright.com.**

Please note that the ASM is in full **compliance with NIH Policy.**

Figure A.4: Reprint permission from American Society of Microbiology.